COMBINING SPHINGOLIPIDOMICS AND COMPUTATIONAL SYSTEMS BIOLOGY TO STUDY RED BLOOD CELL SPHINGOLIPID METABOLISM IN HEALTH AND DISEASE

A Dissertation
Presented to
The Academic Faculty

by

Nathan Frederick Chiappa

In Partial Fulfillment
of the Requirements for the Degree
Doctor of Philosophy in the
Wallace H. Coulter Department of Biomedical Engineering

Georgia Institute of Technology and Emory University
December 2019

COMBINING SPHINGOLIPIDOMICS AND COMPUTATIONAL SYSTEMS BIOLOGY TO STUDY RED BLOOD CELL SPHINGOLIPID METABOLISM IN HEALTH AND DISEASE

Approved by:

Edward Botchwey, PhD, Advisor
Wallace H. Coulter Department of Biomedical Engineering
Georgia Institute of Technology

Alfred Merrill, PhD
School of Biological Sciences
Georgia Institute of Technology

Clinton Joiner, MD, PhD
Department of Pediatrics
Emory University School of Medicine

Mark Styczynski, PhD
School of Chemical and Biomolecular Engineering
Georgia Institute of Technology

Wilbur Lam, MD, PhD
Wallace H. Coulter Department of Biomedical Engineering
Georgia Institute of Technology

Eberhard Voit, PhD
Wallace H. Coulter Department of Biomedical Engineering
Georgia Institute of Technology

Date Approved: 08/23/19

ACKNOWLEDGEMENTS

It is safe to say that I could not have completed this thesis without the help of many people. First and foremost, I want to thank my mom and dad for their unending support through the years. Second, I want to thank my advisor Ed Botchwey for putting up with me for 7 years and for trying to make me a better salesman of my work. I want to thank the two postdocs in the Botchwey lab, Molly Ogle and Hannah Song for helping me with all of the experimental design and for helping to remind me that there is light at the end of the graduate school tunnel. I want to thank my committee members for meeting with me and helping to stear me towards (and sometimes away from) research ideas. I want to thank the members of Dr. Voit's lab for making me feel like family and in particular to Luis Fonseca who met with me on so many occasions to figure out modeling problems. I want to say thank you to Drs. Cameron Sullards and David Bostwick in the IBB mass spectrometry core for teaching me how to do LC-MS/MS analysis. I want to say thank you to Sam and Jingjing from Dr. Merrill's lab for teaching me how to do lipid extraction and for helping me to troubleshoot my analytical biochemistry problems. I want to thank my fellow Botchwey lab grad student, Jada, for supporting me during the very difficult final push to finish my thesis. I absolutely want to thank all of the undergrads that I worked with over the years including Sivlia, Bhargav, Sully, Ryan, Dharani, Ashlee, Abby, and Kelly. I could not have completed all of the work necessary for this thesis with out them. Finally, I want to thank the two brilliant high school students that I got to work with, Miyana and Ciara. They made me feel young again and reminded me of the joy of learning and science.

TABLE OF CONTENTS

LIST OF TABLES

LIST OF FIGURES

LIST OF SYMBOLS AND ABBREVIATIONS

AA	Non-sickle genotype
ACER	Alkaline ceramidase
ATP	Adenosine triphosphate
BSA	Bovine serum albumin
C1P	Ceramide 1-Phosphate
CER	Ceramide
CERK	Ceramide kinase
DHCER	Dihydroceramide
EV	Extracellular vesicles
HexCer	Hexosylceramide
LC-MS/MS	Liquid chromatography tandem mass spectrometry
PBS	Phosphate buffered saline
PLA	Plasma
PS	Phosphatidylserine
RBC	Red blood cell
RET	Reticulocyte
SA	Sphinganine
SA1P	Sphinganine 1-phosphate
SCD	Sickle cell disease
SK	Sphingosine kinase
SM	Sphingomyelin
SO	Sphingosine

SO1P	Sphingosine 1-phosphate
SS	Sickle genotype
WBC	White blood cell

SUMMARY

Sickle cell disease is among the most common hematologic diseases in the world, affecting over 4 million people worldwide. Despite knowing the genetic origin of this disease for decades, our ability to treat sickle cell disease is limited. Thus, an improved understanding of the mechanisms of sickle pathology is desperately needed. One aspect of sickle cell disease pathology that still requires more investigation is the alteration of the membrane lipids. Sickle red blood cell membranes are subject to intense physical and oxidative damage from sickle hemoglobin. Thus, it is reasonable to hypothesize that sickle red blood cell lipid metabolism is dysfunctional. One branch of lipid metabolism that may be particularly important in red blood cells is sphingolipid metabolism. Research has shown that red blood cell sphingolipids regulate cell death, regulate adhesion to endothelial cells, and protect other lipids from oxidation, all of which are areas relevant to sickle cell pathology. Despite this, little is known about red blood cell sphingolipid metabolism under normal or sickle conditions.

In this thesis, we combine liquid chromatography-tandem mass spectrometry-based sphingolipidomics with computational modeling to characterize sphingolipid metabolism in red blood cells and how it is altered in sickle cell disease. First, we collected mechanistic information on red blood cell sphingolipid metabolism from the literature and integrated it into a computational model. This model was used as a tool for determining the importance of different metabolic variables in determining the concentration of sphingolipids in red blood cells and plasma. Second, we measured the homeostatic concentrations of sphingolipids from normal and sickle red blood cells and extracellular vesicles. From these

measurements, we were able to determine that sickle red blood cells have significantly higher concentrations of many different sphingolipid classes. Further, we identified novel changes in the metabolic enzymes of sphingolipid metabolism in sickle red blood cells. Finally, we investigated the contribution of the plasma environment and a specific subset of red blood cells, the reticuolocytes, to the alterations in red blood cell sphingolipid concentrations observed in sickle cell disease. We observed that although there are many changes in red blood cell sphingolipid concentrations, there are few changes in plasma sphingolipid concentrations in sickle cell disease. Further, incubating red blood cells with plasma of the opposite genotype did not affect the red blood cell sphingolipid concentrations. Next, we used two different techniques to isolate reticulocyte-enriched and reticulocyte-depleted sickle red blood cell populations. We then measured the sphingolipid concentrations in the different populations. Our analysis showed that sickle reticulocytes have elevated concentrations of sphingolipids compared to sickle erythrocytes, suggesting that the increased prevalence of reticulocytes in sickle cell disease may contribute to the increased sphingolipid concentrations. However, the differences in reticulocytes are not as widespread as those seen when comparing normal and sickle red blood cells. Thus, there may be other, unidentified, factors contributing to the alteration of red blood cell sphingolipids in sickle cell disease.

The results of this thesis represent significant contributions to our understanding of basic red blood cell biology and to sickle cell disease pathology. Further, the model that we constructed can serve as tool to predict how red blood cell sphingolipid metabolism will behave under novel pathologic and pharmacologic situations.

CHAPTER 1. INTRODUCTION AND SPECIFIC AIMS

1.1 Introduction

The central hypothesis of this thesis is that red blood cell sphingolipid metabolism is dysfunctional in sickle cell disease red blood cells and that this is the result of changes in the red blood cell population itself and in the enviroment. This hypothesis will be tested in the following three specific aims.

1.2 Specific Aims

Aim 1. To construct a computational model of red blood cell sphingolipid metabolism and use it to determine the importance of known changes in sickle red blood cells in determining red blood cell sphingolipid concentrations. First, we will construct a model of red blood cell sphingolipid metabolism based on known biochemical and biophysical details of the metabolic network. Next, we will fit the model to dynamic time-series data from literature and ensure that the model performs reasonably. Finally, we will use the computational model to predict how changes in biophysical and biochemical parameters affect sphingolipid concentrations.

Aim 2. To use LC-MS/MS-based sphingolipidomics and statistical analysis to comprehensively characterize differences in sphingolipid concentrations between normal and sickle cell disease red blood cells. First, we will use LC-MS/MS analysis to measure and compare the concentrations of multiple classes of sphingolipids in normal and sickle red blood cells. Then, we will use multivariate statisitical approaches to analyze the LC-

MS/MS data and infer changes in enzyme activities that may have caused the changes in sphingolipid concentrations in sickle cell disease.

Aim 3. To use LC-MS/MS-based sphingolipidomics to evaluate the importance of the plasma environment and reticulocytes in determining the sphingolipid concentrations in sickle red blood cells. This aim will attempt to find a mechanistic explanation for the changes in red blood cell sphingolipid concentrations observed in aim 2. First, we will isolate red blood cells and plasma from normal and sickle genotype donors and measure the sphingolipid concentrations in the different samples. Next, we will incubate red blood cells in plasma of the opposite genotype to determine if the plasma is capable of altering the red blood cell sphingolipid concentrations. Next, we will isolated sickle reticulocyte-enriched and reticulocyte-depleted red blood cell fractions and use LC-MS/MS to measure the sphingolipid concentrations of the different populations. We will use statistical analysis to determine whether red blood cell sphingolipid concentrations depend on the percent of reticulocytes in the red blood cell population.

1.3 Significance

The work presented in this thesis represents a significant contribution to many fields of study. The computational model of red blood cell sphingolipid metabolism is the first attempt to integrate the currently available information on this system into one place. This is not trivial as the unique biophysical properties of lipids present challenges for the construction and parameterization of such a model. Thus, this model can serve as a templete for future modeling of lipid systems and for how to address the many complications involved with biophysical properties of lipids. The sphingolidomic

characterization of normal and sickle red blood cells is the most comprehensive to date. This characterization will contribute to our knowledge of basic red blood cell biology, but also to our knowledge of sickle cell disease pathology. Our sphingolipidomic characterization of the interaction of plasma and red blood cells will allow us to determine whether the changes in sickle red blood cell sphingolipids are dependent on the cell environment. Finally, our sphingolipidomic characterization of sickle reticulocytes is the most comprehensive to date. Further, this characterization will allow us to determine whether the changes in red blood cell sphingolipids are dependent on changes in the cell population itself.

CHAPTER 2. BACKGROUND

2.1 Sickle Cell Disease is a Widespread Genetic Disease

Sickle cell disease (SCD) is a genetic disease affecting around 100,000 Americans, and more than 4 million people worldwide. It is caused by a genetic mutation in the gene for the beta-globin subunit of hemoglobin. When sickle hemoglobin is deoxygenated, it polymerizes. The polymerized sickle hemoglobin fibers mechanically deform and damage the red blood cell membrane. Further, sickle hemoglobin can precipitate onto the inner leaflet of the red blood cell membrane and oxidatively damage the membrane [1]. Ultimately, the mutation in hemoglobin causes a large number of problems for individuals with SCD. These include hemolytic anemia, inflammation, infections, acute and chronic pain, organ damage, and painful vaso-occlusive crises. The symptoms experienced are heterogeneous from patient to patient and within the same patient over time. Given the diverse and often severe symptoms experienced by people with SCD, there is continued need to research basic disease mechanisms and to develop new treatment options.

2.2 Treatment Options for Sickle Cell Disease Remain Limited

Despite decades of research, treatment options for SCD remain limited. Treatment for SCD patients is often aimed at treating each symptom individually. Children with SCD are given penicillin and the PCV7 vaccine prophylactically to prevent infections. Patients are given NSAIDs and opioids to manage pain. Blood transfusion may be given to dilute the population of sickled RBCs with normal RBCs in cases of severe pain or crisis. This however carries the risk of iron overload and alloimmunization. There are currently only

two FDA-approved disease-modifying drugs for SCD, hydroxyurea and L-glutamine. Hydroxyurea works by increasing the expression of fetal hemoglobin in RBCs, which prevents hemoglobin polymerization [2]. L-glutamine works in part by increasing the RBC's antioxidant defenses [3]. One potential cure for the disease is bone marrow transplant from a non-SCD donor. This has been effective in a small number of cases, but for many patients a suitable matched donor is difficult to find and morbidity associated with graft-versus-host disease is a major concern. Thus, there is still ongoing research to better understand disease mechanisms and develop more effective therapies.

2.3 Sphingolipids Play Many Roles in RBC Biology

Sphingolipids have been shown to affect many RBC properties and processes. Thus, dysfunction of the sphingolipid metabolic system can result in widespread dysfunction in RBCs. Thus, sphingolipids may be an underappreciated therapeutic target in SCD.

2.3.1 Sphingoid Bases

One study showed that sphingosine inhibits the RBC plasma membrane calcium ATPase [4]. This would increase the RBC intracellular calcium concentration. This is consistent with other studies that showed that sphingosine increases intracellular calcium, causes cell shrinkage, causes phosphatidylserine surface exposure, and increases osmotic fragility [5, 6]. One study showed that sphingosine can increase the permeability of RBC ghost membranes to small ions [7]. This is consistent with another study that showed that sphingosine can induce the formation of small pores in RBC ghost membranes [8]. It it not known whether sphinganine can exhibit the same effects as sphingosine.

2.3.2 Sphingoid Base 1-Phosphate

One study showed that, unlike sphingosine, addition of exogenous SO1P does not cause increased intracellular calcium, cell shrinkage, or phosphatidylserine surface exposure [5]. However, when the SO1P exporter MFSD2B was knocked out, the concentrations of SO1P and SA1P in mouse RBCs increased dramatically [9]. This buildup causes stomatocytosis and hemolysis with SA1P being a stronger hemolytic agent than SO1P. A recent study showed that SO1P can bind to deoxygenated hemoglobin which promotes hemoglobin binding to the membrane [10]. This leads to release of membrane-anchored glycolytic enzymes, increased glycolytic flux, and an increase in 2,3-bisphosphoglycerate concentration. This decreases hemoglobin's affinity for oxygen, facilitates oxygen release, and prevents tissue hypoxia.

2.3.3 Ceramides

One study showed that ceramide can activate the RBC plasma membrane calcium ATPase [4]. Ceramide is thus antagonistic with sphingosine in its action on this protein. Another study showned that addition of ceramide to the outer leaflet of RBCs promotes flip-flop of other lipids in the membrane [11]. The same study showed that dihydroceramides do not exert the same effect. In contrast with sphingosine, ceramide is not capable of forming pores in RBC membranes [12]. The production of ceramide is involved in erythrocyte apoptosis (eryptosis) resulting from a wide array of stimuli including osmotic shock [13], and platelet-activating factor [14]. Ceramide production also plays a role in a novel form of erythrocyte necroptosis resulting from exposure to bacterial pore-forming toxins [15].

2.3.4 Sphingomyelins

Sphingomyelins constitute about 25% of the RBC phospholipids [16], so one of the major roles of sphingomyelin is as a structural component of the RBC membrane. Breakdown of sphingomyelin to ceramide in RBCs is a sufficient signal to promote phosphatidylserine (PS) exposure on the RBC surface, cell shrinkage, endovesiculation, membrane protein clustering, microparticle production, and adhesion to endlothelial cells [17, 18]. Breakdown of sphingomyelin also results in the leakage of RBC intracellular contents [19].

2.4 Sphingolipid Composition of Human RBCs is Only Partly Characterized

It is important to establish which sphingolipids have already been quantified in human red blood cells in the literature for multiple reasons. First, to establish where gaps in our current knowledge of RBC sphingolipid composition are. Second, to provide a basis for comparison with the sphingolipid composition of RBCs from SCD individuals. Different studies express sphingolipid concentrations in different units. In order to express concentrations in a common set of units we use the conversion factor of 1 mL of packed RBCs=10_{10} cells and express all concentrations as pmoles per mL of RBCs. The known fatty acyl side chain compositions of the major sphingolipids in red blood cells are summarized in Figure 1.

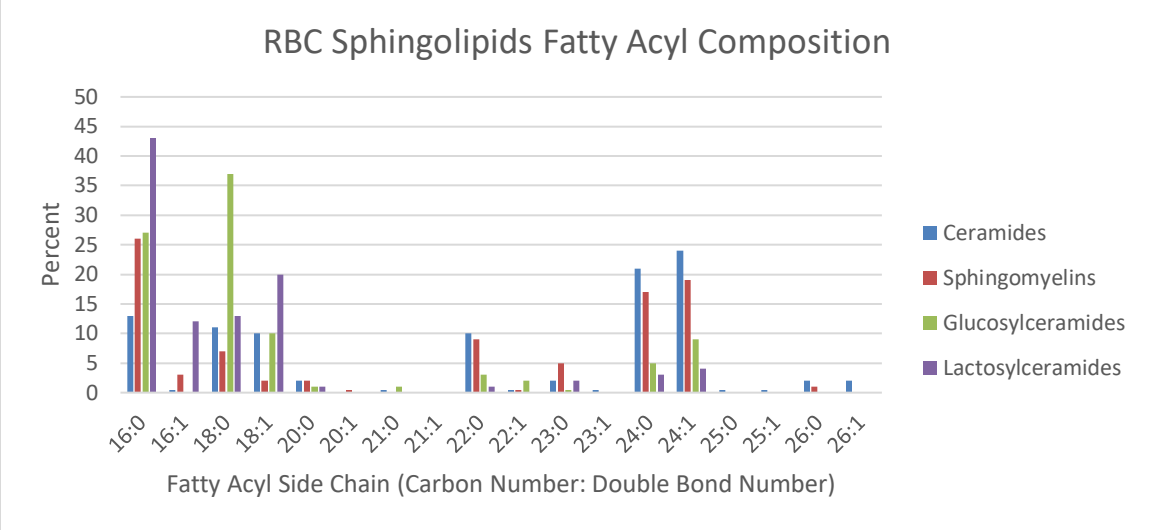

Figure 1. Known Fatty Acyl Side Chain Composition of Sphingolipids in Human Red Blood Cells

Values were taken from references described in the text. The figure is not inclusive of all minor species detected. It is important to notice that even classes of sphingolipids that are immediately adjacent in the sphingolipid metabolic network (see figure 2) do not have the same fatty acyl side chain distribution suggesting some bias in the enzymes that interconvert them.

2.4.1 Sphingomyelins

Sphingomyelins make up about 25 mole% of RBC phospholipids [16]. They have a total concentration in RBCs of about 1 μmol/mL of cells [16]. Multiple studies have reported on the fatty acyl side chain composition of sphingomyelins in RBCs [16, 20-23]. According to these studies, 16:0, 24:0, and 24:1 sphingomyelins are the major contributors to the sphingomyelin pool in human RBCs, together contributing over 60% of the pool. Other major contributors include 18:0, 22:0, and 24:2 sphingomyelins. Interestingly, the study by

Myher et al. also identified minor contributions for sphingomyelins with d16:1, d18:0, and d18:2 sphingoid backbones [23].

Multiple studies have measured the sidedness of sphingomyelin in RBCs by measuring the amount of sphingomyelin that is hydrolyzable by extracellular bacterial sphingomyelinase. These studies concluded that about 15% of RBC sphingomyelin is in the inner leaflet [22, 24, 25]. However, this has been challenged by the observation that upon treatment with bacterial sphingomyelinase, RBCs undergo endovesiculation, which protects internalized sphingomyelin from hydrolysis [26]. A more recent study estimated that about 98% of RBC sphingomyelin is in the outer leaflet [27]. Multiple studies have shown that sphingomyelin in the RBC membrane laterally segregates into microdomains [28-30]. These studies showed that sphingomyelin microdomains seem to disappear when the cells are stretched which may be relevant when RBCs squeeze through capillaries and splenic sinuses. Further, these studies showed that the sphingomyelin microdomains partly overlap with the microdomains of glycosphingolipids like glucosylceramide and GM1. The sidedness and lateral segregation of sphingomyelin may have important consequences for metabolism as the local concentration of sphingomyelin that sphingomyelinases are exposed to will be much higher than the average cell concentration.

2.4.2 Glycosphingolipids

A large number of glycosphingolipids have been identified in red blood cells including P antigen glycosphingolipids [31-37], I antigen glycosphingolipids [38-42], Lewis antigen glycosphingolipids [38, 43], ABO antigen glycosphingolipids [38, 39, 41, 42, 44-53] and

other gangliosides [31, 54-57]. There is also one study that identified sulfatide in red blood cells [58].

Multiple studies have reported concentration values for glycosphingolipids in RBCs [31, 32, 34-36, 59-61]. In RBCs, the globotetraosylceramide concentration is about 0.1 μmol/mL of cells, the GM3 concentration is about 0.004 μmol/mL of cells, the globotriaosylceramide concentration is about 0.01 μmol/mL of cells, the lactosylceramide concentration is about 0.02 μmol/mL of cells, and the glucosylceramide concentration is about 0.005 μmol/mL of cells. This adds up to about 0.14 μmol/mL of cells.

Multiple studies have investigated the fatty acyl composition of glycosphingolipids in RBCs [33, 34, 59]. These studies showed that the major species of globoteraosylceramide are 22:0, 24:0, and 24:1, contributing over 70% of the pool. The major species of globotriaosylceramide are 16:0, 24:0, and 24:1, contributing over 70% over the pool. The major species of lactosylceramide are 16:0, 18:0, and 18:1, contributing over 70% of the pool. The major species of glucosylceramide are 16:0 and 18:0, contributing over 60% of the pool.

Few studies have investigated the membrane sidedness of glycosphingolipids in RBCs. One early study using galactose oxidase to label outer leaflet glycosphingolipids showed that RBC glycosphingolipids are at least partly in the outer leaflet [62]. This study also suggested that these glycosphingolipids are party obscured by cell surface proteins. One study showed that the vast majority of the glycosphingolipid GM3 is located on the outer leaflet of RBCs [27]. Multiple studies have suggested that glycosphingolipids such as glucosylceramide and GM1 laterally segregate into microdomains in the RBC membrane

[28-30]. Further, these studies showed that the microdomains of glycosphingolipids like glucosylceramide and GM1 partially overlap with the microdomains of sphingomyelin. The sidedness and lateral segregation of glycosphingolipids may have important implications for metabolism as the local concentration of glycosphingolipids that enzymes are exposed to will be much higher than the average cell concentration.

2.4.3 Ceramides

The total concentration of ceramides in RBCs is about 0.05 μmol/mL of cells [59, 63]. These same studies also investigated the fatty acyl composition of the ceramide pool in RBCs. They determined that the major species of ceramide are 16:0, 18:0, 18:1, 22:0, 24:0, and 24:1, contributing about 90% of the pool. 20:0, 23:0, 26:0, and 26:1 ceramides have more minor contributions. Interestingly, one study also detected a small amount of ceramides with 2-hydroxy fatty acyl side chains as well as ceramides with 16:0 and 18:2 sphingoid backbones [63].

One study showed that ceramides flip flop between the leaflets of the RBC membrane on a timescale of minutes [64]. Thus, it is likely that ceramide is evenly distributed between the two leaflets under normal conditions. While the steady-state lateral membrane distribution of ceramides in RBC membranes is not known, multiple studies have shown that sphingomyelinase-generated ceramide aggregates into microdomains [17, 65-67].

2.4.4 Sphingoid Bases

Reported concentrations of d18:1 sphingosine in RBCs very widely. Example values include 3 pmol/mL of cells [68], 70 pmol/mL of cells [69], and 100 pmol/mL of cells [70].

This may reflect the very high turnover of d18:1 sphingosine in RBCs as determined partly by the high activity of sphingosine kinase 1(see next section). To the best of our knowledge, the concentration of d18:0 sphinganine has not been reported in human RBCs.

To the best of our knowledge, the membrane distribution of LCBs has not been reported in RBCs. One study that might lend some insight involved incorporating sphingosine into Dioleoylphosphatidylcholine (DOPC) vesicles [71]. When there was no pH gradient between the inside and outside of the vesicle, about half of the sphingosine was localized on the outer leaflet. In contrast, when the interior the vesicle was made acidic relative to the exterior media, all of the sphingosine was sequestered in the inner leaflet. This suggests that uncharged sphingosine is able to spontaneously flip-flop between the inner and outer leaflet of a membrane, but cationic sphingosine is not able to flip-flop.

2.4.5 Sphingoid Base 1-Phosphates

Reported concentrations of d18:1 sphingosine 1-phosphate in RBCs vary, though not to the extent of d18:1 sphingosine. Example values include 0.25 nmol/mL of cells [69], 1 nmol/mL of cells [70], 1.3 nmol/mL of cells [68], 2 nmol/mL of cells [72], and 2.3 nmol/mL of cells [73]. The concentration of d18:0 sphinganine 1-phosphate in human RBCs is about 600 pmole/mL of cells [74].

To the best of our knowledge, the membrane distribution of LCBPs has not been investigated in RBCs.

2.5 Sphingolipid Metabolic Reactions in RBCs are Poorly Characterized

It is important to establish which sphingolipid-metabolizing enzymes are present in RBCs because this will affect any interpretation of changes in sphingolipid concentrations associated with pathological conditions and because it will limit choices for enzyme inhibitors that can be used for therapeutic purposes. The known sphingolipid metabolic network in human RBCs is summarized in figure 2.

Despite the important roles of sphingolipids in RBC biology, the metabolic network connecting those sphingolipids is poorly characterized in RBCs. This is largely due to the fact that RBCs lose all of their organelles during differentiation. Many of the enzymes of sphingolipid metabolism are thought to be associated with specific organelles. For examples, serine palmitoyltransferase, 3-ketosphinganine reductase, ceramide synthase, dihydroceramide desaturase, S1P phosphatase, and S1P lyase have all been shown to be associated with the endoplasmic reticulum. Thus, it is possible that all of these enzymes are removed from RBCs during their terminal differentiation. However, this may not be the case as there have been counterexamples reported in the literature. For example, carnitine palmitoyltransferase, which is usually associated with mitochondria, has been detected in the mature RBC membrane [75]. In fibroblasts, S1P lyase, which is usually endoplasmic reticulum associated, has been found associated with the plasma membrane [76]. Thus, it is possible that sphingolipid metabolizing enzymes may be found in atypical places in the RBC.

To further complicate matters, enzymes that are not permanently associated with the RBC may still be able to act on RBC sphingolipids. Soluble acid sphingomyelinase, neutral sphingomyelinase, and sphingosine kinase 1 activity have been reported in the plasma [69, 77]. These enzymes may be able to latch onto the outer leaflet of the RBC membrane and

metabolize sphingolipids present there. Further, it is possible that enzymes present in the membranes of other cells may be able to metabolize sphingolipids in the RBC membrane. This idea is supported by a study showing that sphingomyelinase present in hen RBC membranes is capable of degrading sphingomyelin in human RBC membranes when the two are mixed together [78].

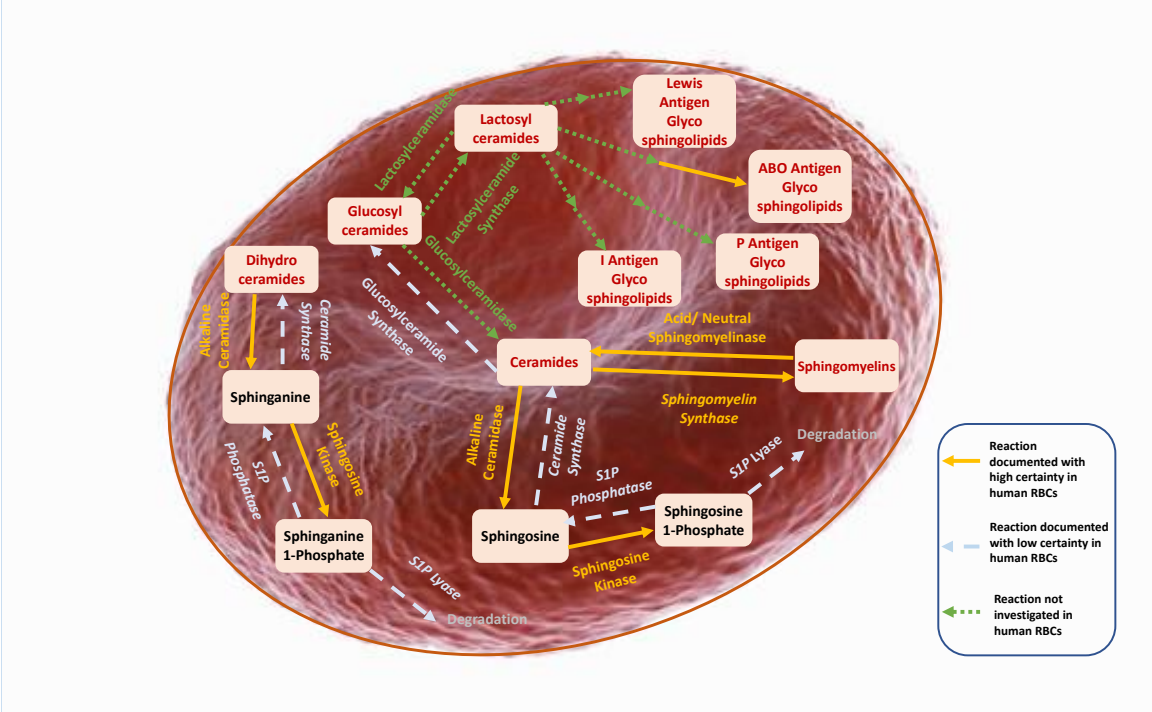

Figure 2. Known Sphingolipid-Metabolizing Enzymes in Human Red Blood Cells. Reactions that have been documented consistently in the literature are shown in yellow. Reactions that have been documented inconsistently in the literature are shown in blue. Reactions that have never been reported in the literature are shown in green.

2.5.1 Serine Palmitoyltransferase

Serine palmitoyltransferase (SPT) catalyzes the conversation of serine and palmitoyl-CoA into 3-ketosphinganine, CoA, and CO_2 which is the first step in de novo sphingolipid metabolism. SPT is the only enzyme in sphingolipid metabolism that has been detected in

RBCs by proteomic techniques [79]. SPT can actually be composed of multiple subunits, SPTLC 1, 2, and 3. Only SPTLC 1 and 2 have been detected in RBCs [79]. It is not known if this enzyme is active in RBCs and, if it is, what its activity level is. Further, since it is not known if the subsequent enzyme in sphingolipid de novo biosynthesis, 3-ketosphinganine reductase, is present in RBCs, it is not clear if SPT meaningfully contributes to the broader sphingolipid network.

2.5.2 Ceramide Synthase

Ceramide synthase catalyzes the conversion of sphingosine and fatty acyl-CoA to ceramide and CoA as well as sphinganine and fatty acyl-CoA to dihydroceramide and CoA. There are 6 known isoforms of ceramide synthase in mammals. The expression of ceramide synthases in RBCs is not clear. In one study where RBCs were incubated with ^{3}H-sphingosine, no conversion to ^{3}H-ceramide was detected [80]. In contrast, in other studies where RBCs were incubated with ^{14}C-fatty acids, incorporation of the fatty acids into ceramide, sphingomyelin, and glycosphingolipids could be detected [81, 82] One study where rat erythrocytes were incubated with ^{3}H-fatty acids showed incorporation into sphingomyelin [83].

2.5.3 Ceramidase

Ceramidase catalyzes the conversion of ceramides into sphingosine and dihydroceramides into sphinganine. There are 5 isoforms of ceramidase in mammals: acid ceramidase, neutral ceramidase, and alkaline ceramidase 1, 2, and 3. Early studies using heavy isotope tracers and activity assays did not detect any ceramidase activity in RBCs [70, 80] Another study did not detect any conversion of bacterial sphingomyelinase-generated ceramide to

sphingosine in RBCs [84]. However, the bacterial sphingomyelinase-generated ceramide was converted to sphingosine after addition of bacterial ceramidase to the RBCs. These results do not support the idea of an active ceramidase endogenous to the RBCs. However, a later report did detect alkaline ceramidase activity in mouse and human RBCs [85]. This report suggested that while RBC may possess activity for all 3 isoforms of alkaline ceramidase, alkaline ceramidase 3 may be dominant. This study also showed that systemic administration of an alkaline ceramidase inhibitor into mice reduced RBC SO and SO1P concentrations. While this reduction cannot uniquely be attributed to RBC alkaline ceramidase because the drug was administered systemically, the results may support a role for RBC alkaline ceramidase in regulating RBC sphingolipids. A recent report using an alkaline ceramidase 2 knockout mouse showed that RBC sphingosine and sphinganine are significantly reduced compared to a wildtype control [86]. While this reduction cannot uniquely be attributed to RBC alkaline ceramidase 2 because the experiment was done with a global knockout mouse, the results may support a role for RBC alkaline ceramidase 2 in regulating RBC sphingolipids.

2.5.4 Sphingosine Kinase

Sphingosine kinase (SK) catalyzes the conversion of sphingosine and ATP to sphingosine 1-phosphate and ADP as well as sphinganine and ATP to sphinganine 1-phosphate and ADP. SK is the only sphingolipid-metabolizing enzyme that has consistently been detected in enzyme activity [70, 72, 87] and tracer [70, 80, 88] studies in RBCs. Sphingosine kinase has 2 isoforms: SK 1 and 2. Sphingosine kinase 1 typically has a cytosolic/ plasma membrane localization while sphingosine kinase 2 typically has a nuclear localization. While it has been claimed that only sphingosine kinase 1 is present in RBCs due to the lack

of a nucleus [72], it should be pointed out that a report from our group detected both SK1 and SK2 in RBCs by western blot [69]. One study reported that SK activity in RBCs is increased by signaling through the adenosine pathway which causes phosphorylation of SK and movement of SK to the plasma membrane [87].

2.5.5 S1P Phosphatase/ Lipid Phosphate Phosphatases

S1P phosphatases and lipid phosphatase phosphatases (LPPs) can both catalyze the dephosphorylation of So1P and SA1P to SO and SA respectively. However, LPPs are less specific and can also dephosphorylate ceramide 1-phosphates and lysophosphatidydic acids [89]. Since these two groups of enzymes have overlapping activity, it can be difficult to distinguish them. The literature on S1P phosphatase/ lipid phosphate phosphatase activity in RBCs is somewhat inconsistent. One study did not detect any activity from these enzymes [70]. However, a later study using a more sensitive technique detected a small amount of activity from these enzymes [90]. It is not clear if this small amount of activity came from platelet/ leukocyte contamination or, even if it is genuine, if it has a significant impact on RBC sphingolipid metabolism.

2.5.6 S1P Lyase

S1P lyase catalyzes the irreversible degradation of SO1P and SA1P to (E)-2-hexadecenal and hexadecanal, respectively, and phosphoethanolamine. The literature on S1P Lyase in RBCs is somewhat inconsistent. One study did not detect any S1P lyase activity in RBCs [70]. However, a later study using a more sensitive assay did detect a small amount of S1P lyase activity in RBCs [90]. It is not clear is this small amount of activity came from

platelet/ leukocyte contamination or, if it is genuine, if it has a significant impact on sphingolipids metabolism in RBCs.

2.5.7 Sphingomyelinase

Sphingomyelinase catalyzes the hydrolysis of sphingomyelin into ceramide and phosphocholine as well as the hydrolysis of dihydrosphingomyelin into dihydroceramide and phosphocholine. There are multiple isoforms of sphingomyelinase including acid sphignomyelinase and multiple neutral sphingomyelinases. The literature on sphingomyelinase activity in RBCs is somewhat inconsistent. One study did not detect any neutral or acid sphingomyelinase activity in RBCs [91]. However, multiple studies have detected sphingomyelinase activity in RBCs in response to a variety of stimuli although the studies often did not clarify which isoform is active [13, 14, 67]. A study that utilized an acid sphingomyelinase knockout mouse showed significant, but not complete, reduction in RBC ceramide compared to the wildtype control [92]. While this effect cannot uniquely be attributed to RBC acid sphingomyelinase because it was a global knockout, the results may support the importance of RBC acid sphingomyelinase in regulating RBC sphingolipids. Another study detected neutral sphingomyelinase activity in RBCs whose activity seems to be dependent on the membrane bending of the RBCs [93]. A study from our lab detected acid sphingomyeinase and a small amount of neutral sphingomyelinase in RBCs [69]. To further confuse the identification of the sphingomyelinase associated with RBCs, it has been shown that acid sphingomyelinase can act at neutral pH if the membrane that it is attached to has been oxidized or hydrolyzed by phospholipase A2 [94].

2.5.8 Sphingomyelin Synthase

The literature on sphingomyelin synthase in RBCs is not entirely consistent. Early studies where RBCs were incubated with ^{3}H-ceramide did not detect any sphingomyelin synthase activity [80, 95, 96]. Later reports did identify recovery of sphingomyelin concentration after activation of sphingomyelinase in RBCs, suggesting sphingomyelin synthase activity [13, 14, 67, 93]. In other studies where RBCs were incubated with ^{14}C-fatty acids, incorporation of the fatty acids into sphingomyelin could be detected [81, 82]. In one study where RBCs were incubated with NBD-dihydroceramide, conversion into NBD-dihydrosphingomyelin was detected [97]. One study where rat erythrocytes were incubated with ^{3}H-fatty acids showed incorporation into sphingomyelin which indicates the presence of sphingomyelin synthase [83].

2.5.9 Glucosylceramide synthase

Glucosylceramide synthase (GCS) catalyzes the conversion of ceramide and UDP-glucose to glucosylceramide and UDP. There is limited data in the literature on GCS in RBCs. One study where RBCs were incubated with ^{3}H-ceramide did not detect incorporation into glycosphingolipids [96]. Another study where RBCs were incubated with ^{14}H-fatty acids did detect incorporation into glycosphingolipids [82]. Another study where RBCs were incubated with NBD-dihydroceramide did not detect conversion into glycosphingolipids [97].

2.5.10 Glucosylceramidase

To our knowledge there have not been any studies investigating glucosylceramidase (GCDase) activity in RBCs. However, β-glucosidase activity has been detected in RBCs [98]. Glucosylceramidase is included in the family of β-glucosidases. One area of research

that might offer guidance is the study of Gaucher disease which is a genetic deficiency of glucosylceramidase 1. RBC glucosylceramide is significantly elevated in individuals with Gaucher disease [61, 99]. While this does not necessarily provide evidence of GCDase in RBCs because Gaucher disease is results in the global absence of GCDase, it could support the presence of GCDase in RBCs.

Given the uncertainty around which sphingolipid-metabolizing enzymes are present in RBCs and/or act on RBC sphingolipids, it is entirely possible that some sphingolipids detected in RBCs under homeostatic conditions are not actively been turned over. In other words, these sphingolipids may have been biosynthesized early in the differentiation of the erythroid cells and simply reside in the RBC membrane throughout its lifespan.

2.6 Changes in Red Blood Cell Sphingolipid Metabolism Have Been Observed in Sickle Cell Disease

Several studies have identified changes in the concentrations of sphingolipids and the activities of sphingolipid-metabolizing enzymes in sickle cell erythrocytes and plasma. Figure 3 summarizes the known changes in red blood cell and plasma sphingolipid metabolism.

A study from our group showed that the activity of both neutral and acid sphingomyelinase as elevated in plasma and erythrocytes from sickle individuals [69]. This study furthered showed increased levels of circulating microparticles, which may be the result of sphingomyelinase-mediated membrane vesiculation. These results are consistent with another study which showed elevated neutral sphingomyelinase activity in serum of sickle individuals [100]. This study also showed decreases in the concentrations of serum

sphingomyelins and ceramides. Taken together, these results suggest that erythrocyte sphingomyelin levels may decrease through increased hydrolysis though sphingomyelinase and decreased influx of sphingomyelin from plasma. To our knowledge, measurements of erythrocyte sphingomyelins in sickle cell have not been reported. While measurements of human erythrocyte ceramides in sickle cell have not been made, erythrocytes from a mouse model of sickle cell show higher levels of ceramides [101]. This is consistent with the higher sphingomyelinase activity observed in erythrocytes and plasma [69, 100].

Multiple studies have demonstrated elevated sphingosine kinase activity in human sickle red blood cells and in red blood cells from a mouse model of sickle cell disease [72, 87]. This is concurrent with an increase in the concentration of SO1P in red blood cells [69, 72, 101] and plasma [69, 72, 101]. A study from our group also demonstrated elevated concentrations of sphingosine in red blood cells and plasma [69]. It has been shown that the elevation of sphingosine kinase activity is caused by elevated plasma adenosine in sickle cell [87]. It has been shown that the elevation in red blood cell SO1P contributes to increased sickling, at least in a mouse model of the disease [72]. It has later shown that SO1P can bind to deoxyhemoglobin and enhance its binding to the cell membrane [101]. This increased the flux of glucose though glycolysis, increases 2,3-bisphosphoglycerate concentration, and further decreases binding of oxygen by hemoglobin.

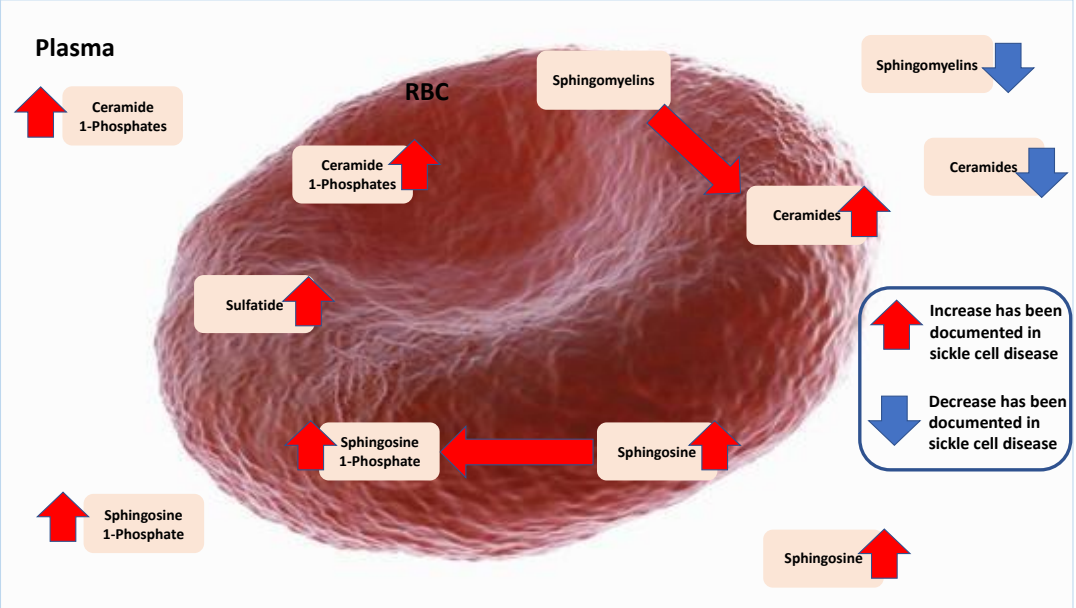

Figure 3. Known Changes in Red Blood Cell Sphingolipid Metabolism in Sickle Cell Disease. Increases in sphingolipid concentration or enzyme activity in SCD are shown by red arrows. Decreases in sphingolipid concentration or enzyme activity in SCD are shown by blue arrows.

CHAPTER 3. INTEGRATION OF BIOCHEMICAL AND BIOPHYSICAL INFORMATION TO PREDICT THE BEHAVIOR OF SPHINGOSINE 1-PHOPSHATE METABOLISM IN RED BLOOD CELLS

3.1 Abstract

Sphingosine 1-phosphate is a bioactive lipid that plays many roles in the blood including regulating endothelial barrier function and regulating energy metabolism in red blood cells. Red blood cells are the largest reservoir of sphingosine 1-phosphate in the blood and also produce about 50% of plasma sphingosine 1-phosphate. It has also been shown that blood levels of sphingosine 1-phosphate are altered in diseases like sickle cell disease and malaria. Despite the importance of sphingosine 1-phosphate in the blood, it is not fully understood how its concentration is regulated. In this study, we constructed a computational model of red blood cell sphingosine 1-phosphate metabolism combining the biophysical and biochemical aspects of sphingosine 1-phosphate metabolism. We validated the performance of the model against data on red blood cell sphingosine 1-phosphate metabolism in vitro. Our results show that red blood cell and plasma sphingosine 1-phosphate concentrations are very sensitive to changes in red blood cell ceramide concentration, hematocrit, and red blood cell sphingosine kinase activity. These results are significant because all three of these variables are altered in sickle cell disease. Thus, our results can help guide the development of more effective treatments for sickle cell disease.

3.2 Introduction

Sphingosine 1-phosphate (SO1P) is a bioactive lipid that plays many roles in the blood. These include maintaining vascular barrier integrity [102], regulating the trafficking of lymphocytes between body compartments [103], and regulating the trafficking of stem cells between body compartments [104]. It has been shown that SO1P also regulates the binding of hemoglobin to the red blood cell (RBC) membrane which regulates RBC energy metabolism [10]. Recently, it was shown that the concentration of SO1P is significantly elevated in the RBCs and plasma of individuals with sickle cell disease (SCD) [69, 72]. Further, it has been shown that SO1P is significantly lowered in the serum of individuals with malaria [105]. Thus, the regulation of the concentration of SO1P in RBCs and in plasma is important in both physiologic and pathologic contexts.

In blood, the majority of SO1P is stored in RBCs, with lesser amounts being stored in platelets and plasma [70] . Studies using mice have suggested that about 50% of plasma SO1P comes from red blood cells with the remainder primarily coming from endothelial cells [106]. Under pathological conditions involving platelet activation, platelets can also contribute significantly to plasma SO1P concentration [80]. Despite the important role of RBCs in storing and releasing SO1P in blood, the details of how RBC SO1P metabolism is regulated remain incompletely understood although some components are known. It has been shown that RBCs possess sphingosine kinase 1 activity capable of producing SO1P from its precursor sphingosine (SO) [70, 80]. Sphingosine kinase 1 can be activated through the adenosine signaling pathway [87]. It was recently been shown that the transporter responsible for exporting SO1P from RBCs is the protein MFSD2B [9]. It has also been shown that various plasma components including albumin and HDL are capable

of extracting SO1P from RBCs [73, 74]. Despite having information on these individual components, we do not understand how the integrated system regulates the concentration of RBC and plasma SO1P.

In individuals with SCD, hematocrit (volume percentage of RBCs in blood) is significantly reduced. Further, it has been shown that sphingosine kinase 1 activity is significantly elevated in SCD RBCs [72]. Finally, it has been shown that the activities of neutral and acid sphingomyelinase, which produce ceramide from sphingomyelin, are significantly elevated in SCD RBCs [69]. However, it is not clear how important each of these factors is in determining the overall increase in SO1P concentration in SCD. In this study, we investigated the relative importance of these three factors in determining the concentrations of SO1P in RBCs and plasma. To do this, we constructed and validated a computational model of RBC SO1P metabolism in vitro. Our results show that RBC and plasma SO1P concentrations are sensitive to changes in RBC ceramide concentration, hematocrit, and red blood cell sphingosine kinase activity. Further, our results suggest that that changes in RBC ceramide concentration may have the most influence in the context of SCD.

3.3 Results

3.3.1 Construction of a mathematical model RBC SO1P metabolism in vitro

We constructed a mathematical model of RBC SO1P metabolism that includes all parts of this metabolic system that are currently known. First, SO reversibly exchanges between plasma and the RBC membrane outer leaflet. Then, SO reversibly flip-flops between the two leaflets of the RBC membrane. SO is phosphorylated to SO1P by sphingosine kinase

1. The sphingosine kinase 1 reaction is activated by membrane phospholipids, especially phosphatidylserine. SO1P is dephosphorylated back to SO by S1P phosphatase or irreversibly degraded by S1P lyase. Inner leaflet SO1P is transported to the outer leaflet by MFSD2B. Outer leaflet SO1P can spontaneously flip back to the inner leaflet. Outer leaflet SO1P also reversibly exchanges with plasma. Finally, inner leaflet SO is produced from the deacylation of ceramide by alkaline ceramidases. A network map representation of the system is given in Figure 4. All enzymatic reaction rates were described by Michaelis-Menten-type equations. All biophysical process rates were described by mass action equations. The full details of the how the model equations and parameter values were decided upon are described in the methods section.

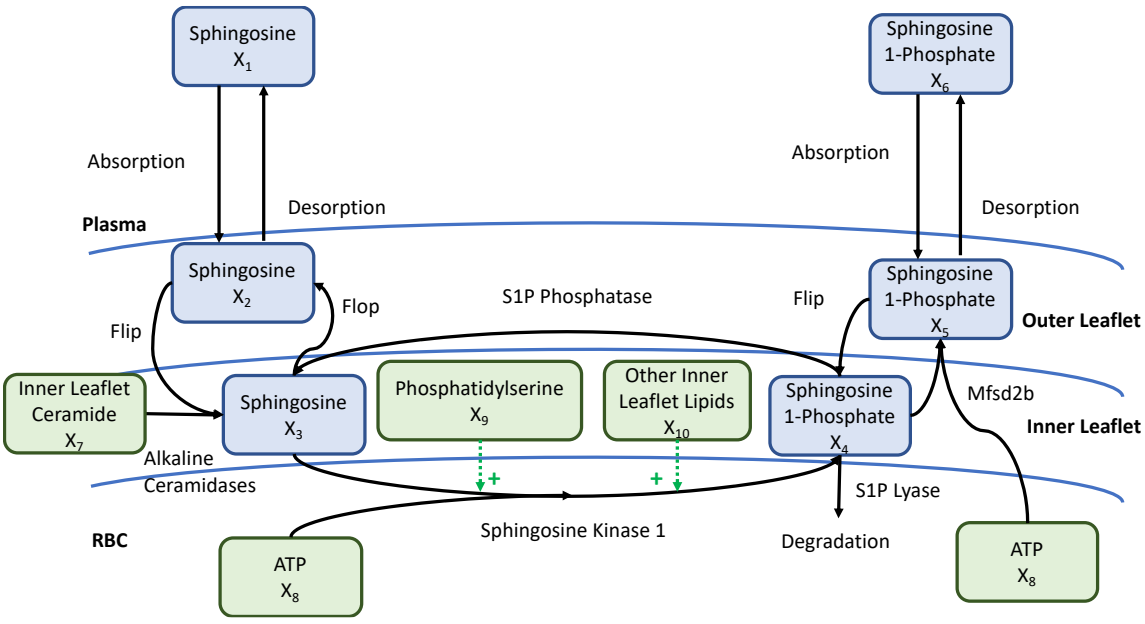

Figure 4. A Mathematical Model of RBC SO1P Metabolism was Constructed Using Known Network Structure. Independent variables, whose values do not change during a given experiment, are shown in green boxes. Dependent variables, whose values do change during a given experiment, are shown in blue boxes. Activation of a process is shown by a

green dotted arrow with a plus sign. Reactions or processes are represented by black arrows.

We first evaluated the ability of our model to fit three different data sets from one study [74]. We optimized the values of the model parameters to each data set by using a constrained nonlinear optimization algorithm. The full details of the algorithm are given in the methods section. For each data set, the optimization algorithm produced 100 optimized parameter sets from which the parameter set with the lowest sum of squared errors was used for further simulations. In the first experiment, described in Hanel et al. 2007, Figure 2, human RBCs were incubated with human plasma at 50% hematocrit for 6 hours. Plasma SO1P concentration was measured at different time points during the incubation. We will refer to this data set as Data Set 1. The optimized fit of the model to this data set is shown in Figure 5.

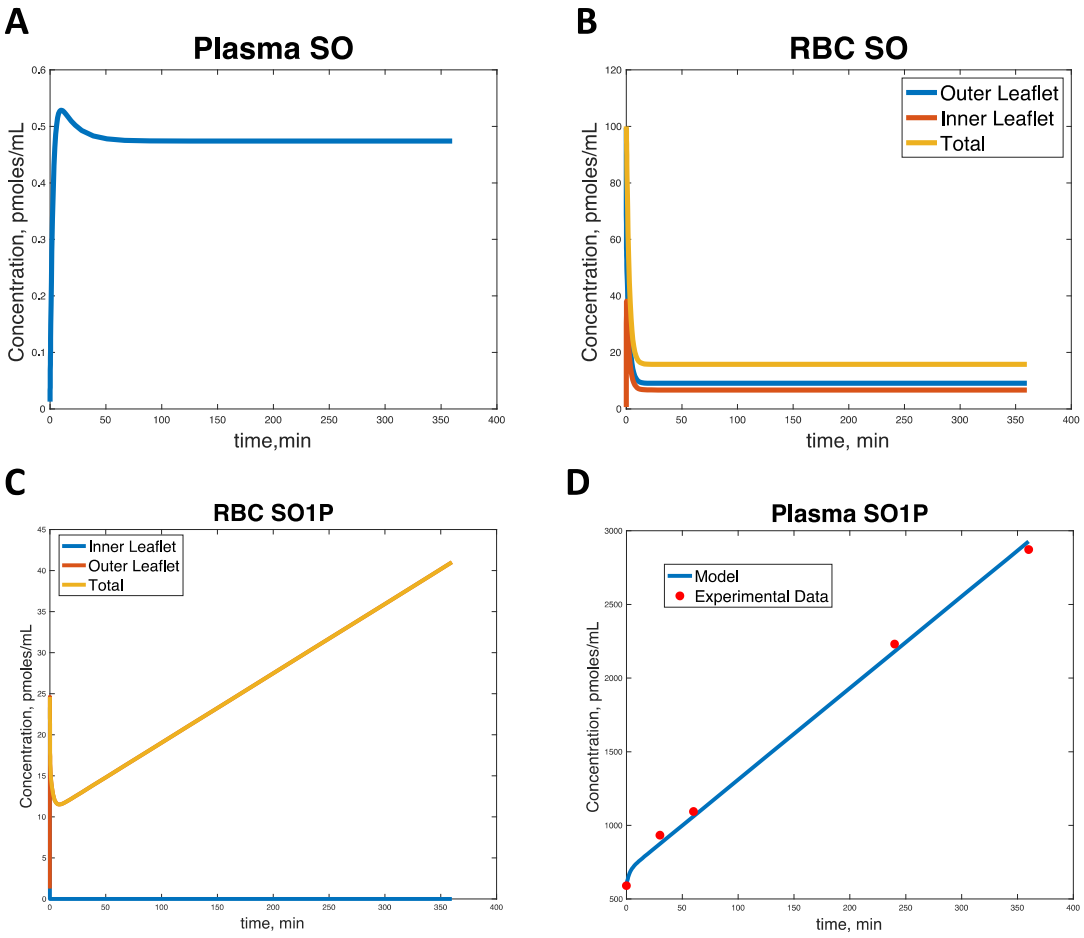

Figure 5. The RBC SO1P Metabolism Model was Fit to Data Set 1. A) Model simulation of plasma SO concentration. B) Model simulation of RBC SO concentration. C) Model simulation of RBC SO1P concentration. D) Model simulation of plasma SO1P concentration.

In the second experiment, described in Hanel et al. 2007, Figure 4A, human RBCs and plasma were incubated at volume ratios of 1:1, 1:2, 1:4, 1:8, and 1:16 for 6 hours. Plasma SO1P concentration was measured at different time points during the incubations. We will refer to this data set as Data Set 2. The optimized fit of the model to this data set is shown in Figure 6.

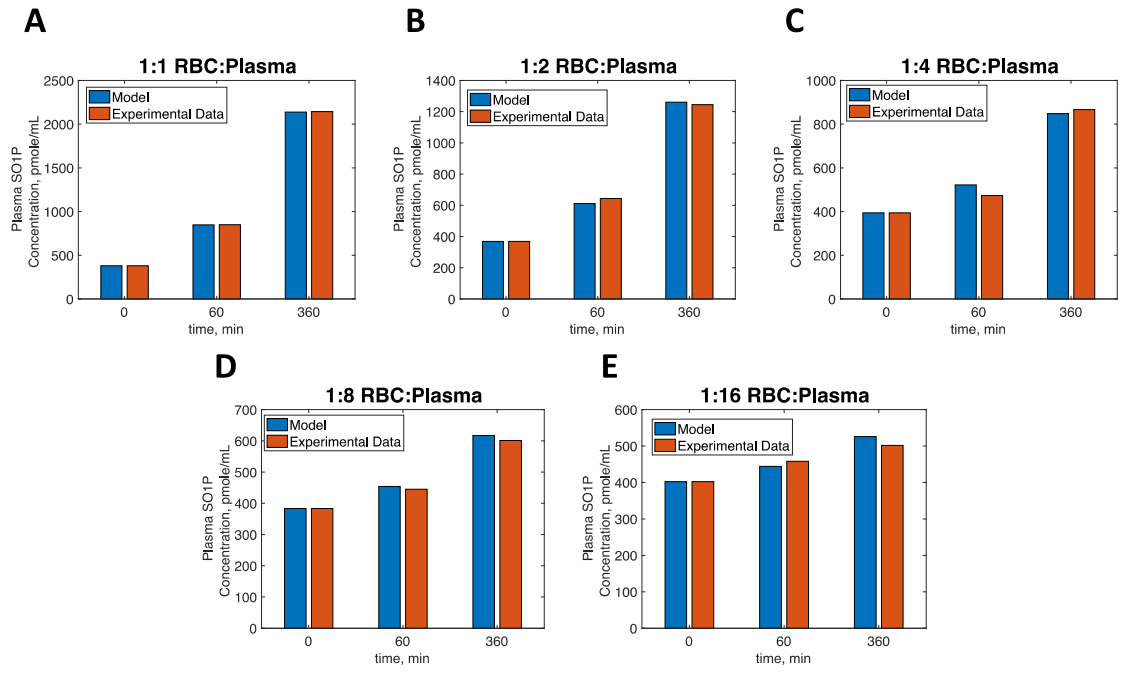

Figure 6. The RBC SO1P Metabolism Model was Fit to Data Set 2. Computational model was simultaneously fit to plasma SO1P concentration data for RBCs and plasma incubated at volume ratios of A) 1:1 B) 1:2 C) 1:4 D) 1:8 E) 1:16.

In the third experiment, described in Hanel et al. 2007, Figure 4B, RBCs and plasma/media were incubated at 50% hematocrit for 6 hours. The plasma was mixed with RPMI media to make plasma percentages of 25%, 50%, 75%, and 100%. Plasma/media SO1P concentration was measured at different time points during the incubations. We will refer to this data set as Data Set 3. The optimized fit of the model to this data set is shown in Figure 7.

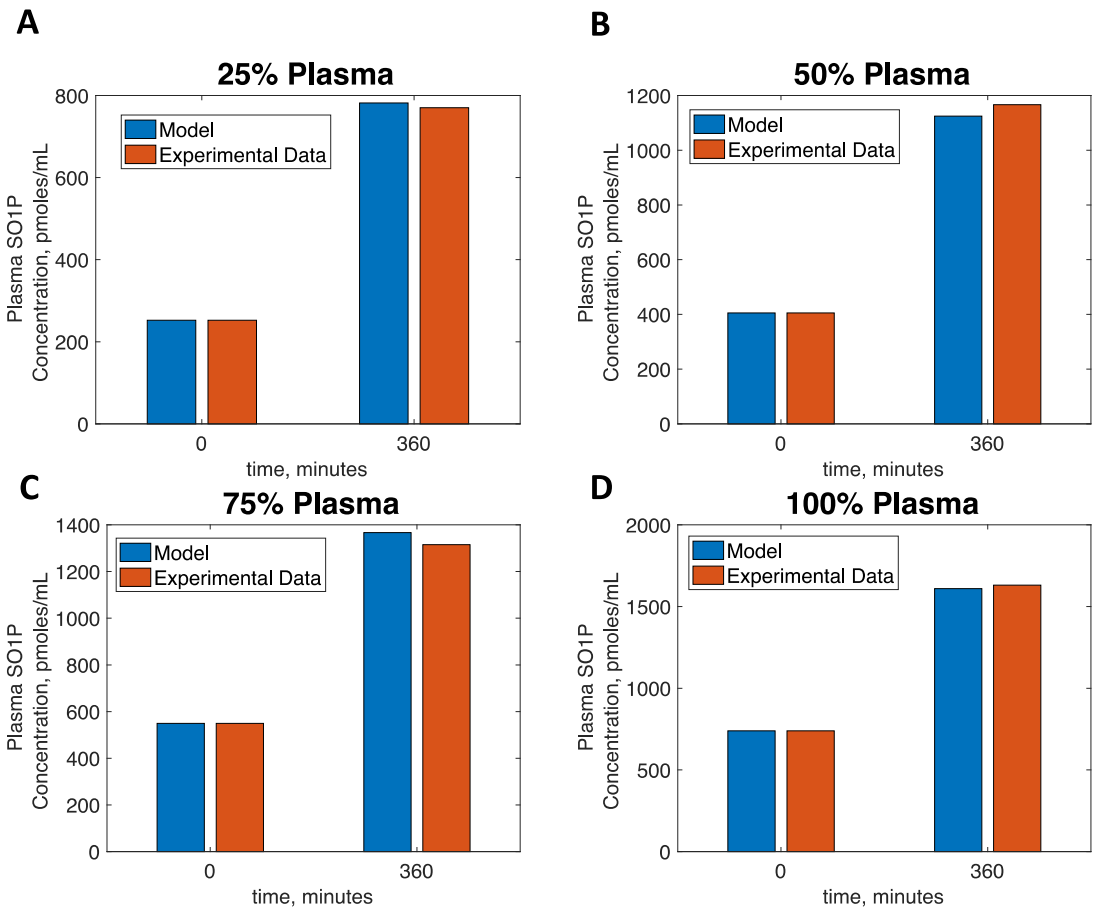

Figure 7. The RBC SO1P Metabolism Model was Fit to Data Set 3. Computational model was simultaneously fit to plasma SO1P concentration data for RBCs incubated at 50% hematocrit with plasma mixed with media to make plasma percentages of A) 25% B) 50% C) 75% D) 100%.

In order to ensure that similar parameter sets are able to provide good model fits to all three data sets, we used principal component analysis to visualize the 100 optimized parameters fits for each data set together in principal component space. The parameter set taken from literature values was also included for comparison. The results of this analysis are shown in Figure 8. As Figure 8 shows, the is almost complete overlap of the optimized parameter sets for all three data sets in one cluster. Examining the loadings of principal component 1, it can be seen that the most significant contributors to that principal component are the

initial concentrations of RBC SO and RBC SO1P. Examining the loadings of principal component 2, the most significant contributors to that principal component are the initial concentration of RBC SO and one of the parameters controlling the rate of exchange of SO1P between the RBC membrane and plasma, $k_{6,5}$. The best-fit parameter values for all three data sets are given in Table 1 with the parameter set taken from literature for comparison. In order to decide on a parameter set to use for further model predictions, we evaluated the total sum of squared errors for all three data sets when using each of the three best-fit parameter sets. The total sum of squared errors for all three data sets for each of the best-fit parameter sets are $5.34*10_6$ for best-fit parameter set 1, $2.24*10_6$ for best-fit parameter set 2, and $3.80*10_6$ for best-fit parameter set 3. Thus, we used best-fit parameter set 2 for model predictions.

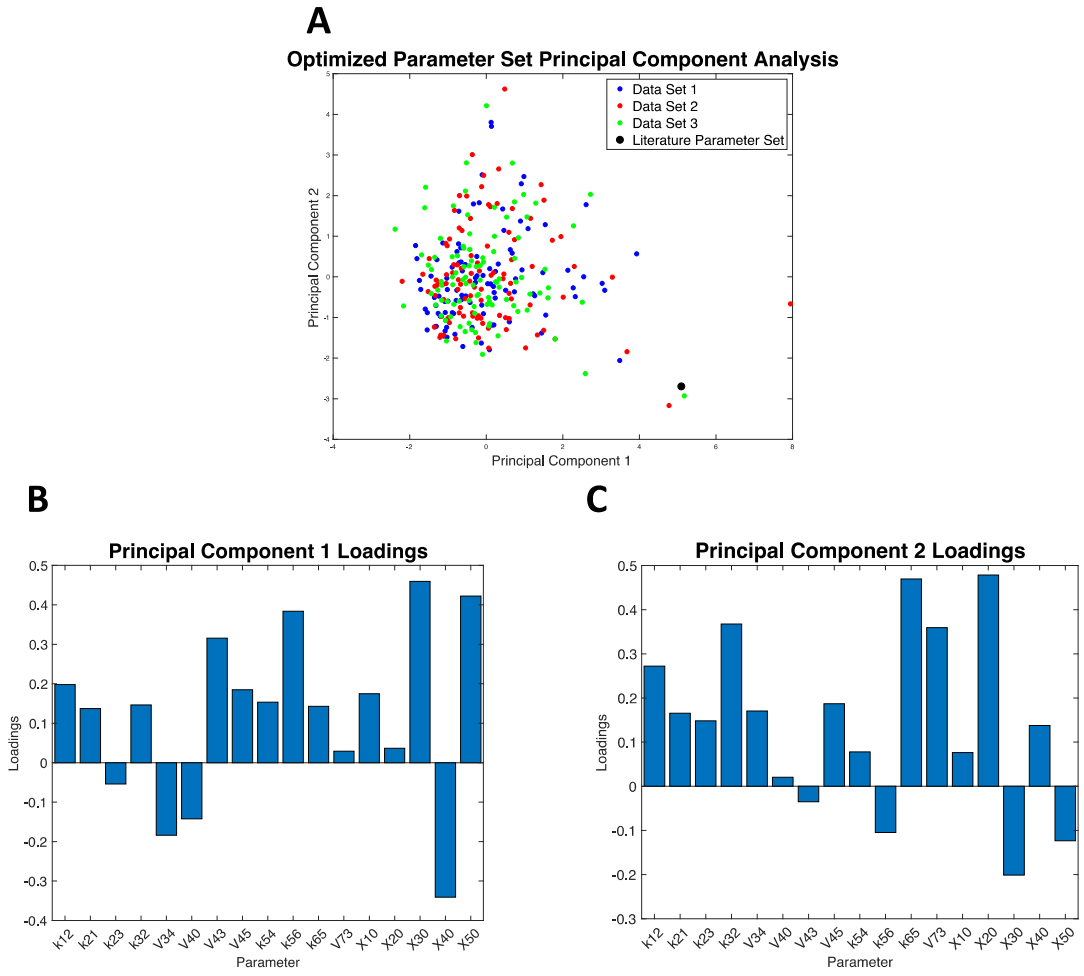

Figure 8. Principal Component Analysis was Performed on the 100 Optimized Parameter Sets for Each Data Set. A) The 100 optimized parameter sets for each of the three data sets as well as the parameter set derived from literature were plotted in principal component space. Parameter sets for data set 1 are given in blue, parameter sets for data set 2 are given in red, parameter sets for data set 3 are given in green, and the literature data set is given in black. B) The loadings of each model parameter in principal component

1 were calculated. C) The loadings of each model parameter in principal component 2 were calculated.

Table 1. The Best-Fit Values of Model Parameters for All Three Data Sets Were Determined Through Nonlinear Optimization

Parameter Name	Literature Value	Best-Fit Value for Data Set 1	Best-Fit Value for Data Set 2	Best-Fit Value for Data Set 3	Units
Mean Square Error	Data Set 1: 781,000 Data Set 2: 108,000 Data Set 3: 72,900	808.6	1,681.2	1,258.3	pmole/mL
$k_{1,2}$	1.39	0.03064535	0.01435555	0.01687903	$min^{-1}mL^{-1}$
$k_{2,1}$	0.01	0.00722663	0.10449552	0.09597118	$min^{-1}mL^{-1}$
$k_{2,3}$	2.77	98.6063044	0.05992106	0.02775253	min^{-1}
$k_{3,2}$	2.77	88.7642583	0.18061132	207.619465	min^{-1}
$V_{3,4}$	10,200	116,098.952	102.065064	185,903.232	pmole/min/mL

$V_{4,0}$	0.0068	0.01620506	0.00656226	0.43415209	pmole/min/mL
$V_{4,3}$	0.0198	0.0166201	0.05874975	0.67541816	pmole/min/mL
$V_{4,5}$	11,900	4,976.86366	12,583.4054	48,4215.764	pmole/min/mL
$k_{5,4}$	0.00083	0.0021011	9.11E-06	6.18E-05	min^{-1}
$k_{5,6}$	1.023	0.40399136	0.03307294	0.06029206	$min^{-1}mL^{-1}$
$k_{6,5}$	1.39	0.55610986	0.0289528	0.01391022	$min^{-1}mL^{-1}$
$k_{7,3}$	57.8	608.947961	2,069.94733	2.26212189	pmole/min/mL
$X_{1,0}$	100	1.45274271	47.0444719	4.78161073	pmole/mL
$X_{2,0}$	50	93.9102973	0.00333579	56.4719848	pmole/mL
$X_{3,0}$	50	0.93935367	0.03391118	1.16529494	pmole/mL
$X_{4,0}$	1000	1,129.42461	948.587869	1,222.15931	pmole/mL
$X_{5,0}$	1000	0.82825168	51.5637221	2.01976342	pmole/mL

3.3.2 Model Predictions

Once we were confident that the model could simulate the behaviour of the system under multiple experimental conditions with similar parameter values, we investigated the

sensitivity of the steady-state in vitro RBC and plasma SO1P concentrations to changes in critical model parameters. It has been shown that in SCD, hematocrit is decreased, sphingosine kinase activity is increased [72], and ceramide concentration is increased [101]. We evaluated the steady-state concentrations of RBC and plasma SO1P in vitro as functions of these three parameters. The results are shown in Figure 9. Figure 9A and B show that as the hematocrit drops from a normal value of 45% to a typical SCD value of 25%, the RBC SO1P concentration drops from 3,192 to 1,335 pmole/mL and the plasma SO1P concentration drops from 3,641 to 1,522 pmole/mL. Figure 9C and D show that as the sphingosine kinase 1 activity rises 50%, which is typical of SCD, the RBC SO1P concentration rises from 3,850 to 5,117 pmole/mL and the plasma SO1P concentration rises from 4,392 to 5,838 pmole/mL. Figure 9E and F show that as the concentration of ceramide increases by 300%, which is typical of SCD [101], the RBC SO1P concentration rises from 3847 to 9433 pmole/mL and the plasma SO1P concentration rises from 4,392 to 10,761. We also estimated the sensitivities of RBC and plasma SO1P to these three parameters numerically. The results are given in Table 2. As the table shows, both concentrations are more sensitive to changes in hematocrit than the other 2 parameters. However, when we take into account the fact that the percent changes in both hematocrit and sphingosine kinase 1 activity in SCD are only about 50% while the percent change in RBC ceramide concentration in SCD is 300%, the increase in ceramide concentration in SCD ultimately has a bigger effect.

Table 2. Sensitivities of RBC and PLA SO1P Concentrations were Estimated

	Hematocrit	Sphingosine Kinase 1 Activity	RBC Ceramide Concentration
RBC SO1P Concentration	1.737	0.710	0.793
Plasma SO1P Concentration	1.982	0.809	0.905

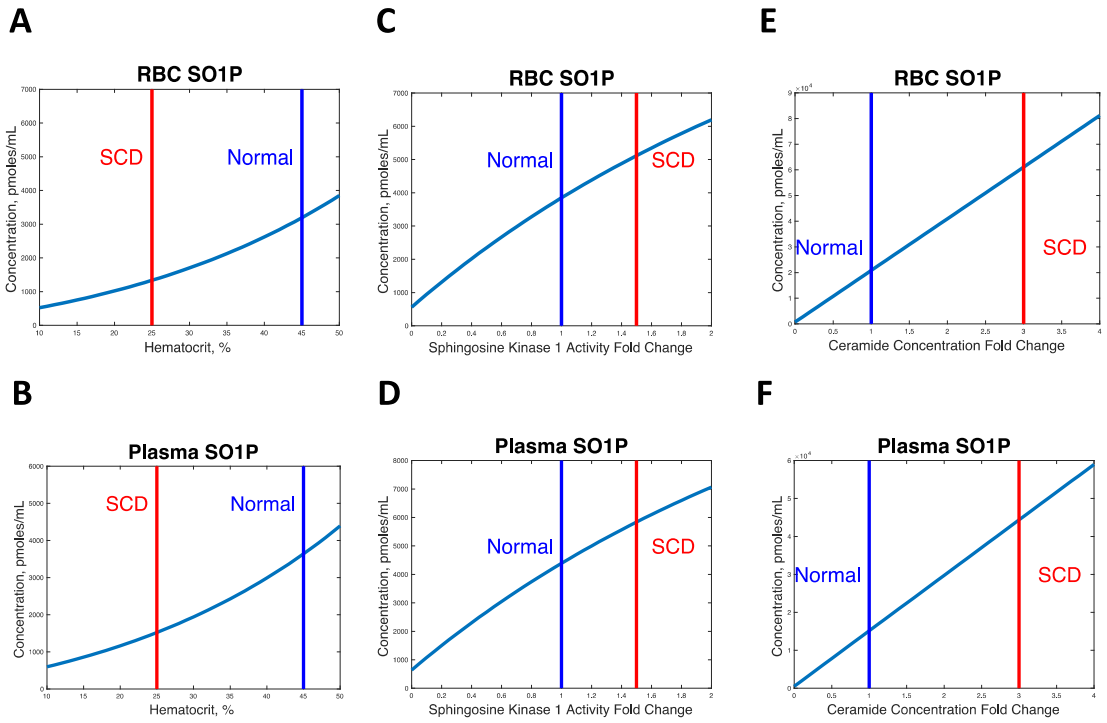

Figure 9. Dependency of RBC and Plasma SO1P Concentrations on Model Parameters was Estimated. The dependency of the in vitro steady-state RBC SO1P concentration on A) hematocrit, C) sphingosine kinase activity, and E) RBC ceramide concentration were estimated. The dependency of the in vitro steady-state plasma SO1P

concentration on B) hematocrit, D) sphingosine kinase, and F) RBC ceramide concentration were estimated. The best-fit parameter sets for data set 2 was used in this analysis.

3.4 Discussion

We have constructed and validated a computational model of RBC SO1P metabolism in vitro using known biochemical and biophysical aspects of the system. The construction of the model was illuminating as it made clear which details of this system are known and which are not. For example, fundamental biophysical parameters for SO and SO1P such as partition coefficients and transbilayer diffusion rates have not been reported and had to be estimated by indirect methods. Thus, there is still a need for experimental investigation of these details. Further, the distributions of SO and SO1P between RBC membrane leaflets has never been reported. Thus, model predictions of concentrations of SO and SO1P in individual leaflets could not be directly validated and further experimental work in this area is needed.

The first major result of our modeling study is that plasma and RBC SO1P concentrations are very sensitive to changes in hematocrit. Our model predicts that as the hematocrit drops from the physiologic range of 40-45% hematocrit to levels seen in SCD (20-25%), the RBC and plasma SO1P concentrations are expected to drop by about 50%. This result is consistent with data from normal and non-sickle anemic individuals [73, 107]. However, RBC and plasma SO1P concentrations increase in SCD [69]. Thus, other changes affecting the metabolic network must occur to outweigh the decrease in concentration caused by anemia.

Another key result of this study is that the concentrations of RBC and plasma SO1P are very sensitive to changes in the concentration of RBC ceramide. The total concentration of ceramide in human RBCs has been estimated to be about 50 μM [63]. It has been shown that RBCs possess the capacity to synthesize ceramide from sphingomyelin through neutral sphingomyelinase [93] and acid sphingomyelinase [69]. The RBC neutral sphingomyelinase seems to be activated by membrane bending. Acid sphingomyelinase activity can be released into circulation by endothelial cells during inflammation [108]. Because SCD is characterized by significant mechanical deformations of the RBC membrane and chronic inflammation, we expect both of these enzymes to increase RBC ceramide. Indeed, we have previously shown that the activities of both sphingomyelinases are increased in SCD RBCs [69]. RBCs also possess sphingomyelin synthase activity which can reversibly convert ceramide to sphingomyelin [93]. The physiologic role of sphingomyelin synthase in RBCs and whether or not sphingomyelin synthase activity is altered in SCD are not currently known. Ceramide can also be deacylated to sphingosine by alkaline ceramidases in RBCs [85]. As noted previously in this study, these enzymes are very sensitive to intracellular calcium concentrations. While the steady-state concentration of free calcium in RBCs is maintained at very low levels, it has been shown that RBC calcium concentration transiently increases in response to a variety of stimuli [109, 110]. This would result in transiently higher activity of alkaline ceramidase. To support the importance of ceramidase in maintaining RBC and plasma SO1P concentrations, it has been shown that when alkaline ceramidase 2 is knocked out in mice, the RBC and plasma SO1P concentrations drop by more than 50% [86]. It has been shown that the calcium concentration in SCD RBCs is significantly higher than in normal RBCs

[111]. Thus, we expect that alkaline ceramidase activity to be higher in SCD RBCs than in normal RBCs and to contribute to the increase in RBC and plasma SO1P concentrations.

Another key result of our study is that the concentrations of RBC and plasma SO1P are sensitive to changes in sphingosine kinase 1. It has been shown that under conditions of sphingosine kinase 1 knockout, the SO1P concentration in RBCs drops to near-zero and the plasma SO1P concentration drops by half [101]. The fact that plasma SO1P only drops by half with sphingosine kinase 1 knockout is likely due to the activity of sphingosine kinase 2, which is present in other cell types such as endothelial cells [106]. These other sources of plasma SO1P are outside the scope of our current model which is restricted to RBCs and plasma in vitro. It has been shown that the RBC and plasma concentrations of SO1P are elevated in individuals with SCD and in a mouse model of SCD [69, 72]. It has further been shown that the activity of sphingosine kinase 1 increases by about 50% in SCD RBCs compared to normal RBCs [87]. Our modeling results are consistent with these observations.

In conclusion, our model which incorporates the known biochemical and biophysical details of RBC SO1P metabolism has allowed us to determine the relative importance of different variables known to be significantly altered by transient physiologic stresses and under pathological conditions. This will allow us to design more effective therapeutic strategies in sickle cell disease and other contexts where RBC SO1P is important.

3.5 Methods

3.5.1 Model Construction

When parameterizing the rate equations, we needed to convert parameters and concentrations into a single set of units. It has been shown that the rates of lipid metabolic reactions depend on the interfacial concentrations lipids, not the bulk concentrations. Therefore, lipid enzyme kinetic parameters are often reported in units of mole% of interfacial molecules. When expressing cellular lipid concentrations, different units are used including lipid per cell, per unit DNA, per unit protein, and per unit lipid phosphate. Thus, some unit conversion is necessary. We chose to convert all model parameters and outputs into units of pmole/mL of cells because this is the units that the experimental data are expressed in. To do this, we assume that the RBC concentration of phospholipid is about 4 μmol/mL of cells [16, 112], the molar ratio of cholesterol to phospholipid in RBC membranes is about 0.8 [16], giving a total of 7.2 μmol total lipid/mL of cells. Based on these values, we used the following conversion factor to convert x mole% to y pmoles/mL.

$$y\frac{pmoles}{mL\ cells} = \frac{x\ pmoles * 100}{pmoles\ lipid\ in\ 1\ leaflet} * \frac{1}{100} * \frac{1\ pmole\ lipid\ in\ 1\ leaflet}{2\ pmoles\ total\ lipid} * \frac{7.2 * 10^6\ pmoles\ total\ lipid}{mL\ cells}$$

Reference concentrations for all dependent and independent variables were taken from literature and are compiled in table 1.

Table 3. Reference Concentrations of Model Dependent and Independent Variables were Collected

Variable Name/ Number	Concentration	Reference
RBC SO/ X_2+X_3	100 pmole/mL	[70]

RBC SO1P/ X_4+X_5	2*10_3 pmole/mL	[70]
RBC Inner Leaflet 18:1 Cer/X_7	2.5*10_6 pmole/mL	[63]
ATP/X_8	1000 μM	[113]
Inner Leaflet Phosphatidylserine/X_9	560 μM	[16]
Other Inner Leaflet Lipids/X_{10}	3040 μM	[16]

Based on the network map presented above, we wrote the following system of differential equations to describe the dynamic mass balances in the system.

Differential Equations	Rate Equations
$\dot{X_1} = \frac{V_R}{V_P} v_{2,1} - v_{1,2}$	$v_{1,2} = k_{1,2} X_1 V_R$
$\dot{X_2} = \frac{V_P}{V_R} v_{1,2} + v_{3,2} - v_{2,1} - v_{2,3}$	$v_{2,1} = k_{2,1} X_2 V_P$
$\dot{X_3} = v_{0,3} + v_{2,3} + v_{4,3} - v_{3,2} - v_{3,4}$	$v_{2,3} = k_{2,3} X_2$
$\dot{X_4} = v_{3,4} + v_{5,4} - v_{4,0} - v_{4,3} - v_{4,5}$	$v_{3,2} = k_{3,2} X_3$
$\dot{X_5} = v_{4,5} + \frac{V_P}{V_R} v_{6,5} - v_{5,4} - v_{5,6}$	$v_{4,5} = \frac{V_{max,4,5} \frac{X_4 * X_8}{K_{m,4,5,4} * K_{m,4,5,8}}}{1 + \frac{X_4}{K_{m,4,5,4}} + \frac{X_8}{K_{m,4,5,8}} + \frac{X_4 * X_8}{K_{m,4,5,4} * K_{m,4,5,8}}}$
$\dot{X_6} = \frac{V_R}{V_P} v_{5,6} - v_{6,5}$	$v_{5,4} = k_{5,4} X_5$

$$v_{5,6} = k_{5,6} X_5 V_P$$

$$v_{6,5} = k_{6,5} X_6 V_R$$

$$v_{3,4} = \frac{\beta * V_{max,3,4} \frac{X_3 X_8 X_9}{K_{m,3,4,3} K_{m,3,4,8} K_{m,3,4,9}} + V_{max,3,4} \frac{X_3 X_8 X_{10}}{K_{m,3,4,3} K_{m,3,4,8} K_{m,3,4,10}}}{\left(1 + \frac{X_8}{K_{m,3,4,8}} + \frac{X_8 X_9}{K_{m,3,4,8} K_{m,3,4,9}} + \frac{X_8 X_{10}}{K_{m,3,4,8} K_{m,3,4,10}} + \frac{X_3 X_8 X_9}{K_{3,4,3} K_{3,4,8} K_{3,4,9}} + \frac{X_3 X_8 X_{10}}{K_{3,4,3} K_{3,4,8} K_{3,4,10}}\right)}$$

$$v_{4,0} = \frac{V_{max,4,0} \frac{X_4}{K_{m,4,0,4}}}{1 + \frac{X_4}{K_{m,4,0,4}}}$$

$$v_{4,3} = \frac{V_{max,4,3} \frac{X_4}{K_{m,4,3,4}}}{1 + \frac{X_4}{K_{m,4,3,4}}}$$

$$v_{7,3} = \frac{V_{max,7,3} \frac{X_7}{K_{m,7,3,7}}}{1 + \frac{X_4}{K_{m,7,3,7}}}$$

Here, $\dot{X}_\iota$ is the time derivative of the concentration of dependent variable i, the $v_{i,j}$ terms refer to the flux converting lipid i into lipid j. An i value of 0 indicates production. A j value of 0 indicates degradation. The details of each v term are given in the next section. V_R refers to the size of RBC compartment and V_P refers to the size of the plasma compartment. Depending on the experimental data source, different units of the size of the RBC compartment have been used including cell number, cell volume, or mg of cellular protein. For the sake of standardization, we will define V_R by the mL of RBCs and V_M as the number of mL of plasma.

Biophysical Processes

Sphingosine Exchange with Media

Multiple studies have shown that RBCs readily uptake SO from media and metabolize it [70, 80, 88]. Mechanistically, this process can be broken into 2 steps: the reversible dissociation from albumin and the reversible absorption into the outer leaflet of the RBC membrane. The binding affinity of albumin for SO has not been reported, but affinity has been reported for SO1P. The K_D for SO1P binding to bovine albumin has been reported to be about 40 μM (40,000 pmol/mL) [114]. While the additional phosphate group on SO1P may affect the K_D value, this is the best estimate currently available for SO binding to albumin. The equilibrium relationship between albumin-bound SO and free SO is given by the following equation.

$$\frac{X_{i,Alb,eq}}{X_{i,aq,eq}} = \frac{Alb}{K_D}$$

Partitioning of a surfactant into a membrane is typically characterized by a partition coefficient, which is defined as follows.

$$K_P = \frac{\frac{n_{S,om}}{n_{L,om}}}{X_{S,aq}}$$

Here $n_{S,om}$ is the number of surfactant molecules in the outer membrane, $n_{L,om}$ is the number of lipid molecules in the outer membrane, and $C_{S,aq}$ is the concentration of surfactant in aqueous solution. The partition coefficient of SO into membranes has not been reported.

However, it has been shown the partition coefficient and critical micelle concentration (CMC) of a surfactant are related through the following inverse relationship [115].

$$K_P = \frac{constant}{CMC}$$

Across many different surfactants with diverse structures, the value of the constant is about 1. The value of the constant for lysophopshatidylcholine (LPC), which is structurally closer to SO, is about 0.1. [116]. The CMC of SO has been estimated to be about 1 μM (1000 pmol/mL) [117]. Putting these together gives an estimate of the partition coefficient for SO of about 10^{-4} mL/pmol. The equilibrium relationship between outer leaflet SO and aqueous SO is given by the following equation.

$$\frac{X_{i,om,eq}}{X_{i,aq,eq}} = K_P * X_{L,om}$$

Putting the two mechanistic steps together, we can estimate the overall equilibrium of SO between albumin and the outer RBC membrane to be as follows.

$$\frac{X_{i,BSA,eq}}{X_{i,om,eq}} = \frac{X_{i,BSA,eq}}{X_{i,aq,eq}} \frac{X_{i,aq,eq}}{X_{i,om,eq}} = \frac{Alb}{K_D} \frac{1}{K_P * X_{L,om}} = \frac{Alb}{40{,}000} \frac{1}{10^{-4} * 3.6 * 10^6}$$

$$= 6.94 * 10^{-8} Alb$$

The concentration of lipids in the outer membrane was assumed to be half the total concentration of lipids in RBCs ($7.2*10^6$ pmoles/mL of cells). For our parameter estimation, a typical plasma albumin concentration of 500 μM (752,00 pmole/mL) was used.

We use the following equations to describe this exchange.

$$v_{1,2} = k_{1,2} X_1 V_R$$

$$v_{2,1} = k_{2,1} X_2 V_P Alb$$

Kinetic parameters for SO exchange between membranes and albumin have not been reported. The best approximation available is for 18:1 fatty acid (oleic acid). In one study the transfer of oleic acid from albumin to isolated RBC membranes took less than 1 minute to reach equilibrium [118]. Using a half-time of 30 seconds and solving for $k_{1,2}$ gives

$$k_{1,2} = \frac{\ln(2)}{0.5\ min * 1\ mL} = 1.39\ min^{-1} mL^{-1}$$

The remaining rate constant can be estimated by solving for the steady-state of media SO, X_1.

$$\dot{X_1} = 0 = k_{2,1} X_2 Alb V_P \frac{V_R}{V_P} - k_{1,2} X_1 V_R$$

$$\frac{X_{1,SS}}{X_{2,SS}} = \frac{k_{2,1} * Alb}{k_{1,2}}$$

Comparing this to equation 5, we can see that

$$\frac{k_{2,1}}{k_{1,2}} = 6.94 * 10^{-8}$$

$$k_{2,1} = 6.94 * 10^{-8} * 1.39 = 9.65 * 10^{-8}\ min^{-1} mL^{-1}$$

Sphingosine Flip Flop

To the best of our knowledge, the transbilayer diffusion (flip flop) of SO in RBC membranes has not been measured. The closest approximation that is available is the behavior of free fatty acids. Flip flop of 18:1 fatty acid (oleic acid) in RBC membranes happens in less than 15 seconds [118]. Thus, we expect SO to rapidly distribute between the membrane leaflets. We used the following rate equations to describe SO flip flop.

$$v_{2,3} = k_{2,3}X_2$$

$$v_{3,2} = k_{3,2}X_3$$

Until more information becomes available, we will assume $k_{2,3}=k_{3,2}=\ln(2)/0.25\ \text{min} = 2.77\ \text{min}^{-1}$

MFSD2B-Mediated SO1P Flopping

The protein MFSD2B has recently been identified as the SO1P transporter in RBCs, although it is not clear how it operates mechanistically [9]. To date, there has only been one study that has investigated the kinetic parameters of RBC SO1P transport. This study was performed in rat RBCs before the identification of MFSD2B as the SO1P transporter [88]. The study identified ATP-dependent and ATP-independent transport of SO1P in RBC membranes. The study showed that the ATP-dependent transporter exhibited Michaelis-Menten-type dependence on both SO1P and ATP concentrations. However, this study did not investigate the kinetic mechanism of the transport reaction. Until more information becomes available, we will assume that a random order mechanism is appropriate. Importantly, this study showed that SO1P transport occurred even without the presence of a carrier protein in the media which suggests that the transporter could be operating as a

floppase. The same study also showed that the ATP-dependent SO1P transporter is not reversible. Taking all of these observations into account, a plausible rate equation for transport/flopping of SO1P from the inner leaflet to the outer leaflet of the RBC membrane is as follows.

$$v_{4,5} = \frac{V_{max,4,5}\frac{X_4 * X_8}{K_{m,4,5,4} * K_{m,4,5,8}}}{1 + \frac{X_4}{K_{m,4,5,4}} + \frac{X_8}{K_{m,4,5,8}} + \frac{X_4 * X_8}{K_{m,4,5,4} * K_{m,4,5,8}}}$$

$V_{max,4,5}$=11,900 pmol/mL/min [88]. The activity of MFSD2B in human RBCs has not been measured. The only available measurement of activity is in rat RBC membranes. Kobayashi et al reported a maximum transport rate of about 700 pmol/min/mg membrane protein. We converted this to a rate per total protein by assuming that membrane protein accounts for 5% of total RBC protein.

$K_{m,4,5,4}$= 72,000 pmole/mL [88]. The K_m value for SO1P was reported as 21 μM in the original paper. Unfortunately, the original paper did not contain enough experimental detail to allow us to properly convert this to mole%. Therefore, for the time being, we used a K_m of 2 mole% which is near the K_m values of the 2 enzymes that use SO1P in RBCs, S1P lyase and S1P phosphatase (see below).

$K_{m,4,5,8}$=130 μM [88]

SO1P Flipping

To the best of our knowledge, the rate of flip flop for SO1P in RBC membranes has not been reported. The flip flop rate constant of the structurally-similar lipid, 18:1

lysophosphatidylcholine (LPC), was estimated to be about 0.00083 min^{-1} [119]. Until measurements become available for SO1P, we will use the value for 18:1 LPC. Though SO1P flip flop could be bidirectional, we assume that MFSD2B-mediated flopping will dominate passive flopping so we only consider passive flipping in this model. We use the following equation to describe the rate of SO1P flipping.

$$v_{5,4} = k_{5,4}X_5$$

$k_{5,4}$ = 0.00083 min^{-1} [120]

SO1P Exchange with Media

As with SO, the exchange of SO1P between the RBC outer membrane and albumin is mechanistically divided into 2 steps: reversible desorption from the outer RBC membrane and reversible binding to albumin. Though the partition coefficient of SO1P into membranes has not been measured, we could use the same inverse relationship that we used with SO to convert the CMC of SO1P into an estimate of the partition coefficient. The CMC of SO1P has been measured to be about 14 uM (14,000 pmol/mL) [117]. Using the inverse relationship results in an estimate of K_P for SO1P of $7.1*10^{-6}$ mL/pmole. The dissociation constant for SO1P binding to bovine albumin has been measured to be about 40 uM (40,000 pmole/mL) [114]. Putting these two mechanistic steps together, the overall equilibrium of the exchange of SO1P between the RBC outer membrane and albumin is as follows.

$$\frac{X_{Alb,eq}}{X_{om,eq}} = \frac{X_{Alb,eq}}{X_{aq,eq}}\frac{X_{aq,eq}}{X_{om,eq}} = \frac{Alb}{K_D}\frac{1}{K_P * X_{L,om}} = \frac{Alb}{40{,}000}\frac{1}{7.1 * 10^{-6} * 3.6 * 10^{6}}$$

$$= 9.78 * 10^{-7} Alb$$

The exchange kinetics of SO1P between the outer leaflet of the RBC membrane and the media is assumed to obey the following equations.

$$v_{5,6} = k_{5,6} X_5 V_P Alb$$

$$v_{6,5} = k_{6,5} X_6 V_R$$

Kinetic details for SO1P exchange between membrane and albumin have not been reported. Thus, we used kinetic information for the structurally-related molecule oleic acid. The remaining rate constant can be estimated by solving for the steady-state of media SO1P, X_6.

$$\dot{X_6} = 0 = k_{5,6} X_5 Alb V_P \frac{V_R}{V_P} - k_{6,5} X_6 V_R$$

$$\frac{X_{6,SS}}{X_{5,SS}} = \frac{k_{5,6} * Alb}{k_{6,5}}$$

Comparing this to equation x, we can see that

$$\frac{k_{5,6}}{k_{6,5}} = 9.78 * 10^{-7}$$

$$k_{5,6} = 9.78 * 10^{-7} * 1.39 = 1.36 * 10^{-6}$$

Biochemical Processes

Sphingosine Kinase 1

Multiple studies have shown that RBCs express sphingosine kinase 1 (SK1) activity [70, 72, 87]. Sphingosine kinase 1 catalyzes the following bi-bi reaction.

Sphingosine + ATP →Sphingosine 1-Phosphate + ADP

It has been reported that SO1P does not exert product inhibition on this reaction up to a concentration of at least 10 μM (~0.25 mole% in their assay), which is orders of magnitude higher than the physiologic concentration of SO1P in RBCs [121]. Therefore, we will not include product inhibition in this model.

SK1 is a water-soluble enzyme that must attach to the membrane surface in order to access its substrate, SO. Thus, in addition to depending on the interfacial concentration of its substrate, the rate of the reaction also depends on the bulk concentration of membrane surface area similar to what has been shown for phospholipase A2 [122]. It has been suggested that once it has bound to the membrane, the ATP-binding site of SK1 is blocked [123]. Thus, there would be an enforced order to the reaction scheme where ATP must bind to SK1 before attachment to the membrane and SK1 must attach to the membrane before it can bind SO. Thus, SK1 would effectively follow an ordered ter-ter reaction scheme. Further, SK1 can bind to and become activated by phosphatidylserine (PS) [124, 125]. Because the reaction can occur without the presence of PS, PS will be considered a non-essential activator. The mechanistic rate equation encapsulating all the above detail derived using the rapid equilibrium assumption is as follows.

$$v_{3,4} = \frac{\beta * V_{max,3,4} \frac{X_3 X_8 X_9}{K_{m,3,4,3} K_{m,3,4,8} K_{m,3,4,9}} + V_{max,3,4} \frac{X_3 X_8 X_{10}}{K_{m,3,4,3} K_{m,3,4,8} K_{m,3,4,10}}}{\left(1 + \frac{X_8}{K_{m,3,4,8}} + \frac{X_8 X_9}{K_{m,3,4,8} K_{m,3,4,9}} + \frac{X_8 X_{10}}{K_{m,3,4,8} K_{m,3,4,10}} + \frac{X_3 X_8 X_9}{K_{3,4,3} K_{3,4,8} K_{3,4,9}} + \frac{X_3 X_8 X_{10}}{K_{3,4,3} K_{3,4,8} K_{3,4,10}}\right)}$$

$V_{max,3,4}$ = 10,200 pmol/min/mL [87].

$K_{m,3,4,3}$ = 12,600 pmole/mL [121]

$K_{m,3,4,8}$ = 77 μM [121]

$K_{m,3,4,9}$ = 0.0042 μM [125]

$K_{m,3,4,10}$ = 0.052 μM [125]

β = 2 [124]

S1P Lyase

There is some uncertainty about the presence of S1P lyase in RBCs. An early study did not detect any activity from this enzyme in RBCs [70]. A later study, using a more sensitive assay, did detect a small amount of activity [90]. Further evidence for the presence of a small amount of S1P lyase activity in RBCs comes from the fact that in RBCs stored under blood bank conditions for 4 weeks, the SO1P concentration decreases by about 75% while the concentration of hexadecenal increases by about 100%. Thus, we included this enzyme in our model. Since S1P lyase is an integral membrane protein, the rate of the reaction depends only on the interfacial concentration of its substrate. S1P lyase catalyzes the following uni-bi reaction.

SO1P → ethanolamine phosphate +hexadecenal

We use the following rate equation to describe S1P lyase.

$$v_{4,0} = \frac{V_{max,4,0}\frac{X_4}{K_{m,4,0,4}}}{1+\frac{X_4}{K_{m,4,0,4}}}$$

$V_{max,4,0}$ = 0.0068 pmol/mL/min [90]. Selim et al. reported an activity of 0.0004 pmol/min/mg membrane protein. We converted this to total protein by assuming that membrane protein accounts for 5% of total protein.

$K_{m,4,0,4}$ = 51,804 pmol/mL [126]. We used the K_m of the synthetic SO1P analogue, NBD-SO1P. In the assay, Triton X-100 concentration was maintained at 1 mM and the K_m was estimated to be 14.6 μM or 1.43 mole%.

S1P Phosphatase

There is some uncertainty about the presence of S1P phosphatase activity in RBCs. An early study did not detect any activity from these enzymes in RBCs [70]. A later study, using a more sensitive assay, did detect a small amount of activity [90]. Thus, we included this enzyme in our model. S1P phosphatase catalyzes the following uni-bi reaction.

SO1P → sphingosine + orthophosphate

We used the following rate equation to describe S1P phosphatase.

$$v_{4,3} = \frac{V_{max,4,3}\frac{X_4}{K_{m,4,3,4}}}{1 + \frac{X_4}{K_{m,4,3,4}}}$$

$V_{max,4,3}$ =0.0198 pmol/mL/min [90]. Selim et al. reported an activity of 0.00117 pmol/min/mg membrane protein. We converted this to total protein by assuming that membrane protein accounts for 5% of total protein.

$K_{m,4}$ = 90,000 [89]. To the best of our knowledge, the K_m value of S1P phosphatase for SO1P has not been reported. Until more data become available, we will use the value for a related enzyme, phosphatidate phosphatase 2B.

Alkaline Ceramidase

Some papers have suggested that RBCs possess some level of alkaline ceramidase (ACER) activity [85, 86], while other studies contradict this [70, 80]. One of the key differences between these studies is the concentration of calcium used in assays. In one study that detected alkaline ceramidase activity in RBCs, the calcium concentration used in the assay was 1 mM whereas no calcium was added in one study that did not detect alkaline ceramidase activity. Calcium is required for ACER 2 activity and significantly activates ACER3 [127, 128]. The normal concentration of ionized calcium in resting RBCs is about 50 nM [129]. Thus, the in situ activities of these enzymes in RBCs are likely to be much less than reported in activity assays. Since ACER3 is less dependent on calcium and also has a higher activity than ACER2 in RBCs, we included this enzyme in our model. ACER3 catalyzes the group of uni-bi reactions of the form

Ceramide → sphingosine + fatty acid

It has been shown that ACER3 does not catalyze the reverse reaction [128]. ACER3 has been shown to only catalyze the hydrolysis of long-chain unsaturated ceramides [130]. The only long-chain ceramide that has been quantified in human RBCs is 18:1 ceramide. Thus, we will use the following equation described this reaction.

$$v_{7,3} = \frac{V_{max,7,3}\frac{X_7}{K_{m,7,3,7}}}{1 + \frac{X_4}{K_{m,7,3,7}}}$$

$V_{max,7,3}$ =57.8 pmole/mL/min [85]. Xu et al. reported an activity of alkaline ceramide towards 18:1 ceramide of 12 pmole/min/mg membrane protein at pH 9.4 and 1 mM calcium. Taking into account the fact that membrane protein only represents 5% of total RBC protein, that the activity of alkaline ceramidase at pH 7.2 is about 50% the activity at pH 9.4, and that the activity at 50 nM calcium is about 57% of the activity at 1 mM calcium (Mao 2001), the final activity estimate is 0.17 pmole/min/mg protein.

$K_{m,7,3,7}$ = 104,760 pmol/mL [127]. The K_m of ACER3 towards 18:1 ceramide has not been reported. Therefore, for the time being, we used the K_m of ACER2 towards 18:1 ceramide, which is 2.91 mole%.

Ceramide Synthase

Ceramide synthase was not included in the model because it has not been detected in RBCs [80].

3.5.2 Extracting Experimental Data from Literature

All of the data used to calibrate and evaluate model performance was taken from previously published literature. However, all the data were originally in graphical form, not tabular form. Therefore, the numerical values had to be extracted from the figures. To do this, we used the digitize2.m function in MATLAB.

3.5.3 Parameter Estimation Using Nonlinear Optimization

The best fit parameters were estimated through nonlinear optimization. First, a search region for each parameter was set between 0.01 times and 100 times the value estimated from literature. Next, 100,000 sets of parameters were generated using a latin hypercube design using the lhsdesign function in MATLAB so that each parameter guess falls within the appropriate bounds. The model was numerically integrated using the ode15s function in MATLAB. From here, the objective function was evaluated for each parameter set. We used the sum of squared errors as the objective function as follows

$$SSE = \sum_{i=1}^{m} (y_i - \hat{y}_i)^2$$

Here, m is the number of data points, y_i is the average value of data point i, and $\hat{y}_i$ is the model prediction for data point i. The 1% of parameter sets that gave the lowest values were then passed to the fmincon function, which uses the interior point method, for nonlinear optimization. At the end of optimization, the parameter set that gave the lowest SSE value was considered to be the best fit parameter set. Mean squared error was also calculated to the best-fit parameter sets by dividing the sum of squared errors by the number of data points fit.

3.5.4 Evaluation of Optimized Parameter Clustering

In order to determine if the 100 optimized parameter sets for each experiment all cluster in the same region of parameter space we performed principal component analysis on the optimized parameter sets using the pca function in MATLAB. The parameter scores for principal components 1 and 2 were plotted to visualize the parameter clusters.

CHAPTER 4. CONCENTRATION CHANGES IN THE MEMBRANE SPHINGOLIPIDS OF SICKLE RED BLOOD CELLS AND EXTRACELLULAR VESICLES

4.1 Abstract

Sickle cell disease is a genetic disease affecting 4.4 million people worldwide and 100,000 people in the United States. Despite decades of research into this disease, few treatment options are available. Thus, a better understanding of fundamental disease mechanisms is needed to enable new treatment options. Studies have shown that sphingolipids play important roles in red blood cells including promoting production of extracellular vesicles. Further, studies focusing on specific parts of the sphingolipid metabolic network have identified alterations in sickle cell disease red blood cells. However, an evaluation of the entire sphingolipid metabolic network has not been conducted in sickle cell red blood cells or extracellular vesicles. In this study we investigated whether red blood cell and plasma-derived extracellular vesicles sphingolipid concentrations are altered in sickle cell disease. We quantified the concentrations of 89 sphingolipids in non-sickle and sickle genotype red blood cells and extracellular vesicles using liquid chromatography tandem mass spectrometry. We then used statistical techniques to infer changes in the underlying enzymes of the metabolic network. We demonstrate that the concentrations of many sphingolipids including ceramides, dihydroceramides, hexosylceramides, lysosphingomyelins, sphingoid bases, and sphingoid base 1-phosphates are significantly elevated in sickle cell disease red blood cells. In contrast, there are few alterations in sphingolipid concentrations in extracellular vesicles.

The statistical analysis indicates elevations in the activities of multiple enzymes such as ceramide kinase. The results of this study suggest that red blood cell sphingolipid concentrations are widely altered in sickle cell disease and that these alterations can be traced to enzymes which may be useful therapeutic targets.

4.2 Introduction

Sickle cell disease (SCD) is a genetic disease affecting 4.4 million people worldwide and 100,000 people in the United States. SCD is caused by a mutation in the gene for the beta-globin subunit of hemoglobin. Because of this mutation, sickle hemoglobin polymerizes in low-oxygen environments which distorts the red blood cell (RBC) membrane into its characteristic sickle shape. Sickle hemoglobin is also less stable than normal hemoglobin which leads to sickle hemoglobin precipitating onto the RBC membrane, forming Heinz bodies [1]. Because of this sickle hemoglobin, RBCs have more oxidative damage to lipids and proteins, they express more phosphatidylserine on their surface, they release more proinflammatory extracellular vesicles (EVs), and they have a dramatically shortened lifespan [131-133]. These pathologic changes in the RBCs lead to many symptoms for people with this disease, including chronic inflammation, organ damage, anemia, painful vaso-occlusive crises, and a significantly shortened life expectancy. Due to the severe reduction in quality of life and the significant healthcare costs, continued investigation into disease mechanisms and development of new therapies is necessary.

Current treatment options for SCD are limited. There are two FDA-approved disease-modifying drugs for SCD: hydroxyurea and L-glutamine. Hydroxyurea works by elevating

the concentration of fetal hemoglobin in red blood cells which outcompetes sickle hemoglobin and prevents hemoglobin polymerization in RBCs [2]. L-glutamine works in part by increasing RBC's antioxidant defenses. While both of these treatments have some efficacy, they do not work in all patients [3]. Other treatment options such as analgesics and blood transfusions mainly reduce symptoms. Bone marrow transplant is currently the only curative option for SCD although it is often difficult to find a compatible donor. Recently, gene editing has been investigated as a curative option for SCD [134]. However, it seems unlikely that this option will be available in the developing world, where most people affected by the disease live, for some time. Thus, a better understanding of the fundamental mechanisms of SCD is needed to enable new treatment options.

Sphingolipids have been shown to play important roles in RBC biology. Increasing the concentration of ceramide in RBCs has been shown to cause increased exposure of phosphatidylserine on their surface, increased release of EVs, and clustering of proteins in the cell membrane [17]. Increasing sphingosine concentration in red blood cells has been shown to cause increased intracellular calcium and increased phosphatidylserine surface exposure [5]. This is consistent with its ability to inhibit the plasma membrane calcium ATPase [4]. Like ceramide, sphingosine is also capable of forming pores in RBC membranes [8]. Sphingosine 1-phosphate has been shown to bind to deoxygenated hemoglobin and enhance its affinity for the red blood cell membrane[10]. This alters red blood cell energy metabolism. Thus, sphingolipids play many roles in RBC biology and they may be a novel target for intervention in SCD.

The overlap of RBC functions that are regulated by sphingolipids and RBC functions that are altered in sickle cell disease suggests that sphingolipids may play a role in SCD

pathology. Indeed, a few studies have shown that some aspects of the sphingolipid metabolic network are altered in SCD red blood cells. One group has shown that sphingosine kinase activity is significantly elevated in SCD RBCs and that this contributes to an elevation in sphingosine 1-phosphate concentration in SCD RBCs [72]. Our group has shown that acid sphingomyelinase activity is significantly elevated in SCD RBCs and plasma [69]. However, these studies have only focused on two points in a large and complicated network. Further, to date, a comprehensive evaluation of SCD RBC sphingolipids has not been performed.

In this study, we asked the questions, "what are the concentrations of sphingolipids in normal RBCs?", "are those concentrations altered in SCD RBCs?" and "which metabolic reactions are active in normal RBCs and are those connections altered in SCD RBCs?". To answer these questions, we quantified the concentrations of 89 different sphingolipids in normal genotype (AA) donors and SCD (SS) donors using liquid chromatography tandem mass spectrometry. We then used multivariate statistical techniques to infer the changes in sphingolipid-metabolizing enzyme activities between AA and SS RBCs.

4.3 Results

4.3.1 Sphingolipid Concentrations are Significantly Elevated in SS RBCs

We isolated RBCs and plasma-derived EVs from the whole blood of 10 AA genotype and 10 SS donors. We then extracted and quantified 89 sphingolipids in the RBCs and EVs by liquid chromatography tandem mass spectrometry (Figure 10A). These included 32 sphingomyelins, 13 hexosylceramides, 16 ceramide 1-phosphates, 13 ceramides, 7 dihydroceramides, 4 lysosphingomyelins, 2 sphingoid bases and 2 sphingoid base 1-

phosphates. In cells, these sphingolipids are interconverted by a complex metabolic network (Figure 10B).

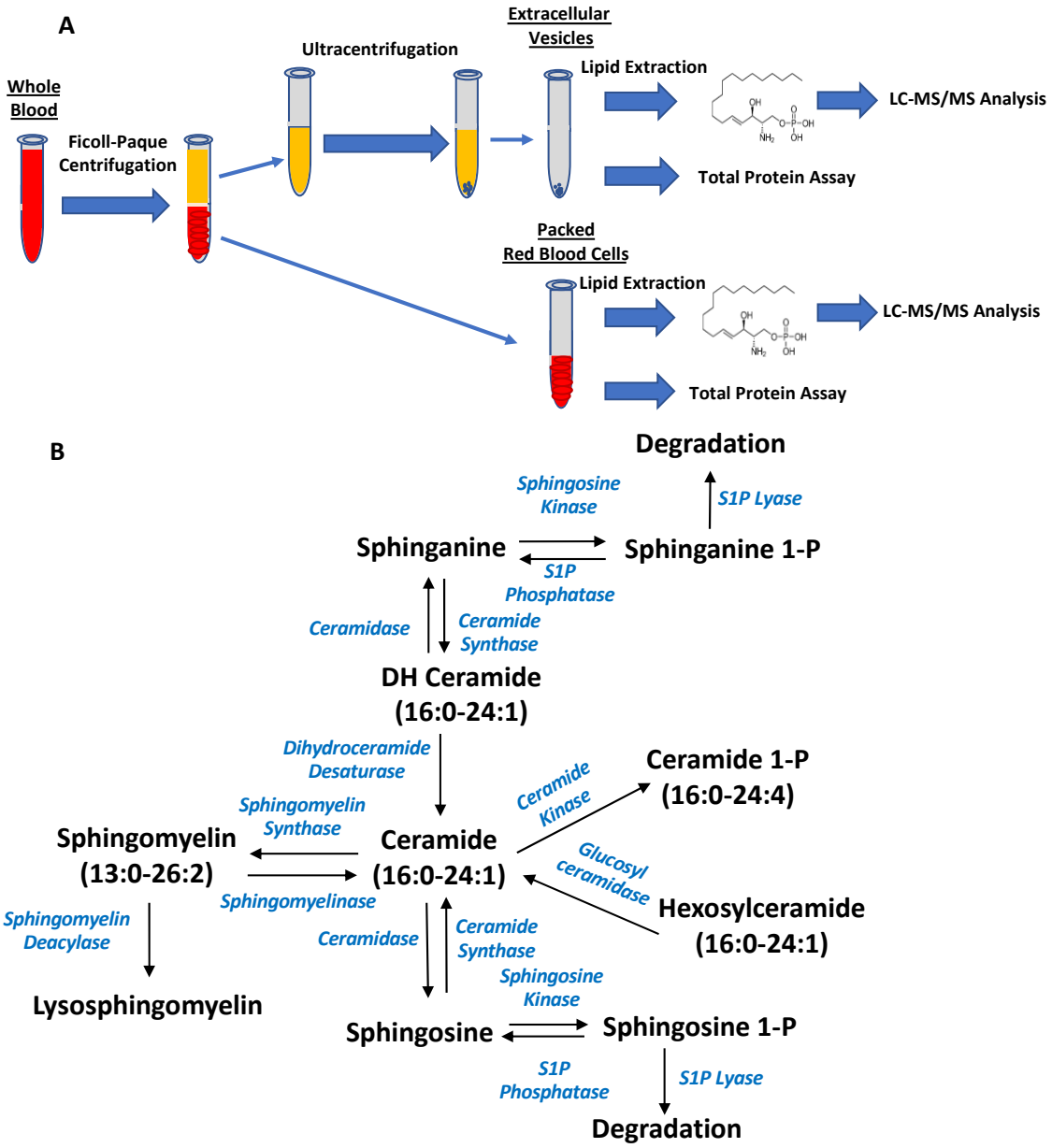

Figure 10. Sphingolipid Analysis of Human AA and SS RBCs and EVs. A) RBCs and EVs were isolated from whole blood. Sphingolipids were then extracted and analyzed by LC-MS/MS. B) Sphingolipids are interconverted by enzymes in a complex metabolic

network. Some lipids can have different fatty acyl side chains represented by carbon number: double bond number. Lipids are given in black, enzymes are given in blue.

Sphingolipid amounts were scaled by total protein amount to compute absolute concentrations. The RBC sphingolipid concentrations are shown in Figure 11.

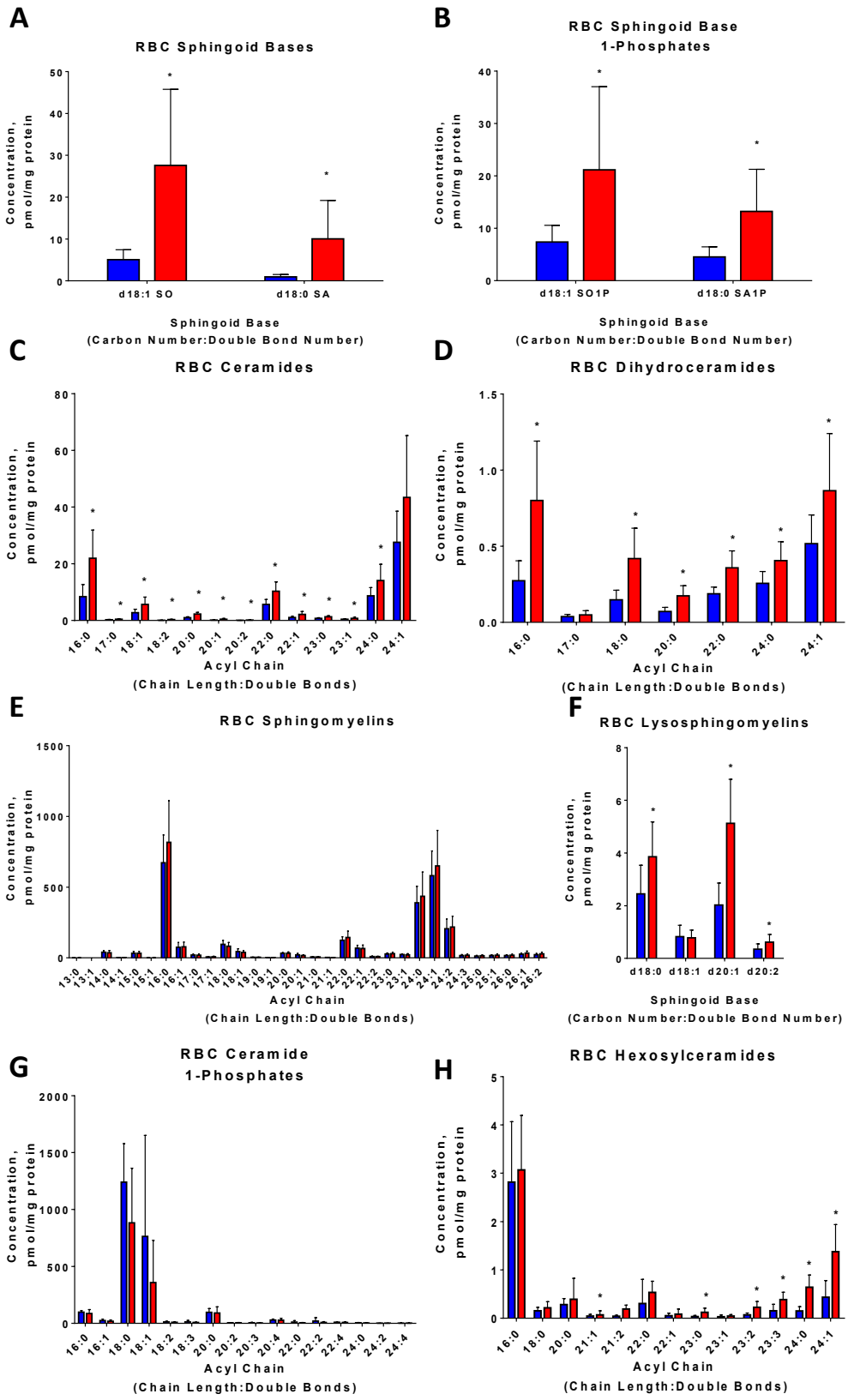
A
RBC Sphingoid Bases
Concentration, pmol/mg protein
d18:1 SO
d18:0 SA
Sphingoid Base
(Carbon Number:Double Bond Number)
B
RBC Sphingoid Base 1-Phosphates
Concentration, pmol/mg protein
d18:1 SO1P
d18:0 SA1P
Sphingoid Base
(Carbon Number:Double Bond Number)
C
RBC Ceramides
Concentration, pmol/mg protein
16:0 17:0 18:1 18:2 20:0 20:1 20:2 22:0 22:1 23:0 23:1 24:0 24:1
Acyl Chain
(Chain Length:Double Bonds)
D
RBC Dihydroceramides
Concentration, pmol/mg protein
16:0 17:0 18:0 20:0 22:0 24:0 24:1
Acyl Chain
(Chain Length:Double Bonds)
E
RBC Sphingomyelins
Concentration, pmol/mg protein
Acyl Chain
(Chain Length:Double Bonds)
F
RBC Lysosphingomyelins
Concentration, pmol/mg protein
d18:0 d18:1 d20:1 d20:2
Sphingoid Base
(Carbon Number:Double Bond Number)
G
RBC Ceramide 1-Phosphates
Concentration, pmol/mg protein
16:0 16:1 18:0 18:1 18:2 18:3 20:0 20:2 20:3 20:4 22:0 22:2 22:4 24:0 24:2 24:4
Acyl Chain
(Chain Length:Double Bonds)
H
RBC Hexosylceramides
Concentration, pmol/mg protein
16:0 18:0 20:0 21:1 21:2 22:0 22:1 23:0 23:1 23:2 23:3 24:0 24:1
Acyl Chain
(Chain Length:Double Bonds)

Figure 11. Sphingolipid Concentrations in AA and SS RBCs were Measured by LC-MS/MS. A) Sphingoid Bases B) Sphingoid Base 1-Phosphates C) Ceramides D) Dihydroceramides E) Sphingomyelins F) Lysosphingomyelins G) Ceramide 1-Phosphates H) Hexosylceramides. AA samples are represented in blue, SS samples are represented in red. Concentrations are in units of pmoles/mg of total protein. * indicated $p<0.05$ using Welch's t-test compared to AA.

Figure 11 shows that the SS RBC samples consistently have higher concentrations of ceramides, dihydroceramides, hexosylceramides, lysosphingomyelins, sphingoid bases, and sphingoid base 1-phosphates. This confirms that the dysfunction of RBC sphingolipid metabolism is not limited to sphingosine 1-phosphate, but is widespread.

4.3.2 Sphingolipid Concentrations are not Significantly Altered in SS EVs

We quantified the same 89 sphingolipids in plasma-derived EVs from 6 AA genotype and 6 SS genotype donors. The absolute concentrations are shown in Figure 12. The figure shows that, in contrast to RBCs, there are few changes in the concentrations of sphingolipids in plasma-derived EVs. SS EVs have lower concentrations some C1Ps, but higher concentrations of some HexCers.

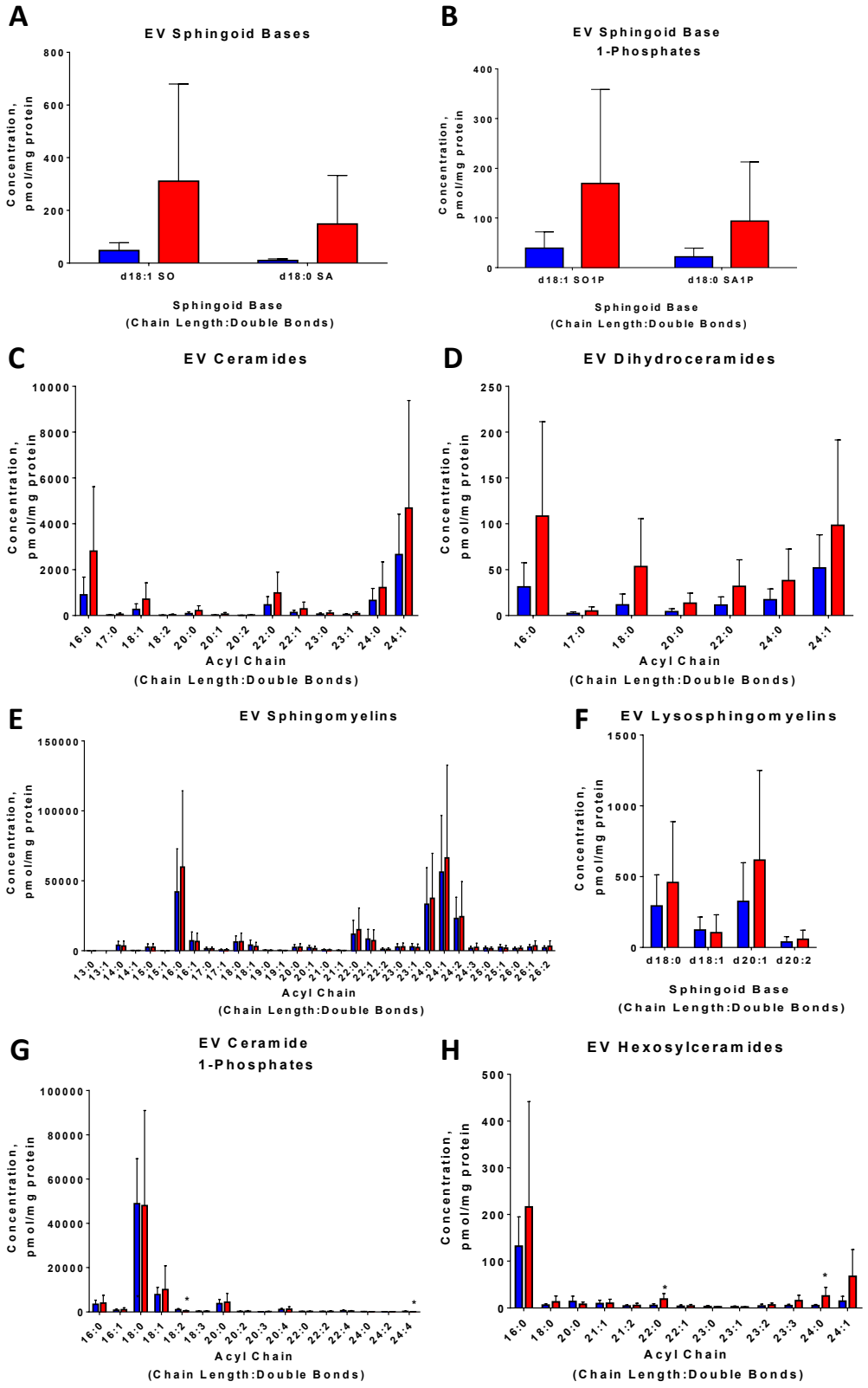
A
EV Sphingoid Bases
Concentration, pmol/mg protein
800
600
400
200
0
d18:1 SO
d18:0 SA
Sphingoid Base
(Chain Length:Double Bonds)
B
EV Sphingoid Base 1-Phosphates
Concentration, pmol/mg protein
400
300
200
100
0
d18:1 SO1P
d18:0 SA1P
Sphingoid Base
(Chain Length:Double Bonds)
C
EV Ceramides
Concentration, pmol/mg protein
10000
8000
6000
4000
2000
0
16:0 17:0 18:1 18:2 20:0 20:1 20:2 22:0 22:1 23:0 23:1 24:0 24:1
Acyl Chain
(Chain Length:Double Bonds)
D
EV Dihydroceramides
Concentration, pmol/mg protein
250
200
150
100
50
0
16:0 17:0 18:0 20:0 22:0 24:0 24:1
Acyl Chain
(Chain Length:Double Bonds)
E
EV Sphingomyelins
Concentration, pmol/mg protein
150000
100000
50000
0
13:0 13:1 14:0 14:1 15:0 15:1 16:0 16:1 17:0 17:1 18:0 18:1 19:0 19:1 20:0 20:1 21:0 21:1 22:0 22:1 22:2 23:0 23:1 24:0 24:1 24:2 24:3 25:0 25:1 26:0 26:1 26:2
Acyl Chain
(Chain Length:Double Bonds)
F
EV Lysosphingomyelins
Concentration, pmol/mg protein
1500
1000
500
0
d18:0 d18:1 d20:1 d20:2
Sphingoid Base
(Chain Length:Double Bonds)
G
EV Ceramide 1-Phosphates
Concentration, pmol/mg protein
100000
80000
60000
40000
20000
0
16:0 16:1 18:0 18:1 18:2 18:3 20:0 20:2 20:3 20:4 22:0 22:2 22:4 24:0 24:2 24:4
Acyl Chain
(Chain Length:Double Bonds)
H
EV Hexosylceramides
Concentration, pmol/mg protein
500
400
300
200
100
0
16:0 18:0 20:0 21:1 21:2 22:0 22:1 23:0 23:1 23:2 23:3 24:0 24:1
Acyl Chain
(Chain Length:Double Bonds)

Figure 12. Sphingolipid Concentrations in AA and SS EVs were Measured by LC-MS/MS. A) Sphingoid Bases B) Sphingoid Base 1-Phosphates C) Ceramides D) Dihydroceramides E) Sphingomyelins F) Lysosphingomyelins G) Ceramide 1-Phosphates H) Hexosylceramides. AA samples are represented in blue, SS samples are represented in red. Concentrations are in units of pmoles/mg of total protein. * indicates $p<0.05$ using Welch's t-test compared to AA.

4.3.3 Principal Component Analysis Shows Separation of RBC and EV Samples by Genotype

The previous analysis investigated differences in individual sphingolipids and identified those that are significantly different in SS samples. Next, we investigated whether the sphingolipid profile of SS samples as a whole are different from that of AA samples. We performed principal component analysis using centered and scaled sphingolipid concentration data from RBCs and EVs. The scores of each RBC sample in principal components 1 and 2 are plotted against each other in figure 13A. Figure 13A shows that the RBC samples from the 2 genotypes do separate along both principal components 1 and 2, supporting the idea that the sphingolipid profiles as a whole are different between the two genotypes. Principal components 1 and 2 together capture over 60% of the total variation in the data. The scores of each EV sample in principal components 1 and 2 are plotted against each other in figure 13B. Figure 13B shows that the EV samples from the 2 genotypes do separate along principal component 2.

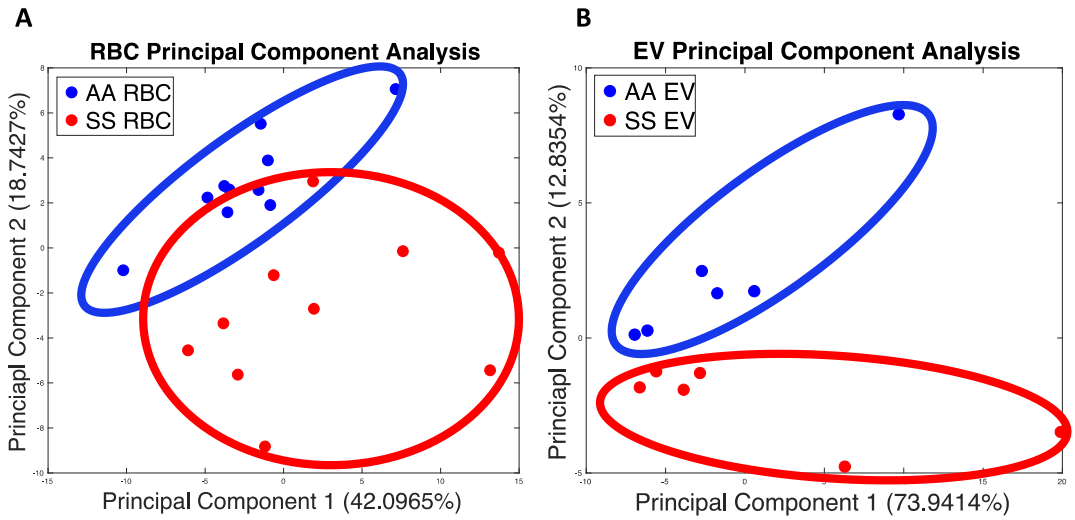

Figure 13. Principal Component Analysis was Performed on RBC and EV Sphingolipid Concentration Data. A) RBC sphingolipid concentrations were rendered in principal component space. Principal component 1 explains about 42% of the variance in the data and principal component 2 explains about 19% of the variance in the data. B) EV sphingolipid concentrations were represented in principal component space. Principal component 1 explains about 74% of the variance in the data and principal component 2 explains about 13% of data variance. AA samples are shown as blue dots and SS samples are shown as red dots.

4.3.4 The Relationships Between RBC Sphingolipids are Altered in SCD

Having established that there are significant changes in the concentrations of sphingolipids in SS RBCs, we then investigated the causes of these changes. Sphingolipids are connected by a complex metabolic network (Figure 10B). However, in SS RBCs it is not known if the activities of sphingolipid-metabolizing enzymes are altered. It has previously been shown that changes in correlation coefficients between pairs of metabolites can be used to identify enzyme activities that may be altered in different cellular states [135]. Thus, we performed correlation analysis on each pair of sphingolipids in the RBC samples. The results are rendered in heat map form in Figure 14. As Figure 14 shows, the overall pattern of correlations between sphingolipids is very different between AA and SS RBCs.

Figure 14. Correlation Coefficients were Calculated for Every Pair of Sphingolipids in AA and SS RBC Samples Correlation Coefficient were calculated for pairs of sphingolipids in A) AA RBCs and B) SS RBCs. Red indicates a correlation coefficient greater than 0. Green indicates a correlation coefficient less than 0. Black indicates a correlation coefficient close to 0.

Next, we particularly focused on whether there were changes in the values of the correlation coefficient of pairs of sphingolipids between AA and SS RBCs that are connected by a metabolic enzyme. It is important to note that sphingolipids with a fatty acyl side chain can only be interconverted with other sphingolipids with the same side chain. For example, 16:0 ceramide can be converted to 16:0 sphingomyelin, but not 18:1 sphingomyelin. We rendered the results of this analysis in Figure 15. For pairs of sphingolipids connected by sphingosine kinase, such as SO and SO1P, the correlation coefficient shift from negative in AA RBCs to positive in SS RBCs, indicating an increase in enzyme activity. This is consistent with previously published data [72]. For pairs of sphingolipids connected by ceramidase, such as ceramides and SO, the correlation coefficients shift from non-statistically significant values in AA RBCs to larger, statistically-significant values in SS RBCs indicating an increase in enzyme activity. For pairs of sphingolipids connected by sphingomyelinase, the correlation coefficients shift from statistically-significant positive values in AA RBCs to non-statistically significant values in SS RBCs, indicating lower enzyme activity. For pairs of sphingolipids connected by hexosylceramidase, the correlation coefficients shift from positive, statistically-significant values in AA RBCs to non-statistically significant values in SS RBCs, indicating a decrease in enzyme activity. Finally, for pairs of sphingolipids connected by

ceramide kinase, the correlation coefficients shift from mostly negative values in AA RBCs to positive values in SS RBCs, indicating an increase in enzyme activity.

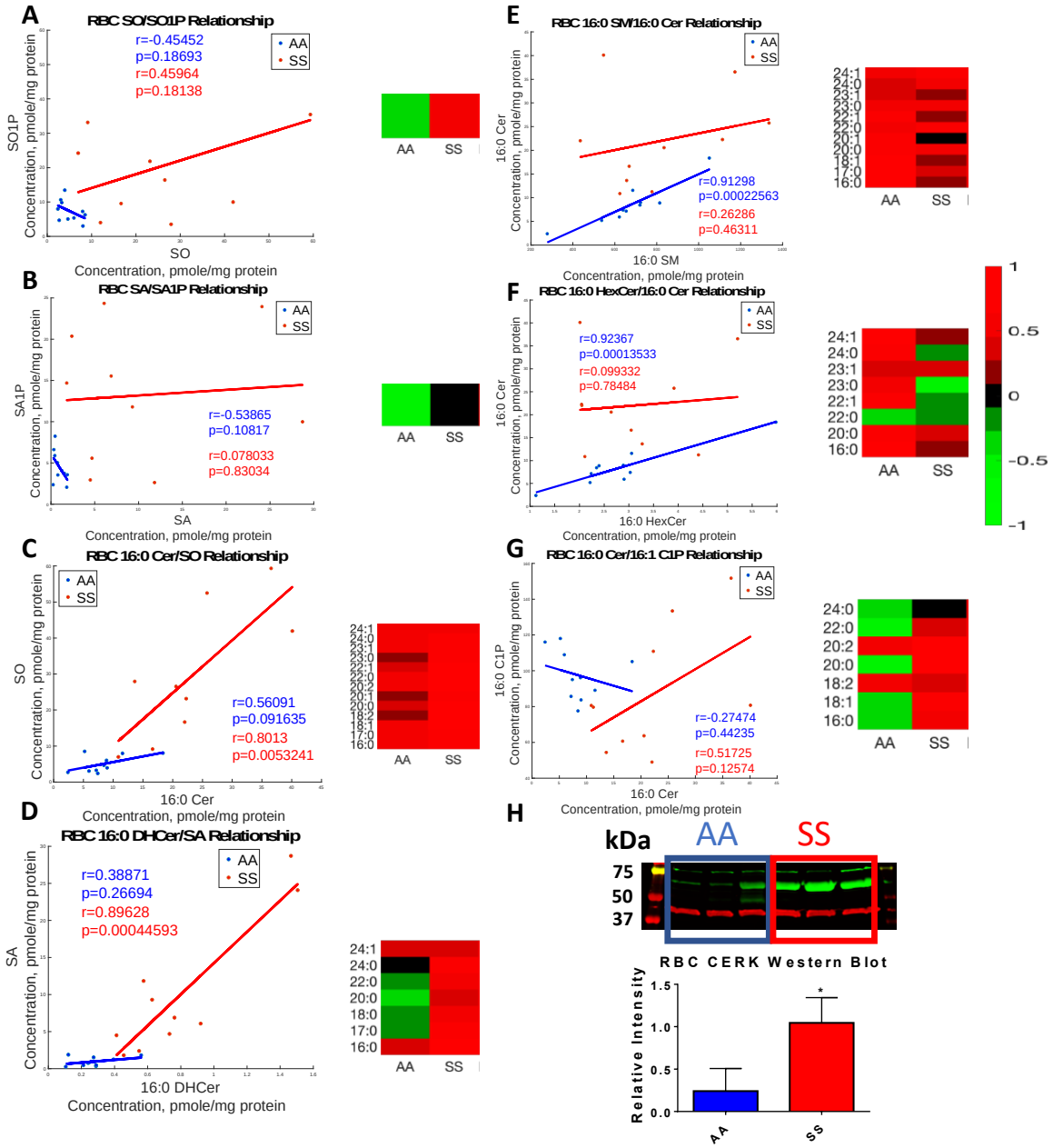

Figure 15. Correlation Analysis was Performed on RBC Sphingolipid Concentration Data. A-G) A representative scatter plot was generated for each group of relationships alongside a heat map representation of the correlation coefficients of all relationships for the group. A) SO/SO1P relationship B) SA/SA1P relationship, C) Ceramide/SO relationships D) Dihydroceramide/SA relationships, E) Sphingomyelin/Ceramide

relationships F) Hexosylceramide/Ceramide relationships G) Ceramide/ Ceramide 1-Phosphate relationships H) A Western Blot was Performed on AA and SS RBCs staining for ceramide kinase (green) and β-Actin (Red). Band intensities were quantified using ImageJ. * indicates $p<0.05$ using Welch's t-test compared to AA.

In order to corroborate the results of the correlation analysis, we investigated the expression of the enzyme ceramide kinase. The expression of this enzyme has not been reported in RBCs. We examined the expression of this enzyme in 3 AA donors and 3 SS donors via Western blot. The results are shown in Figure 15H. As Figure 15H shows, there is a significantly higher expression of ceramide kinase in SS RBCs compared to AA RBCs. This is in agreement with the results of our correlation analysis.

4.4 Discussion

4.4.1 Current Study Results Agree with Previous Data on AA RBCs and Expand Knowledge about SS RBCs

In this study, we quantified the concentrations of 89 sphingolipids in AA and SS RBC samples as well as AA and SS plasma-derived EVs. To our knowledge, this is the most comprehensive evaluation of sphingolipid concentrations in human RBCs for AA or SS donors. Multiple previous reports have measured sphingolipid concentrations in AA RBCs. However, these studies have only measured subsets of sphingolipids at a time such as sphingomyelins [23], ceramides [59, 63], glycosphingolipids [59], sphingoid bases [69], and sphingoid base 1-phosphates [69, 72]. Further, many of these previous studies did not present absolute concentrations of individual sphingolipids, only percentages of total sphingolipids measured. This makes absolute comparison between data sets difficult. When our AA RBC sphingolipid data are considered as percentages, our data agree with these previous studies. For sphingomyelins, hexosylceramides, and ceramides, the 16:0,

24:0, and 24:1 fatty acyl chains are dominant with other fatty acyl chains only making minor contributions. The results of our current study confirm the presence of a large concentration of SO1P noted in previous studies [69, 72] and expand on it by showing a similarly high concentration of SA1P.

To our knowledge, few studies have investigated changes in RBC sphingolipid concentrations in human SS RBCs. A few studies have demonstrated that SO1P concentration is significantly elevated in SS RBCs, which is confirmed by our study [69, 72]. A previous study from our group also showed the SO concentration is elevated in SS RBCs [69]. One study utilizing flow cytometry and a unique sulfatide-binding protein showed a significant increase in the surface expression of the complex glycosphingolipid sulfatide in SS RBCs [58]. To our knowledge, this is the only report to identify the presence of sulfatide in RBCs, AA or SS. One recent study showed significant elevations in the concentrations of ceramides and C1Ps in RBCs in a mouse model for SCD, but did not report absolute concentrations [101]. Thus, the current study is the first major expansion of our knowledge of how sphingolipid concentrations are altered in human SCD RBCs.

4.4.2 Current Study Results Expand Knowledge of Plasma EV Sphingolipid Composition

In this study, we quantified the concentrations of 89 sphingolipids in plasma-derived EVs from AA and SS donors. To our knowledge, this is the first sphingolipid characterization of plasma EVs in AA or SS individuals. There were few differences in sphingolipid concentrations between AA and SS EVs in contrast to the extensive differences in RBCs. This may be due to the generation of EVs from specific sites on the RBC membrane that are not strongly affected by overall changes in sphingolipid concentrations. For example,

sphingolipids have been shown to be heterogeneously distributed in the RBC membrane [136]. This study also showed that sphingolipid-enriched domains are preferentially present in low-curvature areas in the RBC membrane. Thus, there may be differences in the concentrations of sphingolipids in EV-generating areas (high-curvature) and non-EV generating areas (low-curvature) or the RBC membrane. It has been shown that individuals with SCD have higher numbers of EVs in their plasma from RBCs and other cell types [137]. A previous report from our group showed that the increased activity of sphingomyelinase in SS RBCs contributes to increased EV production [69]. Thus, it seems that although individuals with SCD produce more plasma EVs, the sphingolipid composition of those particles is not very different.

4.4.3 Current Study Results Expand Knowledge of Enzymatice Changes in RBC Sphingolipid-Metabolizing Enzymes

In this study, we performed correlation analysis on the concentrations of sphingolipids that are connected by a metabolic enzyme in order to determine changes in the activities of those enzymes. Previously, it has been shown that the activity of sphingosine kinase is elevated in SS RBCs [69, 87]. Our results, which show a change in correlation coefficient from negative in AA RBCs to positive in SS RBCs are consistent with this increase in activity. Our regression analysis also indicated an increase in the activities of ceramidase and ceramide kinase and a decrease in the activity of hexosylceramidase. To our knowledge, the activities or expression levels of these enzymes have not been measured in SS RBCs. Thus, to validate our predictions, we measured ceramide kinase activity in AA and SS RBCs via Western blot. Our results showed a significantly higher expression of ceramide kinase in SS RBCs. To our knowledge, this is the first time the expression of

ceramide kinase has ever been reported in RBCs. Overall, the results of our correlation analysis are consistent with existing data and indicate that the increased concentrations of sphingolipids in SS RBCs are caused by changes in the activities of multiple enzymes in the sphingolipid-metabolic pathway.

4.4.4 The Observed Elevations in Sphingolipid Concentrations May Contribute to Sickle Pathology

Our results showed significant increases in the concentrations of many ceramide species in SS RBCs. Previous studies have shown that increasing the concentration of ceramide in RBCs, either by adding artificial short-chain 6:0 ceramide or by incubating RBCs with bacterial sphingomyelinase causes increased cell surface exposure of phosphatidylserine, which is a marker of apoptosis, increased intracellular calcium, cell shrinkage, membrane endovesiculation, and EV release [17]. Thus, our observation of higher ceramide concentrations is consistent with the observation that sickle RBCs express more cell surface phosphatidylserine [132] and that there are higher concentrations of RBC-derived EVs in SS plasma [137]. The increased RBC ceramide concentration may also play a role in the shortened lifespan of SCD RBCs given that PS exposure is a signal for removal from circulation by macrophages and endothelial cells. Thus, the elevated ceramide in SS RBCs could be a mechanistic cause for these pathologic changes. We also observed significantly elevated concentrations of several dihydroceramides in SCD RBCs. Multiple studies have shown that despite the small difference in structure between ceramides and dihydroceramides (a single double bond in the sphingoid base backbone), dihydroceramides are relatively biologically inert. For example, dihydroceramide is not capable of inducing lipid membrane scrambling whereas ceramide is [11]. Thus, it is not

clear if the increases in RBC dihydroceramide concentrations have a mechanistic impact of SCD pathology.

We observed significant increases in the concentrations of hexosylceramides in SS RBCs. To our knowledge, it is not known whether hexosylceramides per se play a functional role in RBC biology. Rather, it is their downstream metabolic precursors that have recognized functions in RBCs. For example, triaosylceramide and tetraosylceramide, which are downstream products of glucosylceramide, are blood group antigens that are part of the P antigen system. Interestingly, the P antigens act as receptors for parvovirus B19, which is a common cause of infections for people with SCD [138]. Further, sulfatide, which is a downstream product of galactosylceramide, has been shown to play a role in cell adhesion of RBCs to the endothelium [58]. Further, increased sulfatide expression was shown to cause increased adhesion of SCD RBCs to endothelial cells.

We observed increases in the concentrations of sphingoid bases in SCD RBCs. One study showed that increasing the concentration of RBC sphingosine by incubating the cells with high concentrations of extracellular sphingosine causes the cells to expose surface phosphatidylserine, increase intracellular calcium, and shrink in size [5]. This was corroborated by another study which showed that incubating RBCs with sphingosine increased intracellular calcium and made the RBCs much more fragile to osmotic stress [6]. Some of these effects are likely due to the inhibition of RBC plasma membrane calcium ATPase which exports calcium from the RBCs [4]. Further, it has been shown that sphingosine can form pores in RBC membranes [8] and increase their permeability to small ions [7]. Thus, increased RBC sphingosine may contribute to membrane leakiness to small ions in SCD. It is not known if sphinganine exhibits similar effects on RBCs.

We observed significant increases in sphingoid base 1-phosphates in SCD RBCs. It has been shown that incubating RBCs with high concentrations of extracellular SO1P does not cause eryptosis, unlike its precursor SO [5]. However, knockout of the SO1P export protein MFSD2B, which causes an enormous buildup of SO1P and SA1P in the cells, does cause stomatocytosis and hemolysis [9]. Further, it was shown that buildup of SA1P in the RBCs is even more potent and inducing hemolysis than buildup of SO1P [9]. It has been shown that SO1P can modulate glycolysis by affecting the localization of glycolytic enzymes [101]. This is apparently mediated by a direct interaction with deoxygenated hemoglobin. Previous research in mice has shown that RBCs contribute at least 50% of plasma SO1P, with platelets and endothelial cells also being major contributors [106]. SO1P in the plasma is critical for maintaining proper endothelial barrier integrity [102]. Further, SO1P regulates the trafficking of many types of immune cells through the cell surface S1P receptors [103]. Thus, the elevation in RBC SO1P that we observed in this study is consistent with the observed vascular dysfunction and high levels of circulating immune cells observed in people with SCD. We previously reported that the increase in RBC SO1P occurs concurrently with an increase in plasma SO1P [69]. It is not clear whether the increase in SA1P that we observed in this study has any mechanistic impact on SCD pathology.

Altogether, this study has identified widespread dysfunction in the sphingolipid metabolic network in SS RBCs. Altered RBCs sphingolipid concentrations can contribute to SCD pathology in the RBCs and in the whole body. Thus, the entire sphingolipid metabolic network could serve as a novel therapeutic target for SCD treatment. Further research will be needed to determine which enzymes will serve as the most potent therapeutic target.

4.5 Materials and Methods

4.5.1 Red Blood Cell and Plasma Isolation

Whole blood was centrifuged at 200xg for 20 minutes to separate RBCs/white blood cells (WBCs) from platelet-rich plasma. The plasma supernatant was centrifuged again at 1000xg for 10 minutes to pellet platelets. The platelet-poor plasma supernatant was removed and used for further experiments. The RBCs/WBCs from the first centrifugation were washed once in 2 volumes of PBS and centrifuged at 700xg for 7 minutes. The PBS/plasma supernant was then removed. 3 volumes of PBS was added to the RBCs/WBCs and the cell suspension was layered onto 2 volumes of Ficoll-Paque Premium (GE Healthcare) and centrifuged at 400xg for 45 minutes to separate the RBCs and WBCs. After centrifugation, the buffy coat was carefully removed. RBCs were washed once with 2 volumes of PBS and centrifuged at 700xg for 7 minutes.

4.5.2 Sphingolipid Extraction

Sphingolipids were extracted from RBCs using a modification of the procedure described elsewhere [139]. Sphingoid base-type sphingolipids (SO, SA, SO1P, SA1P, LSM) and complex sphingolipids (ceramides, dihydroceramides, sphingomyelins, hexosylceramides, ceramide 1-phosphates) were extracted separately due to their different physical properties. The total sample volume was brought up to 400 μL by adding deionized water. Two 150 μL aliquots from each RBC sample were taken for sphingoid base analysis for complex sphingolipid analysis. An aliquot was also kept for total protein quantification using a BCA assay. 1.5 mL of a 2:1 mixture of methanol:methylene chloride was added to each sphingoid base sample and 1.5 mL of a 2:1 mixture of methanol:chloroform was added to

each complex sphingolipid sample. Next, 50 pmoles of internal standard mixture (Avanti Polar Lipids) was added to each sample. Samples were incubated overnight at 48°C to extract lipids. Next, 150 μL of 1 M KOH in methanol was added to each sample and the cell were incubated at 37°C for 2 hours. This is to cleave the ester bonds of contaminating glycerophospholipids. After incubating, 5 μL of glacial acetic acid was added to all samples to neutralize the KOH. pH was checked using pH strips. 1 mL of chloroform and 2 mLs of deionized water were added to all complex sphingolipid samples to induce phase separation. Sphingoid base and complex sphingolipid samples were centrifuged at 1400 xg for 8 minutes to pellet cell debris. For sphingoid base samples, the supernatant was transferred to a new glass tube. For complex sphingolipid samples, the bottom chloroform phase was transferred to new glass tubes. For sphingoid base samples, 0.5 mL of the 2:1 methanol:methylene chloride mixture was added to the cell debris in the original glass tubes. For complex sphingolipid samples, 1 mL of chloroform was added to the cell debris in the original glass tubes. The original tubes were all centrifuged at 1400 xg for 8 minutes. For sphingoid base samples the second supernatant was added to the first supernatant. For complex sphingolipid samples, the second bottom phase was added to the first bottom phase. Remaining cell debris was discarded. Organic solvents were removed by vacuum drying overnight in a Savant SpeedVac.

4.5.3 Preparation of Samples for LC-MS/MS Analysis

Dried sphingoid base samples were resuspended in 300 μL of a 3:2 mixture of mobile phase A1:mobile phase B1 solvent. Mobile phase A1 consisted of 58:41:1 methanol:water:formic acid and 5 mM ammonium formate. Mobile phase B1 consisted of 99:1 methanol:formic acid and 5 mM ammonium formate. Dried complex sphingolipid samples were

resuspended in 300 uL of mobile phase A2. Mobile phase A2 consisted of 97:21:1 acetonitrile:methanol:formic acid and 5 mM ammonium formate. Resuspended samples were centrifuged at 18,000 xg for 10 minutes to remove any remaining cell debris. The top 200 μL was transferred to an autosampler tube.

4.5.4 Sphingolipid LC-MS/MS Analysis

Sphingoid base samples were separated using a 2.1(i.d.) x 150 mm Phenomenex C18 column and a binary solvent system at a flow rate of 300 μL/min. Prior to injection, the column was equilibrated with 100% Mobile phase A1. After injection, the solvent composition was held a 100% A1 for 5 minutes followed by a linear gradient to 100% B1 over 15 minutes. The solvent composition was held at 100% B1 for 5 min, was dropped back to 100% A over 1 minute, and was then held at 100% A for 4 minutes. Complex sphingolipid samples were separated using a 2.1(i.d) x 150 mm Supelcosil NH2 column and a binary solvent system at a flow rate of 300 μL/min. Prior to injection, the column was equilibrated with 100% mobile phase A2. After injection, the solvent composition was held at 100% A for 5 minutes followed by a linear gradient for 1 minute. The solvent composition was held at 100% B for 14 minutes, was dropped back to 100% A over 1 minute, and was held at 100% A for 9 minutes. Since glucosylceramide and galactosylceramide are not separated by this chromatography method, their concentrations are reported together as hexosylceramide.

4.5.5 Multivariable Data Analysis

Heat map generation, principal component analysis, and correlation analysis were all performed in MATLAB R2018a (Mathworks).

4.5.6 Image Analysis

Western blot bands were quantified using ImageJ (NIH). Peak area of the ceramide kinase band was scaled by the β-actin band to give a relative intensity.

4.5.7 Statistics

Pairwise comparisons between AA and SS samples were performed using Welch's t-test using GraphPad Prism 6. No correction was made for multiple comparisons.

CHAPTER 5. EFFECTS OF PLASMA ENVIRONMENT AND RETICULOCYTES ON SICKLE RED BLOOD CELL SPHINGOLIPIDS

5.1 Abstract

Sickle cell disease is one of the most common hematologic disease in the world, affecting 4.4 million people around the world and over 100,000 people in the United States. Despite decades of research into the disease, we do not fully understand the molecular mechanisms leading to disease symptoms. We previously showed that sickle cell disease red blood cells have higher concentrations of many sphingolipids compared to normal red blood cells. These changes in concentrations could contribute significantly to disease pathology. However, the causes of the changes in sphingolipid concentrations are not clear. We proposed two hypotheses. First, we hypothesized that changes in plasma sphingolipid concentrations could change red blood cell sphingolipid concentrations by exchange of sphingolipids. Second, we hypothesized that sphingolipid concentrations in reticulocytes may be different than in mature erythrocytes and that the increased prevalence of reticulocytes in the sickle red blood cell population is the cause of the previously observed concentration differences. To test the first hypothesis, we collected the plasma and red blood cells from normal and sickle cell donors and measured their sphingolipid concentrations. We also, incubated red blood cells with plasma of the opposite genotype and measured the resulting sphingolipid concentrations. We employed two different methods to produce reticulocyte-enriched and reticulocyte-depleted populations of sickle red blood cells and then we measured the concentrations of sphingolipids in these cell

populations. Our results showed that the sphingolipid concentrations in sickle plasma are not significantly different from normal plasma. Our results further showed that sickle reticulocytes have elevated concentrations of multiple sphingomyelins compared to sickle erythrocytes. Thus, the alterations in red blood cell are not due to changes in plasma, but are partly explained by the increased sphingolipid concentration of reticulocytes.

5.2 Introduction

Sickle cell disease (SCD) is a genetic disease affecting more 4.4 million people worldwide and over 100,000 people in the United States. In a previous study, we showed that the sphingolipid concentrations in sickle cell disease genotype (SS) red blood cells (RBCs) were significantly different from those in normal genotype (AA) RBCs. Specifically, we reported significant increases in hexosylceramides, ceramides, dihydroceramides, lysosphingomyelins, sphingoid bases, and sphingoid base 1-phosphates in SS RBCs. However, the cause of the observed changes in RBC sphingolipid concentrations was not clear.

One hypothesis is that changes in plasma (PLA) sphingolipid concentrations could result in changes in RBC sphingolipid concentrations through exchange of the sphingolipids. It has been shown that the plasma contains a high concentration of sphingolipids [140, 141]. Due to their low solubility in water, sphingolipids are bound to lipoproteins and albumin with different sphingolipids being concentrated in different carrier proteins [140]. Since lipoproteins and albumin are synthesized in the liver, it is possible that plasma sphingolipid concentrations are regulated by the liver. One notable exception to this is sphingosine 1-phosphate (SO1P). Studies have shown that RBCs contribute at about 50% of plasma SO1P

with endothelial cells being the other major contributor [106]. It has been shown that sphingoid bases rapidly transfer from albumin to RBCs in vitro [70, 88]. Further, it has been shown that sphingoid base 1-phosphates transfer from RBCs to albumin and to HDL [73]. The exchange of complex sphingolipids is less well studied, but a few studies suggest that sphingomyelin can exchange between RBCs and lipoproteins over a long timescale [142]. A previous study from our group showed that there are significant increases in the concentrations of sphingosine and sphingosine 1-phosphate in SCD plasma [69]. Recently, it was reported that the concentrations of ceramides and sphingomyelins are significantly lowered in serum from SCD individuals [100]. Thus, it is possible that differences in PLA sphignolipids could result in differences in RBC sphingolipids.

A second hypothesis is that reticulocytes (RET) have different sphingolipid concentrations than mature erythrocytes and the increased prevalence of RETs in the sickle RBC population alters the average properties of the sickle RBC population. In a normal genotype individual, RETs make up 1-2% of the total RBC population. In an individual with SCD, RETs make up 10-20% of the total RBC population. Thus, properties of the reticulocytes will significantly affect the average properties of the RBC population in SCD though not in the normal genotype case. It is known that reticulocytes still retain residual mitochondria and some fragments of the endoplasmic reticulum and Golgi apparatus [143]. Thus, it is possible that enzymes associated with those organelles are still present in reticulocytes. Indeed, it has been shown that fatty acid beta-oxidation, a metabolic pathways that take place in the mitochondria, is absent in mature erythrocytes, but are active in reticulocytes [144]. Several other aspects of lipid metabolism appear to be different in reticulocytes compared to mature erythrocytes. Erythrocytes lack the enzyme acetyl-CoA carboxylase

which prevents de novo fatty acid biosynthesis whereas the full metabolic pathway is active in reticulocytes [145]. Further, reticulocytes seem to be able to synthesize glycerophospholipids de novo whereas erythrocytes cannot [146]. Thus, there are several known metabolic differences between reticulocytes and erythrocytes. However, little is known about sphingolipid concentrations in reticulocytes.

In this study we asked whether sphingolipid concentrations in SS PLA are different from those in AA PLA. Further, we asked whether changing the PLA environment of RBCs could alter their sphingolipid concentrations. Finally, we asked whether the sphingolipid concentrations in SS RETs are different from those in SS erythrocytes. To answer these questions, we isolated RBCs and PLA from AA and SS individuals and measured their sphingolipid concentrations. We also incubated RBCs with PLA of the opposite genotype and measured the resulting RBC sphingolipid concentrations. Further, we used discontinuous gradient density centrifugation and magnetic activated cell sorting (MACS) to isolate sickle reticulocyte-enriched RBC populations of different purities and then quantified their sphingolipid concentrations.

5.3 Results

5.3.1 Sphingolipid Concentrations in SS RBCs are Elevated Compared to Those in AA RBCs

We extracted and quantified the concentrations of 18 sphingolipids in RBC samples from 17 AA and 25 SS donors by LC-MS/MS. These included 7 sphingomyelins, 7 ceramides, 2 sphingoid bases, and 2 sphingoid base 1-phosphates. Our blood fractionation procedure

is shown diagrammatically in Figure 16. The results of the quantification of RBC sphingolipids are shown in Figure 17.

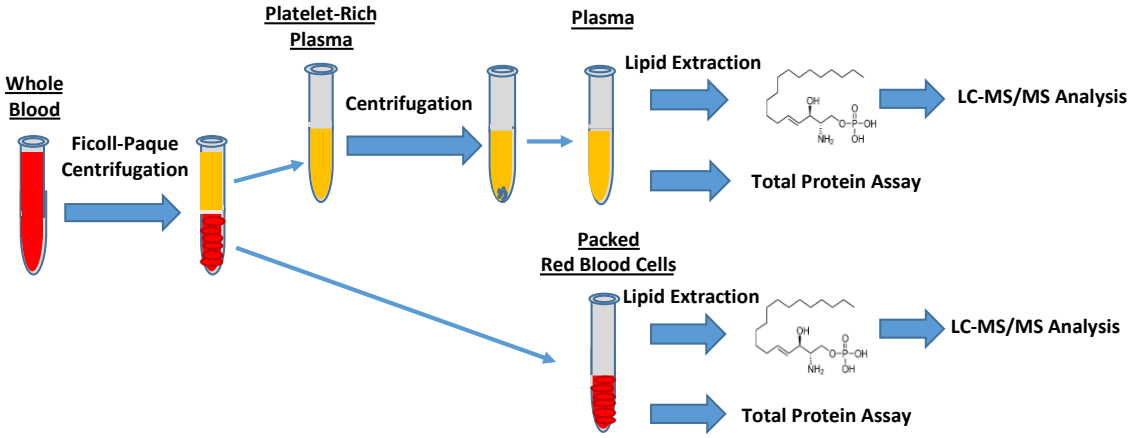

Figure 16. Sphingolipid Analysis of Human AA and SS RBCs and PLA. Human RBCs and PLA were isolated from whole blood. Sphingolipids were then extracted and analyzed by LC-MS/MS.

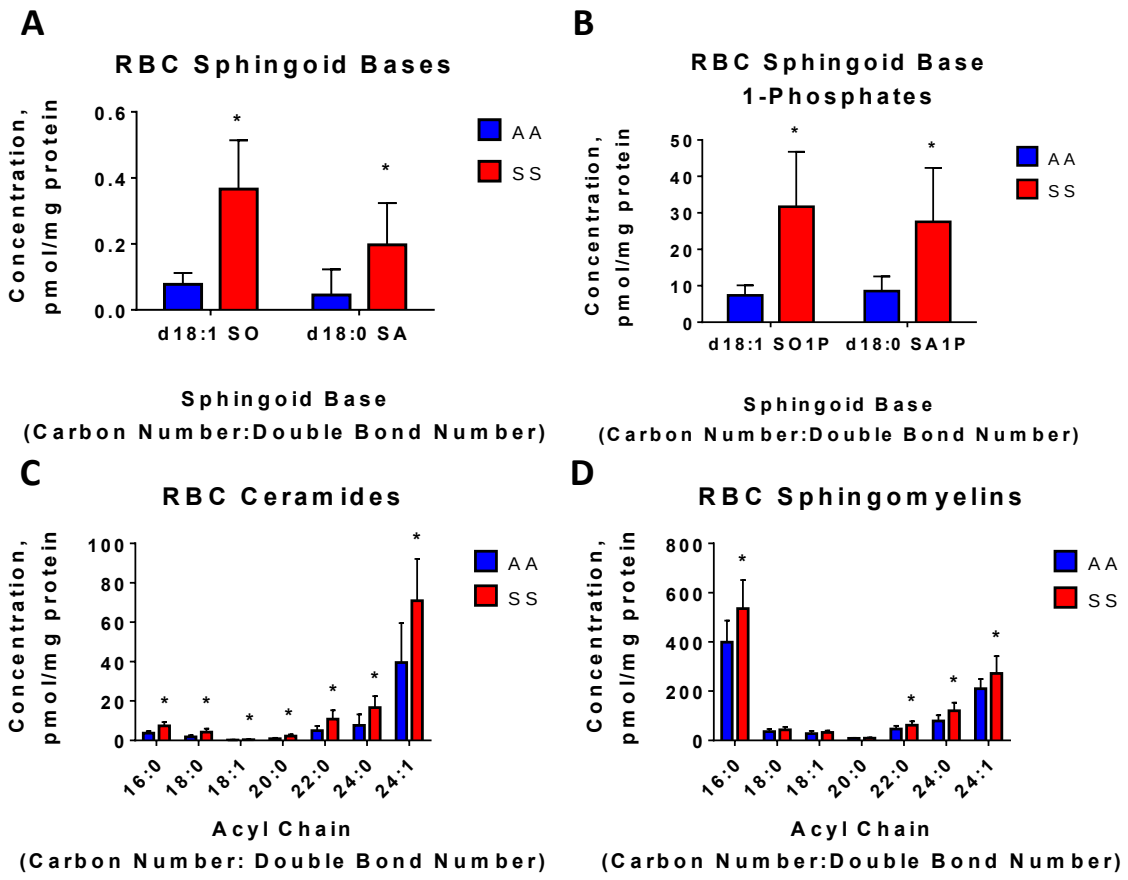

Figure 17. Sphingolipid Concentrations in AA and SS RBCs were Quantified by LC-MS/MS. A) Sphingoid bases B) Sphingoid Base 1-Phosphates C) Ceramides D) Sphingomyelins. Results from AA samples are shown in blue, results from SS samples are shown in red. Concentrations are given in units of pmoles/mg protein. * indicates $p<0.05$ compared to AA using a t-test with correction for multiple comparisons using the Holm-Sidak method.

As Figure 17 shows, the concentrations of 4 of the sphingomyelins, all 8 of the ceramides, both of the sphingoid bases, and both of the sphingoid base 1-phosphates were significantly elevated in SS RBCs.

5.3.2 Only Sphingosine and Sphingosine 1-Phosphate Concentrations are Elevated in SS PLA

We also extracted and quantified the concentrations of the same 18 sphingolipids in PLA samples from 16 AA and 19 SS donors. The results of the quantification of PLA sphingolipids are shown in Figure 18. As Figure 18 shows, only the concentrations of SO and SO1P are significantly elevated in SS PLA.

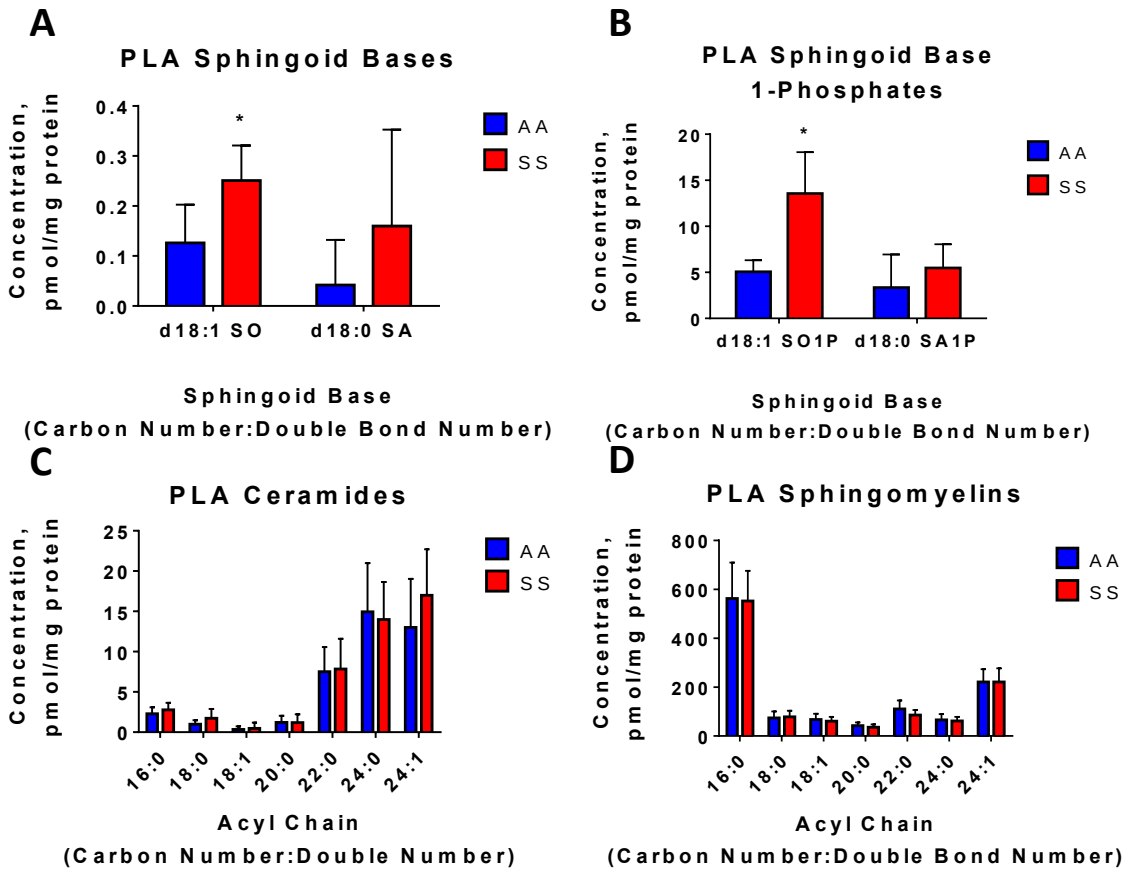

Figure 18. Sphingolipid Concentrations in AA and SS PLA were Quantified by LC-MS/MS. A) Sphingoid bases B) Sphingoid Base 1-Phosphates C) Ceramides D) Sphingomyelins. Results from AA samples are shown in blue, results from SS samples are shown in red. Concentrations are given in units of pmoles/mg protein. * indicates $p<0.05$ compared to AA using a t-test with correction for multiple comparisons using the Holm-Sidak method.

5.3.3 RBC and PLA Genotypes Separate Base on Sphingolipid Concentrations

The previous analysis examined each sphingolipid individually and identified those that are significantly different between AA and SS samples. Next, we evaluated whether the sphingolipid profile of SS samples as a whole is different from that of AA samples. To do this, we performed principal component analysis on the RBC and PLA samples. The scores of the RBC samples in principal components 1 and 2 are plotted against each other in Figure 19A. Together, principal components 1 and 2 capture over 70% of the variation in the data. As Figure 19A shows, AA and SS RBC samples separate from one another along principal components 1 and 2. The scores of the PLA samples in principal component 1 and 2 are plotted against each other in Figure 19B. Together, principal components 1 and 2 capture over 50% of the variation in the data. As Figure 18B shows, AA and SS PLA samples also separate from one another, though only along principal component 2.

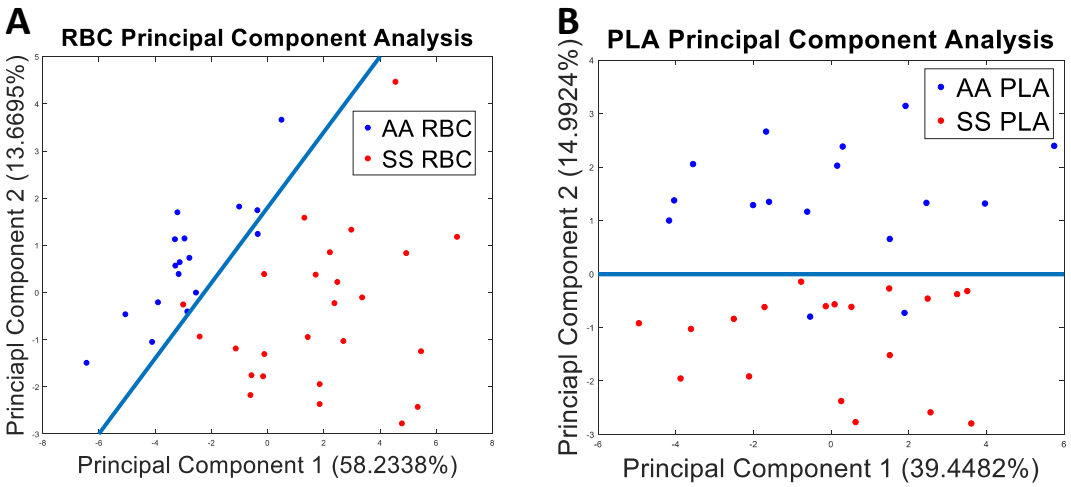

Figure 19. Principal Component Analysis was Performed on RBC and PLA Sphingolipid Concentration Data. A) RBC sphingolipid concentrations were represented in principal component space. B) PLA sphingolipid concentrations were represented in

principal component space. AA samples are shown as blue dots and SS samples are shown as red dots.

5.3.4 Plasma Environment Does Not Significantly Affect RBC Sphingolipid Concentrations

In order to investigate whether changes in the plasma environment in individuals with SCD can explain the changes observed sphingolipid concentrations in SCD RBCs, we incubated AA and SS RBCs in AA and SS PLA for 24 hours and subsequently measured the sphingolipid concentrations in the RBCs and PLA. The resulting concentration data were analyzed by 2-way ANOVA with multiple comparison tests. The RBC sphingolipid concentrations are shown in Figure 20.

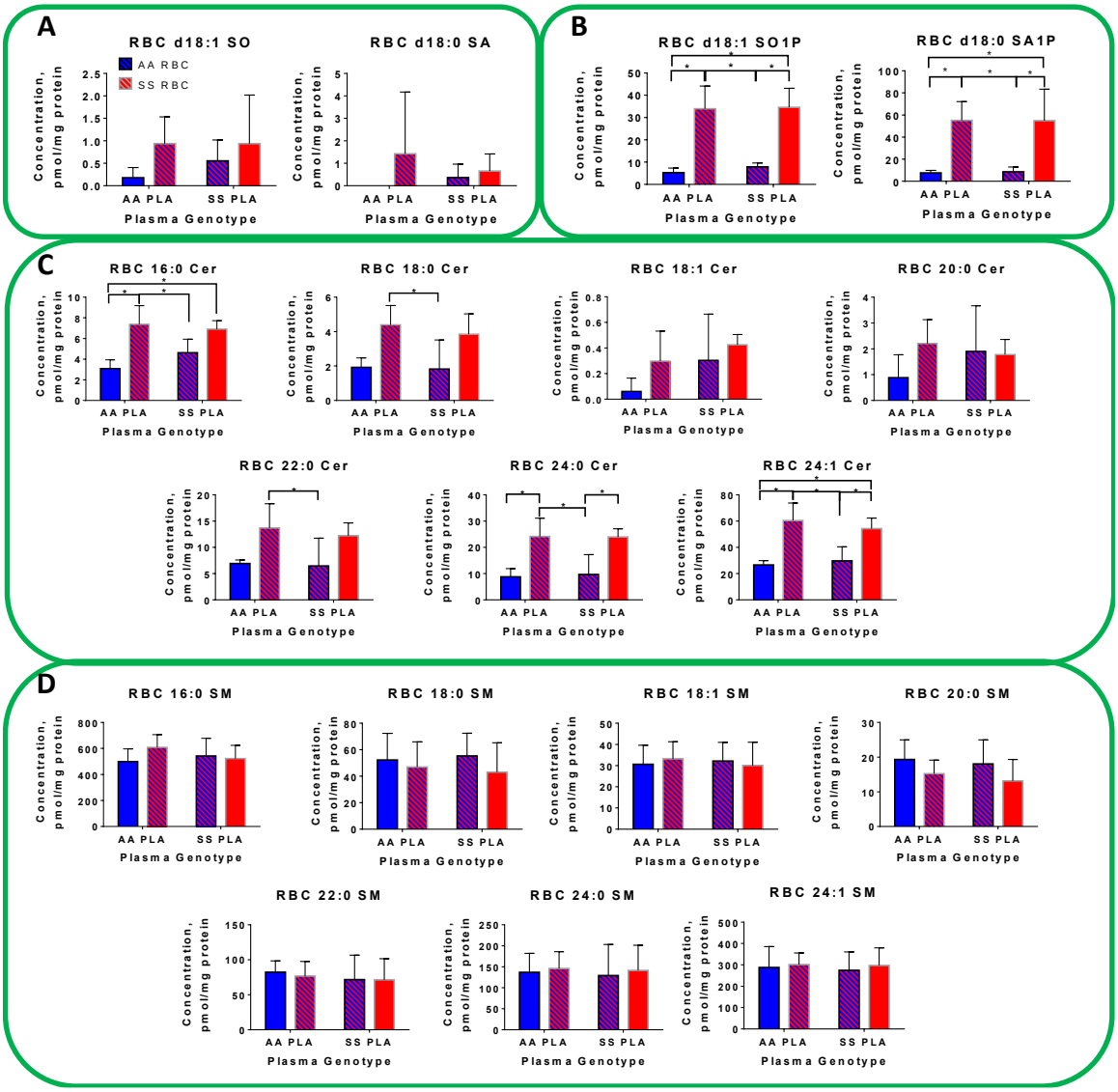

Figure 20. AA and SS RBCs were Incubated in PLA from AA and SS Donors and the RBC Sphingolipid Concentrations were Measured. RBC concentrations of A) sphingoid bases B) sphingoid base 1-phosphates C) ceramides and D) sphingomyelins were measured after incubating RBCs with plasma of different genotypes. AA RBCs incubated with AA PLA is indicated by solid blue bars, AA RBCs incubated with SS PLA is indicated by blue bars with red stripes, SS RBCs incubated with AA PLA is indicated by red bars with blue stripes, and SS RBCs incubated with SS PLA is indicated by solid red bars. * indicates $p<0.05$ in a 2-way ANOVA with post hoc multiple comparison t-tests.

As Figure 20A shows, there were no significant effects of either RBC genotype or PLA genotype on RBC sphingoid base concentrations. In contrast, Figure 20B shows that the RBC genotype, but not the PLA genotype did have a significant effect on RBC sphingoid

base 1-phosphate concentrations. As Figure 20C shows, the RBC genotype, but not the PLA genotype had a significant effect on RBC 16:0, 18:0, 22:0, 24:0, and 24:1 ceramide concentrations. Finally, as Figure 20D shows, neither the RBC genotype nor the PLA genotype had an effect on RBC sphingomyelin concentrations. Thus, the genotype of the PLA did not affect the concentrations of any RBC sphingolipid concentrations. The sphingolipid concentrations in the PLA after the incubation are shown in Figure 21. As Figure 21 shows, the PLA genotype did not have a significant effect on any of the PLA sphingolipid concentrations. The RBC genotype had a significant effect on PLA SO1P concentration only.

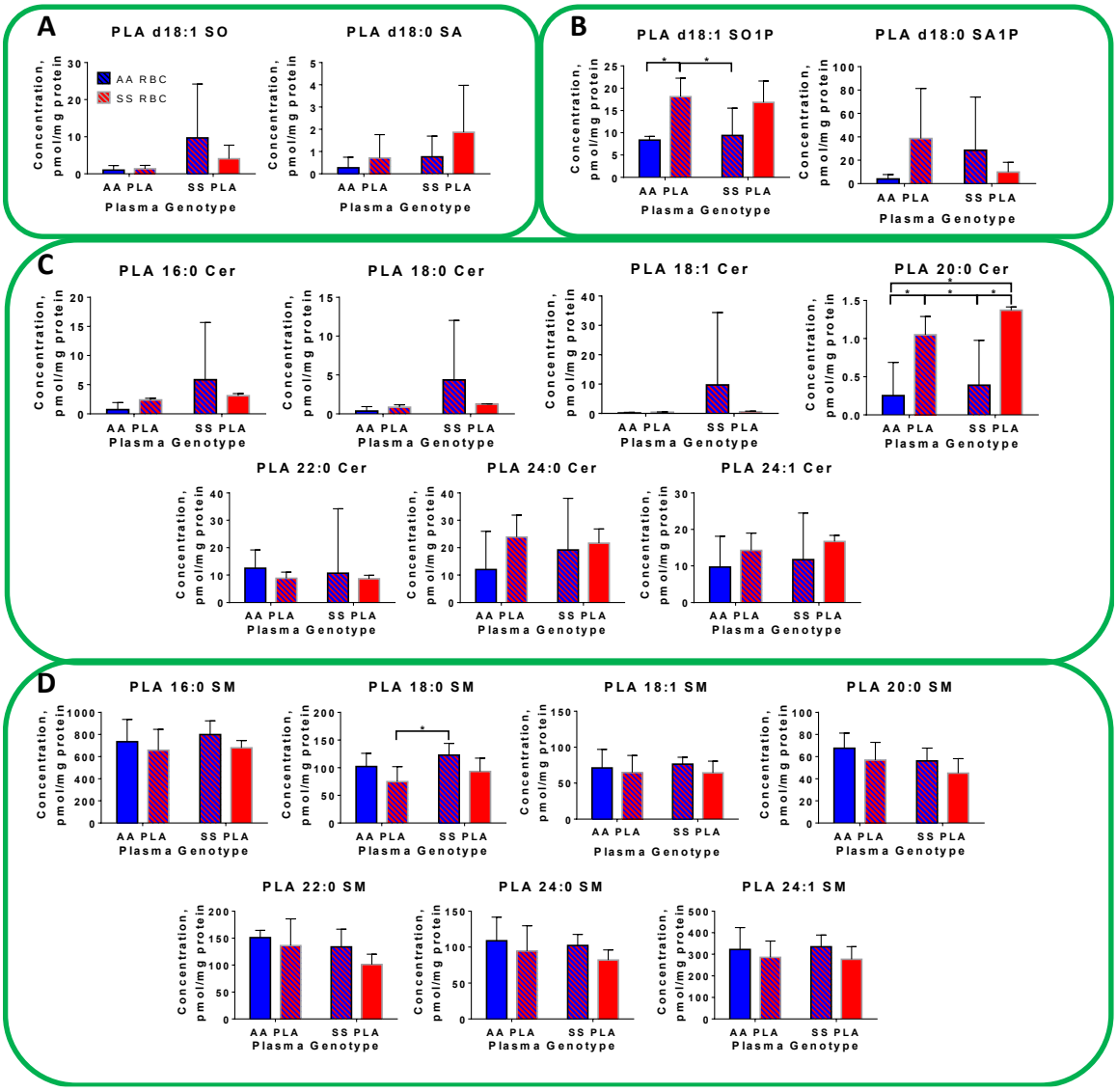

Figure 21. AA and SS RBCs were Incubated in PLA from AA and SS Donors and the PLA Sphingolipid Concentrations were Measured. PLA concentrations of A) sphingoid bases B) sphingoid base 1-phosphates C) ceramides and D) sphingomyelins were measured after incubating RBCs with plasma of different genotypes. AA RBCs incubated with AA PLA is indicated by solid blue bars, AA RBCs incubated with SS PLA is indicated by blue bars with red stripes, SS RBCs incubated with AA PLA is indicated by red bars with blue stripes, and SS RBCs incubated with SS PLA is indicated by solid red bars. * indicates $p<0.05$ in a 2-way ANOVA with post hoc multiple comparison t-tests.

5.3.5 Sphingomyelin and Sphingosine Concentrations are Elevated in SS RETs

Next, we investigated whether differences in sphingolipid concentrations in the SS RETs could explain the elevations in SS RBC sphingolipid concentrations. To do this, we first fractionated SS RBCs using discontinuous density gradient centrifugation on Optiprep. After fractionation, an aliquot was taken from each layer to analyze reticulocyte percentage by flow cytometry and an aliquot was taken for sphingolipid quantification by LC-MS/MS. Our procedure is shown diagrammatically in Figure 22A. Next, we performed linear regression analysis on the SS RBC sphingolipid concentration data and the reticulocyte % values from flow cytometry. The results of this analysis are shown in Fig 23. SO was the only sphingolipid that had a statistically significant positive slope ($p<0.0491$).

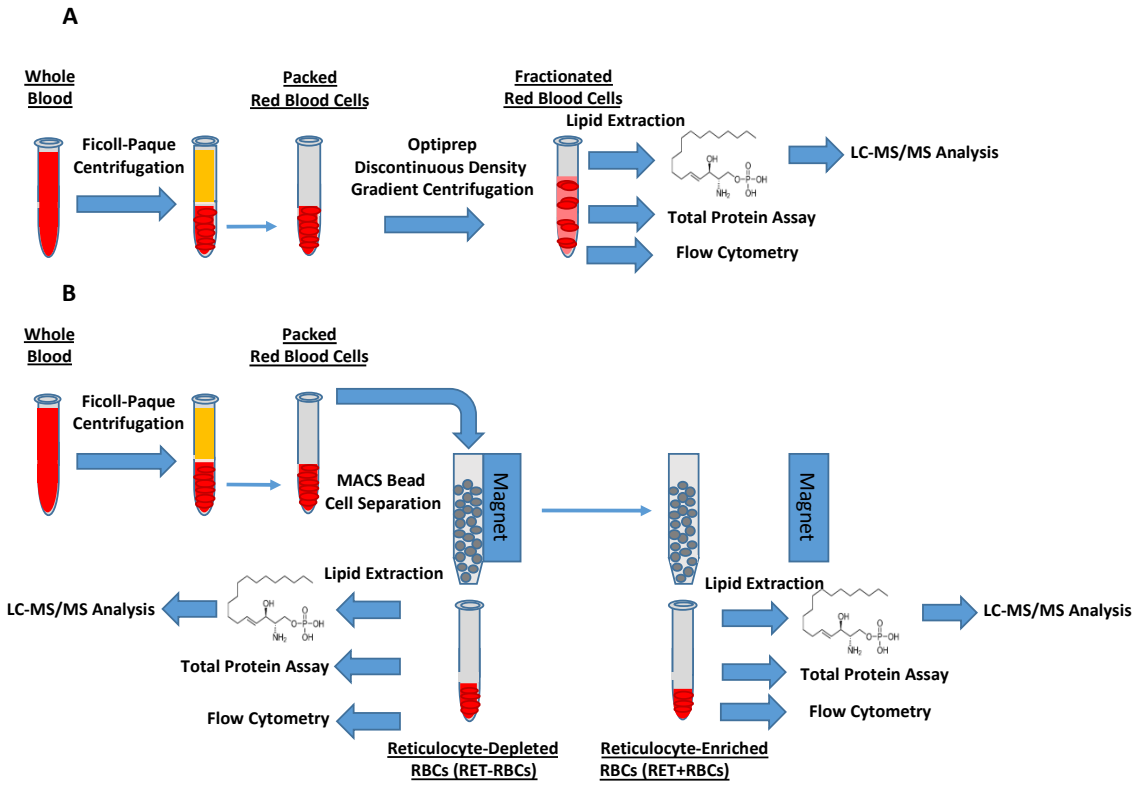

Figure 22. Sphingolipid Analysis of Human SS Reticulocytes. A) Packed SS RBCs were fractionated using Optiprep discontinuous density gradient centrifugation. The reticulocyte percentage in each layer was determined by flow cytometry. Sphingolipids were also extracted and analyzed by LC-MS/MS. B) Packed SS RBCs were fractionated using

MACS into reticulocyte-enriched and reticulocyte-depleted RBC populations. The reticulocyte percentage in each populations was determined by flow cytometry. Sphingolipids were also extracted and analyzed by LC-MS/MS.

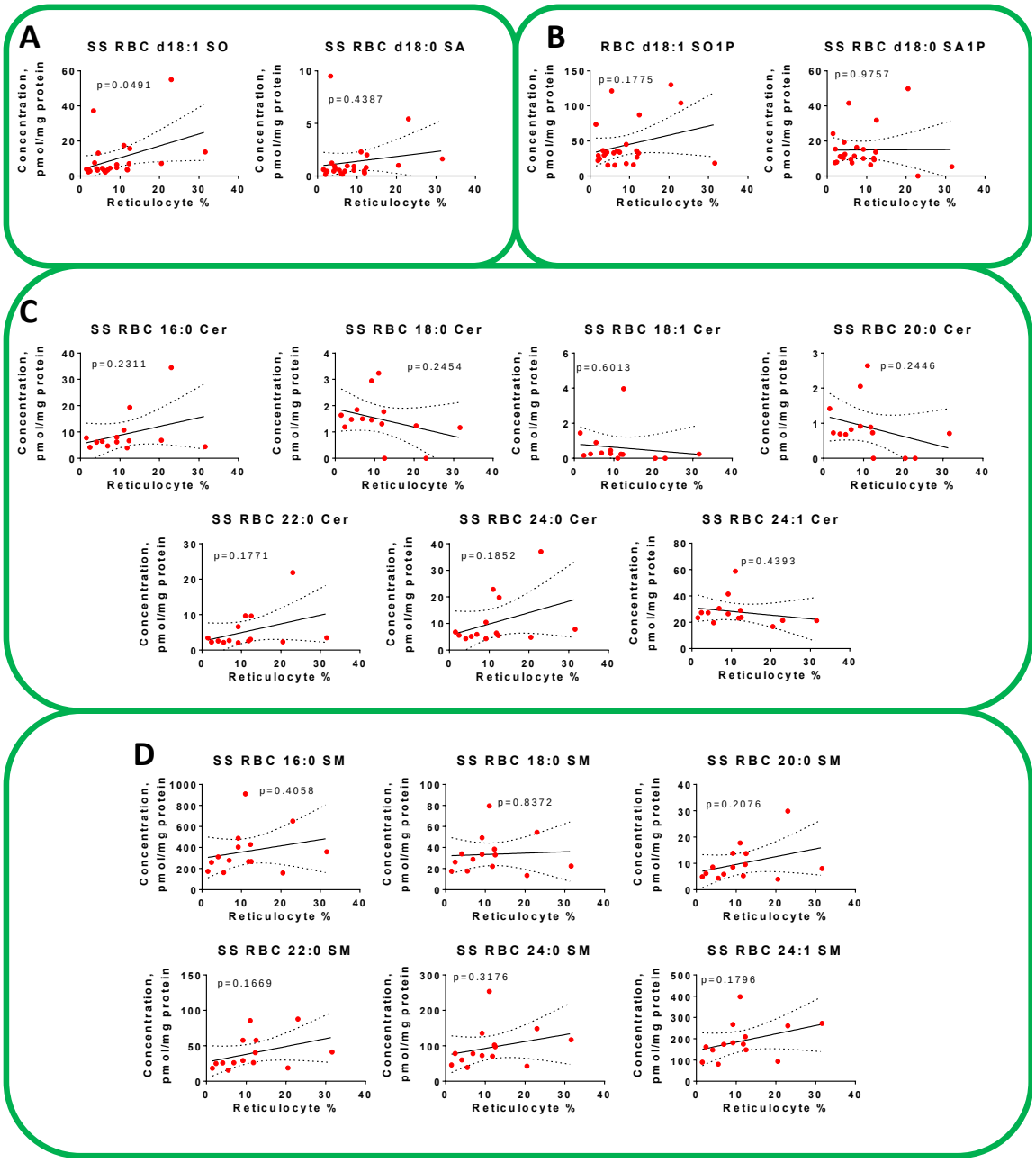

Figure 23. Linear Regression Analysis on RBC Sphingolipid Concentrations and Reticulocyte % was Performed for Optiprep-Separated SS RBCs. Linear regression between the concentrations of A) sphingoid bases B) sphingoid base 1-phosphates C) ceramides and D) sphingomyelins and the reticulocyte% in SS RBC populations was performed. p-values were calculated for the null hypothesis that the regression slope is 0.

Solid black lines indicate the best-fit line. Dotted black curves indicate the 95% confidence interval of the best-fit line.

One limitation of the Optiprep-based SS RBC fractionation is that we could only reach about 30% RET purity. Thus, we used an alternative approach for isolating RETs of a higher purity. We used the magnetic activated cell sorting (MACS) technique using Anti-CD71-coated magnetic beads to separate CD71+SS RETs from the rest of the SS RBC population. After separation, we quantified the percentage of reticulocytes in each fraction using flow cytometry and the sphingolipid concentrations using LC-MS/MS. Our procedure is shown diagrammatically in Figure 22B. Next, we performed linear regression analysis on the SS RBC sphingolipid concentration data and the reticulocyte % values from flow cytometry. The results of this analysis are shown in Fig 24.

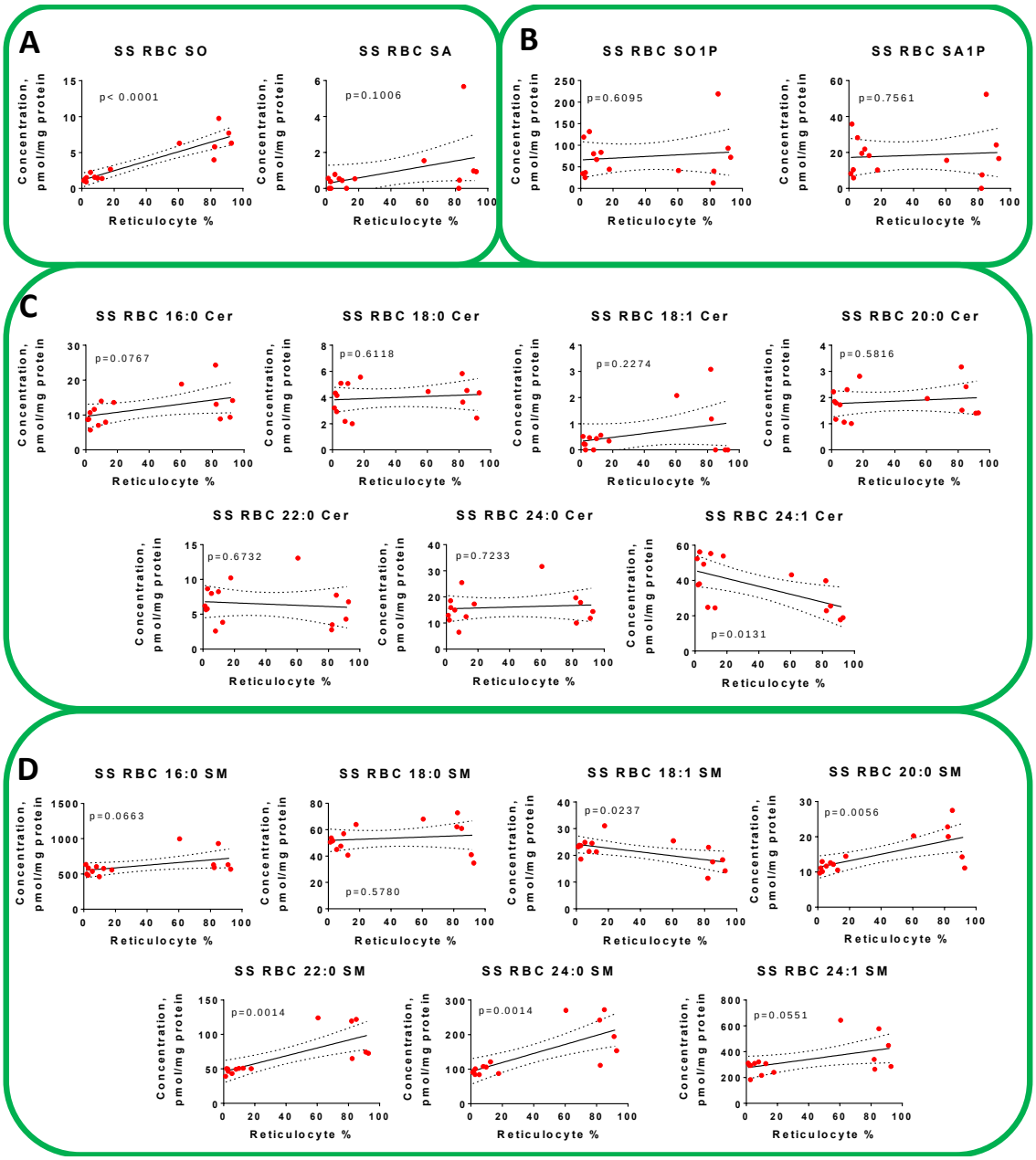

Figure 24. Linear Regression Analysis of RBC Sphingolipid Concentrations and Reticulocyte % was Performed for MACS-Separated SS RBCs. Linear regression between the concentrations of A) sphingoid bases B) sphingoid base 1-phosphates C) ceramides and D) sphingomyelins and the reticulocyte% in SS RBC populations was performed. p-values were calculated for the null hypothesis that the regression slope is 0.

Solid black lines indicate the best-fit line. Dotted black curves indicate the 95% confidence interval of the best-fit line.

As Figure 24A shows, and in agreement with the Optiprep-based SS RBC fractionation, the regression slope for SO was statistically significant, indicating that SS RETs have a concentration of SO that SS erythrocytes. Figure 24B shows that there were no statistically-significant relationships between sphingoid base 1-phosphate concentrations and reticulocyte %. Figure 24C shows that only 24:1 Cer had a statistically-significant negative regression slope, indicating SS RETs have lower concentrations of this ceramide species than SS erythrocytes. Finally, Figure 24D shows that 20:0, 22:0 and 24:0 SM all had statistically-significant positive regression slopes and 18:1 SM had a statistically-significant negative regression slope.

5.4 Discussion

In this study, we measured the concentrations of 18 sphingolipids in human RBC samples from AA and SS donors. We showed that the concentrations of sphingoid bases, sphingoid base 1-phosphates, ceramides, and sphingomyelins are elevated in SS RBCs. This is largely in agreement with previous studies from our group and others [69, 72]. However, this is the first study we are aware of that showed an elevation in sphingomyelin concentrations in SS RBCs. Considering that our current study used more donor samples than our previous study, we likely had more statistical power to detect differences in sphingomyelin concentrations.

We also measured the concentrations of 18 sphingolipids in human PLA samples from AA and SS donors. We showed that, in contrast to RBCs, there were few significant differences in sphingolipid concentrations in SS PLA. SO and SO1P were the only sphingolipids with

significantly elevated concentrations in SS PLA. The elevations in the concentrations of SO and SO1P in SS PLA are consistent with a previous report from our group [69]. A recent report showed that serum from SS donors has lower concentrations of many ceramides and sphingomyelins [100]. It has been shown that the serum and plasma concentrations of SO1P differ significantly due to release of SO1P from activated platelets [147]. Thus, it is possible that the differences between our current plasma sphingolipid results and the previous serum sphingolipid report are similarly rooted in platelet activation.

We incubated AA and SS RBCs with AA and SS PLA and subsequently measured the sphingolipid concentrations in the RBCs and PLA. We showed that while the PLA genotype did not significantly affect the concentrations of any of the RBC sphingolipids, the RBC genotype did significantly affect the concentrations of many RBC sphingolipids. This suggests that the differences in RBC sphingolipid concentrations observed in SCD are not mediated by the PLA. We also showed that the genotype of the RBC does have an impact on the PLA concentration of SO1P. It has been shown that RBCs actively produce and SO1P by the action of sphingosine kinase 1 [87] and export SO1P by the action of MFSD2B [9]. Thus, the effect of RBC genotype on PLA SO1P may reflect elevated activity of one or both of these proteins.

We used two different methods to fractionate SS RBCs into populations with varying enrichments of RETs and measured the concentrations of sphingolipids in the different populations. To the best of our knowledge, our study is the most comprehensive study of the sphingolipid content of human reticulocytes to date. Previous studies of the sphingolipid composition of reticulocytes have been deficient in that 1) they have mostly

been in animals and not humans, 2) they have only measured sphingomyelin, and 3) they have not measured the acyl chain subspecies of sphingomyelin. A study using rat erythrocytes showed that the sphingomyelin content as a percent of total phospholipid content decreases during in vitro differentiation from reticulocyte to erythrocyte [148]. This is consistent with our observation the RET+ SS RBCs have higher sphingomyelin concentrations than RET- SS RBCs.

Little is known about sphingolipid metabolism in reticulocytes. One study showed no difference in sphingosine kinase 1 activity between mature erythrocytes and reticulocyte in transgenic mouse model of sickle cell disease [72]. We could not find any other references to sphingolipid metabolism in reticulocytes in the literature. Multiple studies have shown that reticulocytes possess parts of lipid metabolism that mature erythrocytes do not. These include de novo biosynthesis of fatty acid and glycerophospholipids. Thus, it is possible that reticulocytes also contain additional sphingolipid metabolic activity.

Not much is known about functional roles of sphingolipids in reticulocytes beyond the recognized roles they play in RBCs generally. A recent report demonstrated that SO1P regulates the expression of the mitophagy genes Pink1 and Bnip3l in mouse late erythroid cells [149]. They further showed that exogenously adding SO1P could promote erythroid differentiation. These results may provide an explanation for the elevated SO1P that we have observed in SS RBCs relative to AA RBCs as SS erythroid progenitors are undergoing erythropoiesis at an accelerated rate. Another study in mice showed that intravenous administration of sphingomyelin resulted in an increase in iron utilization by the bone marrow and an increase in the number of circulating reticulocytes [150].

5.5 Materials and Methods

5.5.1 Isolation of Red Blood Cells and Plasma from Whole Blood

Whole blood was centrifuged at 200xg for 20 minutes to separate RBCs/WBCs from platelet-rich plasma. The plasma supernatant was centrifuged again at 1000xg for 10 minutes to pellet platelets. The platelet-poor plasma supernatant was removed and used for further experiments. The RBCs/WBCs from the first centrifugation were washed once in 2 volumes of PBS and centrifuged at 700xg for 7 minutes. The PBS/plasma supernant was then removed. 3 volumes of PBS was added to the RBCs/WBCs and the cell suspension was layered onto 2 volumes of Ficoll-Paque Premium (GE Healthcare) and centrifuged at 400xg for 45 minutes to separate the RBCs and WBCs. After centrifugation, the buffy coat was carefully removed. RBCs were washed once with 2 volumes of PBS and centrifuged at 700xg for 7 minutes.

5.5.2 Fractionation of SS RBCs using discontinuous density gradient centrifugation

Optiprep density gradient medium (Sigma Aldrich) was mixed with PBS to make solutions with densities of 1.08, 1.09, and 1.10 mg/mL. These solutions were gently stacked on top of each other, with the 1.10 mg/mL layer at the bottom. A 1:1 mixture of SS RBCs and PBS was gently place on top of the Optiprep layers. The tubes containing the RBCs and Optiprep were centrifuged to fractionate the RBCs between the different layers. After centrifugation, the layers were separated for further analysis.

5.5.3 Fractionation of SS RBCs using MACS

100 μL of SS RBCs were mixed with 800 μL of 0.2% BSA in PBS and 200 μL of Anti-CD71-coated magnetic beads (Miltenyi Biotec). The cell suspensions were mixed on a rotor at 4°C for 1 hour to allow the magnetic beads to bind to the reticulocytes. LS MACS columns (Miltenyi Biotec) were attached to a QuaddroMACS Separator stand (Miltenyi Biotec). The columns were wetted by passing 3 mL of BSA/PBS through the columns. The volumes of the cell suspensions were brought up to 3 mL with BSA/PBS and the entire cell suspension was layered onto the MACS column. The populations of RBCs that did not bind to the columns were collected in 15 mL tubes below the columns. The columns were washed with 3 more mL of BSA/PBS to completely wash out unbound cells. New 15 mL tubes were placed under the columns and the columns were removed from the stand. The column was washed twice with 3 mL of BSA/PBS to wash out the magnetic-bead bound RBCs. The resulting populations of RBCs will be referred to as RET+RBCs for the reticulocyte-enriched RBC population, and RET-RBCs for the reticulocyte-depleted RBC population.

5.5.4 Quantification of reticulocyte percent by flow cytometry

RBC populations were stained with Thiazole Orange as described previously [151]. Thiazole Orange is a nucleic acid stain. Since reticulocytes still have residual mRNA, but mature erythrocytes do not, Thiazole Orange can be used to distinguish the two cell types. The percentage of positively stained cells in each sample was determined using a BD LSRFortessa flow cytometer.

5.5.5 Sphingolipid Extraction for Steady-State Sphingolipidomic Analysis

Sphingolipids were extracted from RBCs populations using a modification of the procedure described elsewhere [139]. Samples were allowed to thaw on ice for 15 minutes. The total sample volume was brought up to 350 μL with deionized water. Sphingoid base-type sphingolipids (SO, SA, SO1P, SA1P, LSM) and complex sphingolipids (ceramides, sphingomyelins, hexosylceramides) were extracted separately due to their different physical properties. Two 150 μL aliquots from each RBC sample were taken for sphingoid base analysis and for complex sphingolipid analysis. An aliquot was also kept on ice for total protein quantification using a BCA assay. 1.5 mL of a 2:1 mixture of methanol:methylene chloride was added to each sphingoid base sample and 1.5 mL of a 2:1 mixture of methanol:chloroform was added to each complex sphingolipid sample. Next, 50 pmoles of internal standard mixture (Avanti Polar Lipids) was added to each sample. Samples were incubated overnight at 48°C to extract lipids. Next, 150 μL of 1 M KOH in methanol was added to each sample and the cell were incubated at 37°C for 2 hours. This is to cleave the ester bonds of contaminating glycerophospholipids. After incubating, 4 μL of glacial acetic acid was added to all samples to neutralize the pH. pH was checked using pH strips. 1 mL of chloroform and 2 mLs of deionized water were added to all complex sphingolipid samples to induce phase separation. Sphingoid base and complex sphingolipid samples were centrifuged at 1400 xg for 8 minutes to pellet cell debris. For sphingoid base samples, the supernatant was transferred to a new glass tube. For complex sphingolipid samples, the bottom chloroform phase was transferred to new glass tubes. For sphingoid base samples, 0.5 mL of the 2:1 methanol:methylene chloride mixture was added to the cell debris in the original glass tubes. For complex sphingolipid samples, 1 mL of chloroform was added to the cell debris in the original glass tubes. The

original tubes were all centrifuged at 1400 xg for 8 minutes. For sphingoid base samples the second supernatant was added to the first supernatant. For complex sphingolipid samples, the second bottom phase was added to the first bottom phase. Remaining cell debris was discarded. Organic solvents in the sample tubes were removed by vacuum drying overnight in a Savant SpeedVac.

5.5.6 Total protein quantification using BCA assay

Total protein concentrations in RBC and media samples were quantified using a BCA assay (Thermo Scientific) according to manufacturer's instructions. Protein absorbance was measured using a SpectraMax spectrophotometer (Molecular Devices).

5.5.7 Preparation of samples for LC-MS/MS Analysis

Dried sphingoid base samples were resuspended in 300 μL of a 3:2 mixture of mobile phase A1:mobile phase B1 solvent. Mobile phase A1 solvent consisted of 58:41:1 methanol:water:formic acid and 5 mM ammonium formate. Mobile phase B1 solvent consisted of 99:1 methanol:formic acid and 5 mM ammonium formate. Dried complex sphingolipid samples were resuspended in 300 μL of mobile phase A2 solvent. Mobile phase A2 solvent consisted of 97:2:1 acetonitrile:methanol:formic acid and 5 mM ammonium formate. Resuspended samples were centrifuged at 16,000 xg for 10 minutes to remove any remaining cell debris. The top 200 μL from each was then transferred to an autosampler tube for analysis.

5.5.8 Sphingolipid LC-MS/MS Analysis

Sphingoid base samples were separated using a 2.1(i.d.) x 150 mm Phenomenex C18 column and a binary solvent system at a flow rate of 300 μL/min. Prior to injection, the column was equilibrated with 100% Mobile phase A1. After injection, the solvent composition was held a 100% A1 for 5 minutes followed by a linear gradient to 100% B1 over 15 minutes. The solvent composition was held at 100% B1 for 5 min, was dropped back to 100% A over 1 minute, and was then held at 100% A for 4 minutes. Complex sphingolipid samples were separated using a 2.1(i.d) x 150 mm Supelcosil NH2 column and a binary solvent system at a flow rate of 300 μL/min. Prior to injection, the column was equilibrated with 100% mobile phase A2. After injection, the solvent composition was held at 100% A for 5 minutes followed by a linear gradient for 1 minute. The solvent composition was held at 100% B for 14 minutes, was dropped back to 100% A over 1 minute, and was held at 100% A for 9 minutes. Since glucosylceramide and galactosylceramide are not separated by this chromatography method, their concentrations are reported together as hexosylceramide.

5.5.9 Statistical Analysis

For comparisons of sphingolipid concentrations between two groups, statistical significance was determined using unpaired t-tests correction for multiple comparisons using the Holm-Sidak method. For determination of the effects of RBC and PLA gentotpe on RBC and PLA sphingolipid concentrations, 2-way ANOVA was performed with post-hoc t-tests corrected for multiple comparisons with the Holm-Sidak method.

CHAPTER 6. CONCLUSIONS AND FUTURE DIRECTIONS

6.1 Overall summary

This work represents a significant contribution to multiple fields of study including hematology, lipid biochemistry, and mathematical biology. Specifically, we have expanded our understanding of normal red blood cell biology, sickle cell pathology, and the roles that sphingolipids play in both cases. Further, we have constructed the first computational model of RBC SO1P metabolism. This model can be a powerful tool in contexts where RBC SO1P plays an important role including hypoxia stress [10], sickle cell disease [87] , and immunomodulation [103].

In aim 1, we compiled, for the first time, all of the biochemical and biophysical information currently available in the literature on human red blood cell SO1P metabolism into a computational model. The construction of the model in and of itself is useful as it highlights what is known and what is not known about RBC sphingolipid metabolism. Despite many gaps in our knowledge, we constructed a model that reasonably represents RBC SO1P metabolism in vitro. We then fit our model to multiple dynamic data sets allowing for fine-tuning of enzyme activities and biophysical transport processes. We showed that RBC and PLA SO1P concentrations are highly sensitive to changes in hematocrit and less sensitive to changes in the activity of sphingosine kinase 1 and the RBC concentration of ceramide.

In aim 2, we expanded our scope and examined differences in the entire sphingolipid metabolic between normal and sickle RBCs. We used LC-MS/MS to measure the

concentrations of 89 sphingolipids in both RBC populations making this the most comprehensive sphingolipidomic analysis conducted to date in normal or sickle RBCs. We identified widespread eleveations in the concentrations of sphingolipids in sickle red RBCs. Further using correlation analysis, we showed evidence of alterations of many of the enzymes that interconvert ceramides with other classes of sphingolipids in sickle RBCs.

In aim 3, we focused on identifying the cause of the changes in sphingolipid concentrations in sickle RBCs. We measured the concentrations of sphingolipids in normal and sickle plasma. We showed that there are few differences in sickle plasma compared to normal plasma. We then used two different technqiues to isolate sickle RBC populations of varying degree of enrichment in reticulocytes. We then measured the concentrations of sphingolipids in these different RBC populations. We showed that reticulocyte-enriched populations consistently have elevated concentrations of sphingomyelins as well as the sphingoid base sphingosine.

6.2 Expansion of time-series experiments and modeling to complex sphingolipids

The scope of our modeling efforts was limited to the immediate metabolism of SO1P because many of the biochemical details of complex sphingolipid metabolism are not known in RBCs. Generating time series data by perturbing complex sphingolipid metabolism directly may give us enough information to overcome this limitation.

The time-series experiments performed as part of this thesis were limited to the addition of SO to RBCs in vitro. This was partly for practical reasons. First, SO can bind to albumin which makes it easy to disperse SO into aqueous cell media at high concentrations. Second, SO has a modest solubility in water. Studies have shown that the rate of transfer of a lipid

from one carrier to another is directly proportional to the water solubility of the lipid. Thus, it is relatively easy to deliver SO to RBCs on a short time scale. Expanding our analysis to the complex sphingolipids requires overcoming some practical challenges. First, long-chain complex sphingolipids do not bind to albumin. Thus, an alternative carrier must be used to get complex sphingolipids into cell media. Second, long-chain complex sphingolipids have little to no water solubility. Thus, even if a carrier is used, it will take long periods of time to achieve any significant delivery to the RBCs.

As a first step towards expanding our time-series methodology to complex sphingolipids, short-chain complex sphingolipids can be used. Short chain complex sphingolipids with C2 or C6 (though apparently not C12) fatty acyl side chains are still able to bind to albumin. Further, they still exhibit a modest solubility in water which enables relatively fast transfer to cells. The downside of using these short-chain sphingolipids is that they are not naturally occuring. Thus, the rates at which enzymes process these short-chain sphingolipids may be very different from those for natural long-chain sphingolipids.

6.3 Use of stable isotope tracers in dynamic time-series analysis

In the dynamic time-series studies performed for this thesis, RBCs were exposed to relatively large extracellular concentrations of SO to induce dynamic behavior in the metabolic pathway. This was done in order to bring the concentrations of sphingolipids in very small samples above the limit of detection of the mass spectrometer and to create clearly observable dynamics. However, it is possible that exposure to such large concentrations of SO may have been stressful for the cells. While it is possible that using

smaller concentrations of SO could alleviate these concerns, it is also possible that using stable isotopes is a better solution.

6.4 Extension of model to the in vivo context

The modeling studies presented in this thesis were strictly focused on the behavior of RBC SO1P metabolism in vitro. However, enough detail is known about SO1P relase from RBCs and metabolism in plasma that the model could easily be extended to the in vivo context. Further details could be incorporated such as differences in the binding and metabolism of SO1P bound to albumin or HDL in plasma. Further, models of the other major contributors to plasma SO1P, endothelial cells and platelets, could be built and integrated with the red blood cell model to give a moreintegrated picture of SO1P metabolism in blood.

CHAPTER 7. REFERENCES

1. Liu, S.C., et al., *Red cell membrane remodeling in sickle cell anemia. Sequestration of membrane lipids and proteins in Heinz bodies.* J Clin Invest, 1996. **97**(1): p. 29-36.

2. Charache, S., et al., *Hydroxyurea-induced augmentation of fetal hemoglobin production in patients with sickle cell anemia.* Blood, 1987. **69**(1): p. 109-16.

3. Niihara, Y., et al., *Oral L-glutamine therapy for sickle cell anemia: I. Subjective clinical improvement and favorable change in red cell NAD redox potential.* Am J Hematol, 1998. **58**(2): p. 117-21.

4. Colina, C., V. Cervino, and G. Benaim, *Ceramide and sphingosine have an antagonistic effect on the plasma-membrane Ca2+-ATPase from human erythrocytes.* Biochem J, 2002. **362**(Pt 1): p. 247-51.

5. Qadri, S.M., et al., *Sphingosine but not sphingosine-1-phosphate stimulates suicidal erythrocyte death.* Cell Physiol Biochem, 2011. **28**(2): p. 339-46.

6. von Wnuck Lipinski, K., et al., *Hepatocyte nuclear factor 1A deficiency causes hemolytic anemia in mice by altering erythrocyte sphingolipid homeostasis.* Blood, 2017. **130**(25): p. 2786-2798.

7. Contreras, F.X., et al., *Sphingosine increases the permeability of model and cell membranes.* Biophys J, 2006. **90**(11): p. 4085-92.

8. Siskind, L.J., et al., *Sphingosine forms channels in membranes that differ greatly from those formed by ceramide.* J Bioenerg Biomembr, 2005. **37**(4): p. 227-36.

9. Vu, T.M., et al., *Mfsd2b is essential for the sphingosine-1-phosphate export in erythrocytes and platelets.* Nature, 2017. **550**(7677): p. 524-528.

10. Sun, K., et al., *Sphingosine-1-phosphate promotes erythrocyte glycolysis and oxygen release for adaptation to high-altitude hypoxia.* Nat Commun, 2016. **7**: p. 12086.

11. Contreras, F.X., et al., *Asymmetric addition of ceramides but not dihydroceramides promotes transbilayer (flip-flop) lipid motion in membranes.* Biophys J, 2005. **88**(1): p. 348-59.

12. Siskind, L.J., R.N. Kolesnick, and M. Colombini, *Ceramide forms channels in mitochondrial outer membranes at physiologically relevant concentrations.* Mitochondrion, 2006. **6**(3): p. 118-25.

13. Lang, K.S., et al., *Involvement of ceramide in hyperosmotic shock-induced death of erythrocytes.* Cell Death Differ, 2004. **11**(2): p. 231-43.

14. Lang, P.A., et al., *Stimulation of erythrocyte ceramide formation by platelet-activating factor.* J Cell Sci, 2005. **118**(Pt 6): p. 1233-43.

15. LaRocca, T.J., et al., *Human-specific bacterial pore-forming toxins induce programmed necrosis in erythrocytes.* MBio, 2014. **5**(5): p. e01251-14.

16. Dodge, J.T. and G.B. Phillips, *Composition of phospholipids and of phospholipid fatty acids and aldehydes in human red cells.* J Lipid Res, 1967. **8**(6): p. 667-75.

17. Dinkla, S., et al., *Functional consequences of sphingomyelinase-induced changes in erythrocyte membrane structure.* Cell Death Dis, 2012. **3**: p. e410.

18. Abed, M., et al., *Sphingomyelinase-induced adhesion of eryptotic erythrocytes to endothelial cells.* Am J Physiol Cell Physiol, 2012. **303**(9): p. C991-9.

19. Ruiz-Arguello, M.B., et al., *Different effects of enzyme-generated ceramides and diacylglycerols in phospholipid membrane fusion and leakage.* J Biol Chem, 1996. **271**(43): p. 26616-21.

20. Ways, P. and D.J. Hanahan, *Characterization and quantification of red cell lipids in normal man.* J Lipid Res, 1964. **5**(3): p. 318-28.

21. Gercken, G., et al., *Fatty acid composition of phospholipids in erythrocytes of adults, normal newborn infants, and neonates with Rh erythroblastosis.* Pediatr Res, 1972. **6**(5): p. 487-94.

22. Boegheim, J.P., Jr., et al., *The sphingomyelin pools in the outer and inner layer of the human erythrocyte membrane are composed of different molecular species.* Biochim Biophys Acta, 1983. **735**(3): p. 438-42.

23. Myher, J.J., A. Kuksis, and S. Pind, *Molecular species of glycerophospholipids and sphingomyelins of human plasma: comparison to red blood cells.* Lipids, 1989. **24**(5): p. 408-18.

24. Verkleij, A.J., et al., *The asymmetric distribution of phospholipids in the human red cell membrane. A combined study using phospholipases and freeze-etch electron microscopy.* Biochim Biophys Acta, 1973. **323**(2): p. 178-93.

25. Zwaal, R.F., et al., *Organization of phospholipids in human red cell membranes as detected by the action of various purified phospholipases.* Biochim Biophys Acta, 1975. **406**(1): p. 83-96.

26. Allan, D. and C.M. Walklin, *Endovesiculation of human erythrocytes exposed to sphingomyelinase C: a possible explanation for the enzyme-resistant pool of sphingomyelin.* Biochim Biophys Acta, 1988. **938**(3): p. 403-10.

27. Murate, M., et al., *Transbilayer distribution of lipids at nano scale.* J Cell Sci, 2015. **128**(8): p. 1627-38.

28. Tyteca, D., et al., *Three unrelated sphingomyelin analogs spontaneously cluster into plasma membrane micrometric domains.* Biochim Biophys Acta, 2010. **1798**(5): p. 909-27.

29. Carquin, M., et al., *Endogenous sphingomyelin segregates into submicrometric domains in the living erythrocyte membrane.* J Lipid Res, 2014. **55**(7): p. 1331-42.

30. D'Auria, L., et al., *Segregation of fluorescent membrane lipids into distinct micrometric domains: evidence for phase compartmentation of natural lipids?* PLoS One, 2011. **6**(2): p. e17021.

31. Dawson, G., *Detection of glycosphingolipids in small samples of human tissue.* Ann Clin Lab Sci, 1972. **2**(4): p. 274-84.

32. Fletcher, K.S., E.G. Bremer, and G.A. Schwarting, *P blood group regulation of glycosphingolipid levels in human erythrocytes.* J Biol Chem, 1979. **254**(22): p. 11196-8.

33. Koscielak, J., et al., *Structures and fatty acid compositions of neutral glycosphingolipids of human plasma.* Biochim Biophys Acta, 1978. **530**(3): p. 385-93.

34. Marcus, D.M., M. Naiki, and S.K. Kundu, *Abnormalities in the glycosphingolipid content of human Pk and p erythrocytes.* Proc Natl Acad Sci U S A, 1976. **73**(9): p. 3263-7.

35. Vance, D.E. and C.C. Sweeley, *Quantitative determination of the neutral glycosyl ceramides in human blood.* J Lipid Res, 1967. **8**(6): p. 621-30.

36. Vance, D.E., W. Krivit, and C.C. Sweeley, *Concentrations of glycosyl ceramides in plasma and red cells in Fabry's disease, a glycolipid lipidosis.* J Lipid Res, 1969. **10**(2): p. 188-92.

37. Yamakawa, T., S. Yokoyama, and N. Kiso, *Structure of main globoside of human erythrocytes.* J Biochem, 1962. **52**: p. 228-9.

38. Hakomori, S. and G.D. Strycharz, *Investigations on cellular blood-group substances. I. Isolation and chemical composition of blood-group ABH and Le-b isoantigens of sphingoglycolipid nature.* Biochemistry, 1968. **7**(4): p. 1279-86.

39. Gardas, A. and J. Koscielak, *Megaloglycolipids--unusually complex glycosphingolipids of human erythrocyte membrane with A, B, H and I blood group specificity.* FEBS Lett, 1974. **42**(1): p. 101-4.

40. Feizi, T., et al., *Blood-group-Ii-active gangliosides of human erythrocyte membranes.* Biochem J, 1978. **173**(1): p. 245-54.

41. Koscielak, J., et al., *Isolation and characterization of poly(glycosyl)ceramides (megaloglycolipids) with A, H and I blood-group activities.* Eur J Biochem, 1976. **71**(1): p. 9-18.

42. Watanabe, K., R.A. Laine, and S.I. Hakomori, *On neutral fucoglycolipids having long, branched carbohydrate chains: H-active and I-active glycosphingolipids of human erythrocyte membranes.* Biochemistry, 1975. **14**(12): p. 2725-33.

43. Hauser, R., *Observations on the Lewis (a) and Lewis (b) activity of erythrocytes.* Int J Legal Med, 1995. **108**(1): p. 50-2.

44. Dejter-Juszynski, M., et al., *Blood-group ABH-specific macroglycolipids of human erythrocytes: isolation in high yield from a crude membrane glycoprotein fraction.* Eur J Biochem, 1978. **83**(2): p. 363-73.

45. Hakomori, S., K. Stellner, and K. Watanabe, *Four antigenic variants of blood group A glycolipid: examples of highly complex, branched chain glycolipid of animal cell membrane.* Biochem Biophys Res Commun, 1972. **49**(4): p. 1061-8.

46. Koscielak, J., et al., *Structures of fucose-containing glycolipids with H and B blood-group activity and of sialic acid and glucosamine-containing glycolipid of human-erythrocyte membrane.* Eur J Biochem, 1973. **37**(2): p. 214-25.

47. Stellner, K., K. Watanabe, and S. Hakomori, *Isolation and characterization of glycosphingolipids with blood group H specificity from membranes of human erythrocytes.* Biochemistry, 1973. **12**(4): p. 656-61.

48. Schenkel-Brunner, H., *Blood-group-ABH antigens of human erythrocytes. Quantitative studies on the distribution of H antigenic sites among different classes of membrane components.* Eur J Biochem, 1980. **104**(2): p. 529-34.

49. Larson, G. and B.E. Samuelsson, *Blood group type glycosphingolipids of human cord blood erythrocytes.* J Biochem, 1980. **88**(3): p. 647-57.

50. Kushi, Y., et al., *Characterization of blood group ABO(H)-active gangliosides in type AB erythrocytes and structural analysis of type A-active ganglioside variants in type A human erythrocytes.* Biochim Biophys Acta, 2001. **1525**(1-2): p. 58-69.

51. Kushi, Y., et al., *Characterization of blood-group-ABO(H)-active glycosphingolipids in type-AB human erythrocytes.* Eur J Biochem, 1995. **231**(3): p. 862-7.

52. Kannagi, R., S.B. Levery, and S. Hakomori, *Blood group H antigen with globo-series structure. Isolation and characterization from human blood group O erythrocytes.* FEBS Lett, 1984. **175**(2): p. 397-401.

53. Hanfland, P., et al., *Purification and structures of branched blood-group-B-active glycosphingolipids from human erythrocyte membranes.* Eur J Biochem, 1984. **145**(3): p. 531-42.

54. Ackerman, G.A., K.W. Wolken, and F.B. Gelder, *Surface distribution of monosialoganglioside GM1 on human blood cells and the effect of exogenous GM1 and neuraminidase on cholera toxin surface labeling. A quantitative immunocytochemical study.* J Histochem Cytochem, 1980. **28**(10): p. 1100-12.

55. Blanchard, D., et al., *Identification of a novel ganglioside on erythrocytes with blood group Cad specificity.* J Biol Chem, 1985. **260**(13): p. 7813-6.

56. Mrowczynska, L. and H. Hagerstrand, *Patching of ganglioside(M1) in human erythrocytes - distribution of CD47 and CD59 in patched and curved membrane.* Mol Membr Biol, 2008. **25**(3): p. 258-65.

57. Portoukalian, J., et al., *Alteration of gangliosides in plasma and red cells of humans bearing melanoma tumors.* Biochem Biophys Res Commun, 1978. **85**(3): p. 916-20.

58. Zhou, Z., et al., *Erythrocyte membrane sulfatide plays a crucial role in the adhesion of sickle erythrocytes to endothelium.* Thromb Haemost, 2011. **105**(6): p. 1046-52.

59. Bouhours, J.F., D. Bouhours, and J. Delaunay, *Abnormal fatty acid composition of erythrocyte glycosphingolipids in congenital dyserythropoietic anemia type II.* J Lipid Res, 1985. **26**(4): p. 435-41.

60. Ullman, M.D. and R.H. McCluer, *Quantitative analysis of plasma neutral glycosphingolipids by high performance liquid chromatography of their perbenzoyl derivatives.* J Lipid Res, 1977. **18**(3): p. 371-8.

61. Nilsson, O., et al., *Increased cerebroside concentration in plasma and erythrocytes in Gaucher disease: significant differences between type I and type III.* Clin Genet, 1982. **22**(5): p. 274-9.

62. Gahmberg, C.G. and S.I. Hakomori, *External labeling of cell surface galactose and galactosamine in glycolipid and glycoprotein of human erythrocytes.* J Biol Chem, 1973. **248**(12): p. 4311-7.

63. Bouhours, J.F. and D. Bouhours, *Identification of free ceramide in human erythrocyte membrane.* J Lipid Res, 1984. **25**(6): p. 613-9.

64. Lopez-Montero, I., et al., *Rapid transbilayer movement of ceramides in phospholipid vesicles and in human erythrocytes.* J Biol Chem, 2005. **280**(27): p. 25811-9.

65. Lang, F., et al., *Osmotic shock-induced suicidal death of erythrocytes.* Acta Physiol (Oxf), 2006. **187**(1-2): p. 191-8.

66. Montes, L.R., et al., *Ceramide-enriched membrane domains in red blood cells and the mechanism of sphingomyelinase-induced hot-cold hemolysis.* Biochemistry, 2008. **47**(43): p. 11222-30.

67. Ahyayauch, H., et al., *Pb(II) Induces Scramblase Activation and Ceramide-Domain Generation in Red Blood Cells.* Sci Rep, 2018. **8**(1): p. 7456.

68. Chipeaux, C., et al., *Optimization of ultra-high pressure liquid chromatography - tandem mass spectrometry determination in plasma and red blood cells of four sphingolipids and their evaluation as biomarker candidates of Gaucher's disease.* J Chromatogr A, 2017. **1525**: p. 116-125.

69. Awojoodu, A.O., et al., *Acid sphingomyelinase is activated in sickle cell erythrocytes and contributes to inflammatory microparticle generation in SCD.* Blood, 2014. **124**(12): p. 1941-50.

70. Ito, K., et al., *Lack of sphingosine 1-phosphate-degrading enzymes in erythrocytes.* Biochem Biophys Res Commun, 2007. **357**(1): p. 212-7.

71. Hope, M.J. and P.R. Cullis, *Lipid asymmetry induced by transmembrane pH gradients in large unilamellar vesicles.* J Biol Chem, 1987. **262**(9): p. 4360-6.

72. Zhang, Y., et al., *Elevated sphingosine-1-phosphate promotes sickling and sickle cell disease progression.* J Clin Invest, 2014. **124**(6): p. 2750-61.

73. Bode, C., et al., *Erythrocytes serve as a reservoir for cellular and extracellular sphingosine 1-phosphate.* J Cell Biochem, 2010. **109**(6): p. 1232-43.

74. Hanel, P., P. Andreani, and M.H. Graler, *Erythrocytes store and release sphingosine 1-phosphate in blood.* FASEB J, 2007. **21**(4): p. 1202-9.

75. Arduini, A., et al., *Role of carnitine and carnitine palmitoyltransferase as integral components of the pathway for membrane phospholipid fatty acid turnover in intact human erythrocytes.* J Biol Chem, 1992. **267**(18): p. 12673-81.

76. Engel, N., et al., *First evidence of SGPL1 expression in the cell membrane silencing the extracellular S1P siren in mammary epithelial cells.* PLoS One, 2018. **13**(5): p. e0196854.

77. Holopainen, J.M., et al., *Sphingomyelinase activity associated with human plasma low density lipoprotein.* J Biol Chem, 2000. **275**(22): p. 16484-9.

78. Record, M., A. Loyter, and S. Gatt, *Utilization of membranous lipid substrates by membranous enzymes. Hydrolysis of sphingomyelin in erythrocyte 'ghosts' and liposomes by the membranous sphingomyelinase of chicken erythrocyte 'ghosts'.* Biochem J, 1980. **187**(1): p. 115-21.

79. Bryk, A.H. and J.R. Wisniewski, *Quantitative Analysis of Human Red Blood Cell Proteome.* J Proteome Res, 2017. **16**(8): p. 2752-2761.

80. Yang, L., et al., *Metabolism and functional effects of sphingolipids in blood cells.* Br J Haematol, 1999. **107**(2): p. 282-93.

81. Oliveira, M.M. and M. Vaughan, *Incorporation of Fatty Acids into Phospholipids of Erythrocyte Membranes.* J Lipid Res, 1964. **5**: p. 156-62.

82. Couto, A.S., et al., *Glycosphingolipids in Plasmodium falciparum. Presence of an active glucosylceramide synthase.* Eur J Biochem, 2004. **271**(11): p. 2204-14.

83. Le Petit-Thevenin, J., et al., *Selective modulation of membrane sphingomyelin fatty acid turnover by nigericin. A study in the rat reticulocyte.* Life Sci, 1996. **59**(19): p. PL289-94.

84. Okino, N. and M. Ito, *Ceramidase enhances phospholipase C-induced hemolysis by Pseudomonas aeruginosa.* J Biol Chem, 2007. **282**(9): p. 6021-30.

85. Xu, R., et al., *Role of alkaline ceramidases in the generation of sphingosine and its phosphate in erythrocytes.* FASEB J, 2010. **24**(7): p. 2507-15.

86. Li, F., et al., *Alkaline ceramidase 2 is essential for the homeostasis of plasma sphingoid bases and their phosphates.* FASEB J, 2018. **32**(6): p. 3058-3069.

87. Sun, K., et al., *Elevated adenosine signaling via adenosine A2B receptor induces normal and sickle erythrocyte sphingosine kinase 1 activity.* Blood, 2015. **125**(10): p. 1643-52.

88. Kobayashi, N., et al., *Characterization of the ATP-dependent sphingosine 1-phosphate transporter in rat erythrocytes.* J Biol Chem, 2009. **284**(32): p. 21192-200.

89. Roberts, R., V.A. Sciorra, and A.J. Morris, *Human type 2 phosphatidic acid phosphohydrolases. Substrate specificity of the type 2a, 2b, and 2c enzymes and cell surface activity of the 2a isoform.* J Biol Chem, 1998. **273**(34): p. 22059-67.

90. Selim, S., et al., *Plasma levels of sphingosine 1-phosphate are strongly correlated with haematocrit, but variably restored by red blood cell transfusions.* Clin Sci (Lond), 2011. **121**(12): p. 565-72.

91. Hanada, K., et al., *Neutral sphingomyelinase activity dependent on Mg2+ and anionic phospholipids in the intraerythrocytic malaria parasite Plasmodium falciparum.* Biochem J, 2000. **346 Pt 3**: p. 671-7.

92. Brand, V., et al., *Influence of amitriptyline on eryptosis, parasitemia and survival of Plasmodium berghei-infected mice.* Cell Physiol Biochem, 2008. **22**(5-6): p. 405-12.

93. Lopez, D.J., et al., *Accumulated bending energy elicits neutral sphingomyelinase activity in human red blood cells.* Biophys J, 2012. **102**(9): p. 2077-85.

94. Schissel, S.L., et al., *Secretory sphingomyelinase, a product of the acid sphingomyelinase gene, can hydrolyze atherogenic lipoproteins at neutral pH. Implications for atherosclerotic lesion development.* J Biol Chem, 1998. **273**(5): p. 2738-46.

95. Haldar, K., et al., *The accumulation and metabolism of a fluorescent ceramide derivative in Plasmodium falciparum-infected erythrocytes.* Mol Biochem Parasitol, 1991. **49**(1): p. 143-56.

96. Ansorge, I., et al., *Plasmodium falciparum-infected erythrocytes utilize a synthetic truncated ceramide precursor for synthesis and secretion of truncated sphingomyelin.* Biochem J, 1995. **308 (Pt 1)**: p. 335-41.

97. Pinero, T.A., et al., *Effect of tamoxifen on the sphingolipid biosynthetic pathway in the different intraerythrocytic stages of the apicomplexa Plasmodium falciparum.* Biochem Biophys Res Commun, 2018. **497**(4): p. 1082-1088.

98. Goi, G., et al., *Alterations in the activity of several glycohydrolases in red blood cell membrane from type 2 diabetes mellitus patients*. Metabolism, 1999. **48**(7): p. 817-21.

99. Erikson, A., et al., *Ten years' experience of enzyme infusion therapy of Norrbottnian (type 3) Gaucher disease.* Acta Paediatr, 2006. **95**(3): p. 312-7.

100. Aslan, M., et al., *Decreased Serum Levels of Sphingomyelins and Ceramides in Sickle Cell Disease Patients.* Lipids, 2018. **53**(3): p. 313-322.

101. Sun, K., et al., *Structural and Functional Insight of Sphingosine 1-Phosphate-Mediated Pathogenic Metabolic Reprogramming in Sickle Cell Disease.* Sci Rep, 2017. **7**(1): p. 15281.

102. Wilkerson, B.A., et al., *Sphingosine 1-phosphate (S1P) carrier-dependent regulation of endothelial barrier: high density lipoprotein (HDL)-S1P prolongs endothelial barrier enhancement as compared with albumin-S1P via effects on levels, trafficking, and signaling of S1P1.* J Biol Chem, 2012. **287**(53): p. 44645-53.

103. Mandala, S., et al., *Alteration of lymphocyte trafficking by sphingosine-1-phosphate receptor agonists.* Science, 2002. **296**(5566): p. 346-9.

104. Juarez, J.G., et al., *Sphingosine-1-phosphate facilitates trafficking of hematopoietic stem cells and their mobilization by CXCR4 antagonists in mice.* Blood, 2012. **119**(3): p. 707-16.

105. Punsawad, C. and P. Viriyavejakul, *Reduction in serum sphingosine 1-phosphate concentration in malaria.* PLoS One, 2017. **12**(6): p. e0180631.

106. Venkataraman, K., et al., *Vascular endothelium as a contributor of plasma sphingosine 1-phosphate.* Circ Res, 2008. **102**(6): p. 669-76.

107. Ohkawa, R., et al., *Plasma sphingosine-1-phosphate measurement in healthy subjects: close correlation with red blood cell parameters.* Ann Clin Biochem, 2008. **45**(Pt 4): p. 356-63.

108. Marathe, S., et al., *Human vascular endothelial cells are a rich and regulatable source of secretory sphingomyelinase. Implications for early atherogenesis and ceramide-mediated cell signaling.* J Biol Chem, 1998. **273**(7): p. 4081-8.

109. Gatidis, S., M. Foller, and F. Lang, *Hemin-induced suicidal erythrocyte death.* Ann Hematol, 2009. **88**(8): p. 721-6.

110. Niemoeller, O.M., et al., *Retinoic acid induced suicidal erythrocyte death.* Cell Physiol Biochem, 2008. **21**(1-3): p. 193-202.

111. Steinberg, M.H., et al., *Erythrocyte calcium abnormalities and the clinical severity of sickling disorders.* Br J Haematol, 1978. **40**(4): p. 533-39.

112. Broekhuyse, R.M., *Improved lipid extraction of erythrocytes.* Clin Chim Acta, 1974. **51**(3): p. 341-3.

113. Beutler, E. and C.K. Mathai, *A comparison of normal red cell ATP levels as measured by the firefly system and the hexokinase system.* Blood, 1967. **30**(3): p. 311-20.

114. Fleming, J.K., et al., *A novel approach for measuring sphingosine-1-phosphate and lysophosphatidic acid binding to carrier proteins using monoclonal antibodies and the Kinetic Exclusion Assay.* J Lipid Res, 2016. **57**(9): p. 1737-47.

115. Heerklotz, H. and J. Seelig, *Correlation of membrane/water partition coefficients of detergents with the critical micelle concentration.* Biophys J, 2000. **78**(5): p. 2435-40.

116. Henriksen, J.R., et al., *Understanding detergent effects on lipid membranes: a model study of lysolipids.* Biophys J, 2010. **98**(10): p. 2199-205.

117. Sasaki, H., et al., *pH dependence of sphingosine aggregation.* Biophys J, 2009. **96**(7): p. 2727-33.

118. Broring, K., C.W. Haest, and B. Deuticke, *Translocation of oleic acid across the erythrocyte membrane. Evidence for a fast process.* Biochim Biophys Acta, 1989. **986**(2): p. 321-31.

119. Classen, J., B. Deuticke, and C.W. Haest, *Nonmediated flip-flop of phospholipid analogues in the erythrocyte membrane as probed by palmitoylcarnitine: basic properties and influence of membrane modification.* J Membr Biol, 1989. **111**(2): p. 169-78.

120. Vondenhof, A., et al., *Band 3, an accidental flippase for anionic phospholipids?* Biochemistry, 1994. **33**(15): p. 4517-20.

121. Pitson, S.M., et al., *Human sphingosine kinase: purification, molecular cloning and characterization of the native and recombinant enzymes.* Biochem J, 2000. **350 Pt 2**: p. 429-41.

122. Deems, R.A., *Interfacial enzyme kinetics at the phospholipid/water interface: practical considerations.* Anal Biochem, 2000. **287**(1): p. 1-16.

123. Pulkoski-Gross, M.J., et al., *An intrinsic lipid-binding interface controls sphingosine kinase 1 function.* J Lipid Res, 2018. **59**(3): p. 462-474.

124. Olivera, A., J. Rosenthal, and S. Spiegel, *Effect of acidic phospholipids on sphingosine kinase.* J Cell Biochem, 1996. **60**(4): p. 529-37.

125. Stahelin, R.V., et al., *The mechanism of membrane targeting of human sphingosine kinase 1.* J Biol Chem, 2005. **280**(52): p. 43030-8.

126. Bandhuvula, P., H. Fyrst, and J.D. Saba, *A rapid fluorescence assay for sphingosine-1-phosphate lyase enzyme activity.* J Lipid Res, 2007. **48**(12): p. 2769-78.

127. Sun, W., et al., *Substrate specificity, membrane topology, and activity regulation of human alkaline ceramidase 2 (ACER2).* J Biol Chem, 2010. **285**(12): p. 8995-9007.

128. Mao, C., et al., *Cloning and characterization of a novel human alkaline ceramidase. A mammalian enzyme that hydrolyzes phytoceramide.* J Biol Chem, 2001. **276**(28): p. 26577-88.

129. Bogdanova, A., et al., *Calcium in red blood cells-a perilous balance.* Int J Mol Sci, 2013. **14**(5): p. 9848-72.

130. Hu, W., et al., *Alkaline ceramidase 3 (ACER3) hydrolyzes unsaturated long-chain ceramides, and its down-regulation inhibits both cell proliferation and apoptosis.* J Biol Chem, 2010. **285**(11): p. 7964-76.

131. Nur, E., et al., *Increased efflux of oxidized glutathione (GSSG) causes glutathione depletion and potentially diminishes antioxidant defense in sickle erythrocytes.* Biochim Biophys Acta, 2011. **1812**(11): p. 1412-7.

132. Weiss, E., et al., *Deoxygenation-induced and Ca(2+) dependent phosphatidylserine externalisation in red blood cells from normal individuals and sickle cell patients.* Cell Calcium, 2012. **51**(1): p. 51-6.

133. van Beers, E.J., et al., *Circulating erythrocyte-derived microparticles are associated with coagulation activation in sickle cell disease.* Haematologica, 2009. **94**(11): p. 1513-9.

134. Poletti, V., et al., *Pre-clinical Development of a Lentiviral Vector Expressing the Anti-sickling betaAS3 Globin for Gene Therapy for Sickle Cell Disease.* Mol Ther Methods Clin Dev, 2018. **11**: p. 167-179.

135. Steuer, R., et al., *Observing and interpreting correlations in metabolomic networks.* Bioinformatics, 2003. **19**(8): p. 1019-26.

136. Leonard, C., et al., *Contribution of plasma membrane lipid domains to red blood cell (re)shaping.* Sci Rep, 2017. **7**(1): p. 4264.

137. Garnier, Y., et al., *Differences of microparticle patterns between sickle cell anemia and hemoglobin SC patients.* PLoS One, 2017. **12**(5): p. e0177397.

138. Regaya, F., et al., *Parvovirus B19 infection in Tunisian patients with sickle-cell anemia and acute erythroblastopenia.* BMC Infect Dis, 2007. **7**: p. 123.

139. Shaner, R.L., et al., *Quantitative analysis of sphingolipids for lipidomics using triple quadrupole and quadrupole linear ion trap mass spectrometers.* J Lipid Res, 2009. **50**(8): p. 1692-707.

140. Hammad, S.M., et al., *Blood sphingolipidomics in healthy humans: impact of sample collection methodology.* J Lipid Res, 2010. **51**(10): p. 3074-87.

141. Scherer, M., et al., *Sphingolipid profiling of human plasma and FPLC-separated lipoprotein fractions by hydrophilic interaction chromatography tandem mass spectrometry.* Biochim Biophys Acta, 2011. **1811**(2): p. 68-75.

142. Reed, C.F., *Phospholipid exchange between plasma and erythrocytes in man and the dog.* J Clin Invest, 1968. **47**(4): p. 749-60.

143. Griffiths, R.E., et al., *Maturing reticulocytes internalize plasma membrane in glycophorin A-containing vesicles that fuse with autophagosomes before exocytosis.* Blood, 2012. **119**(26): p. 6296-306.

144. Schultze, M., et al., *The oxidation of fatty acids by rabbit reticulocytes and their isolated mitochondria.* Eur J Biochem, 1972. **27**(1): p. 43-7.

145. Pittman, J.G. and D.B. Martin, *Fatty acid biosynthesis in human erythrocytes: evidence in mature erythrocytes for an incomplete long chain fatty acid synthesizing system.* J Clin Invest, 1966. **45**(2): p. 165-72.

146. Ballas, S.K. and E.R. Burka, *Pathways of de novo phospholipid synthesis in reticulocytes.* Biochim Biophys Acta, 1974. **337**(2): p. 239-47.

147. Ono, Y., et al., *Sphingosine 1-phosphate release from platelets during clot formation: close correlation between platelet count and serum sphingosine 1-phosphate concentration.* Lipids Health Dis, 2013. **12**: p. 20.

148. Carayon, K., et al., *Proteolipidic composition of exosomes changes during reticulocyte maturation.* J Biol Chem, 2011. **286**(39): p. 34426-39.

149. Yang, C., et al., *Sphingosine-1-phosphate signaling modulates terminal erythroid differentiation through the regulation of mitophagy.* Exp Hematol, 2019.

150. Scaro, J.L., et al., *Effects of sphingolipids on erythroblastic maturation in the mouse.* Experientia, 1982. **38**(3): p. 401-3.

151. Lee, L.G., C.H. Chen, and L.A. Chiu, *Thiazole orange: a new dye for reticulocyte analysis.* Cytometry, 1986. **7**(6): p. 508-17.